



저작자표시-비영리-변경금지 2.0 대한민국

이용자는 아래의 조건을 따르는 경우에 한하여 자유롭게

- 이 저작물을 복제, 배포, 전송, 전시, 공연 및 방송할 수 있습니다.

다음과 같은 조건을 따라야 합니다:



저작자표시. 귀하는 원저작자를 표시하여야 합니다.



비영리. 귀하는 이 저작물을 영리 목적으로 이용할 수 없습니다.



변경금지. 귀하는 이 저작물을 개작, 변형 또는 가공할 수 없습니다.

- 귀하는, 이 저작물의 재이용이나 배포의 경우, 이 저작물에 적용된 이용허락조건을 명확하게 나타내어야 합니다.
- 저작권자로부터 별도의 허가를 받으면 이러한 조건들은 적용되지 않습니다.

저작권법에 따른 이용자의 권리는 위의 내용에 의하여 영향을 받지 않습니다.

이것은 [이용허락규약\(Legal Code\)](#)을 이해하기 쉽게 요약한 것입니다.

[Disclaimer](#)



A THESIS

FOR THE DEGREE OF DOCTOR OF PHILOSOPHY

Development of Functional Food and Medical Drug
Materials Using Antidiabetic Compounds Isolated
from Brown Seaweeds

Seung-Hong Lee

Department of Biotechnology

GRADUATE SCHOOL

JEJU NATIONAL UNIVERSITY

August, 2011

Development of Functional Food and Medical Drug Materials Using
Antidiabetic Compounds Isolated from Brown Seaweeds

Seung-Hong Lee

2011

A THESIS

FOR THE DEGREE OF DOCTOR OF PHILOSOPHY

**Development of Functional Food and Medical Drug
Materials Using Antidiabetic Compounds Isolated
from Brown Seaweeds**

Seung-Hong Lee

Department of Biotechnology

GRADUATE SCHOOL

JEJU NATIONAL UNIVERSITY

August, 2011


**Development of Functional Food and Medical Drug
Materials Using Antidiabetic Compounds Isolated
from Brown Seaweeds**

**Seung-Hong Lee
(Supervised by Professor You-Jin Jeon)**


A thesis submitted in partial fulfillment of the requirement for the degree of
DOCTOR OF PHILOSOPHY

2011. 08.

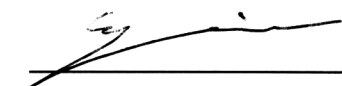
This thesis has been examined and approved by



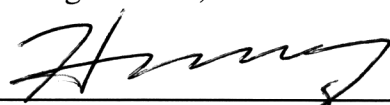
Thesis director, Gi-Young Kim, Prof. of Marine Life Science



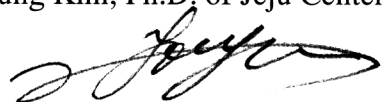
Dae-Ho Lee, Prof. of Medicine



Seuncheon Lee, Prof. of Marine Life Science



Daekyung Kim, Ph.D. of Jeju Center, Korea Basic Science Institute



You-Jin Jeon, Prof. of Marine Life Science

2011. 08

Date

**Department of Biotechnology
GRADUATE SCHOOL
JEJU NATIONAL UNIVERSITY**

CONTENTS

국문초록 vi

LIST OF FIGURESx

LIST OF TABLESxvii

INTRODUCTION1

Part I . Screening of α -glucosidase inhibitory and glucose uptake effects of brown seaweeds and isolation of potential anti-diabetic compounds

ABSTRACT 15

MATERIALS AND METHODS16

General experimental procedures16

Materials16

Extraction procedure of 80% methanolic extracts from brown algae.....17

Inhibition assay for α -glucosidase activity.....17

Cell culture19

Glucose uptake assay	19
Extraction and isolation of octaphlorethol A (OPA).....	20
Statistical analysis	20
RESULTS AND DISCUSSIONS	22
Part II. Octaphlorethol A isolated from <i>Ishige sinicola</i> inhibits α-glucosidase and α-amylase <i>in vitro</i> and alleviates hyperglycemia in diabetic mice	
ABSTRACT	36
MATERIALS AND METHODS	38
Materials	38
Inhibitory effect of OPA on α-glucosidase and α-amylase <i>in vitro</i>.....	38
Experimental animals.....	39
Measurement of postprandial blood glucose level.....	39
Intraperitoneal glucose tolerance test (IPGTT).....	40
Type 2 diabetic mice and experimental design.....	40
Statistical analysis.....	41
RESULTS	42

DISCUSSIONS51

**Part III. Octaphlorethol A isolated from *Ishige sinicola* stimulates glucose uptake
in skeletal muscle cells by activating Akt and AMPK pathway**

ABSTRACT57

MATERIALS AND METHODS59

Materials59

Cell culture59

MTT assay60

LDH Cytotoxicity Assay.....60

Glucose uptake assay.....61

Western blot analysis.....61

Plasma membrane fractionation and immunoblot analysis.....62

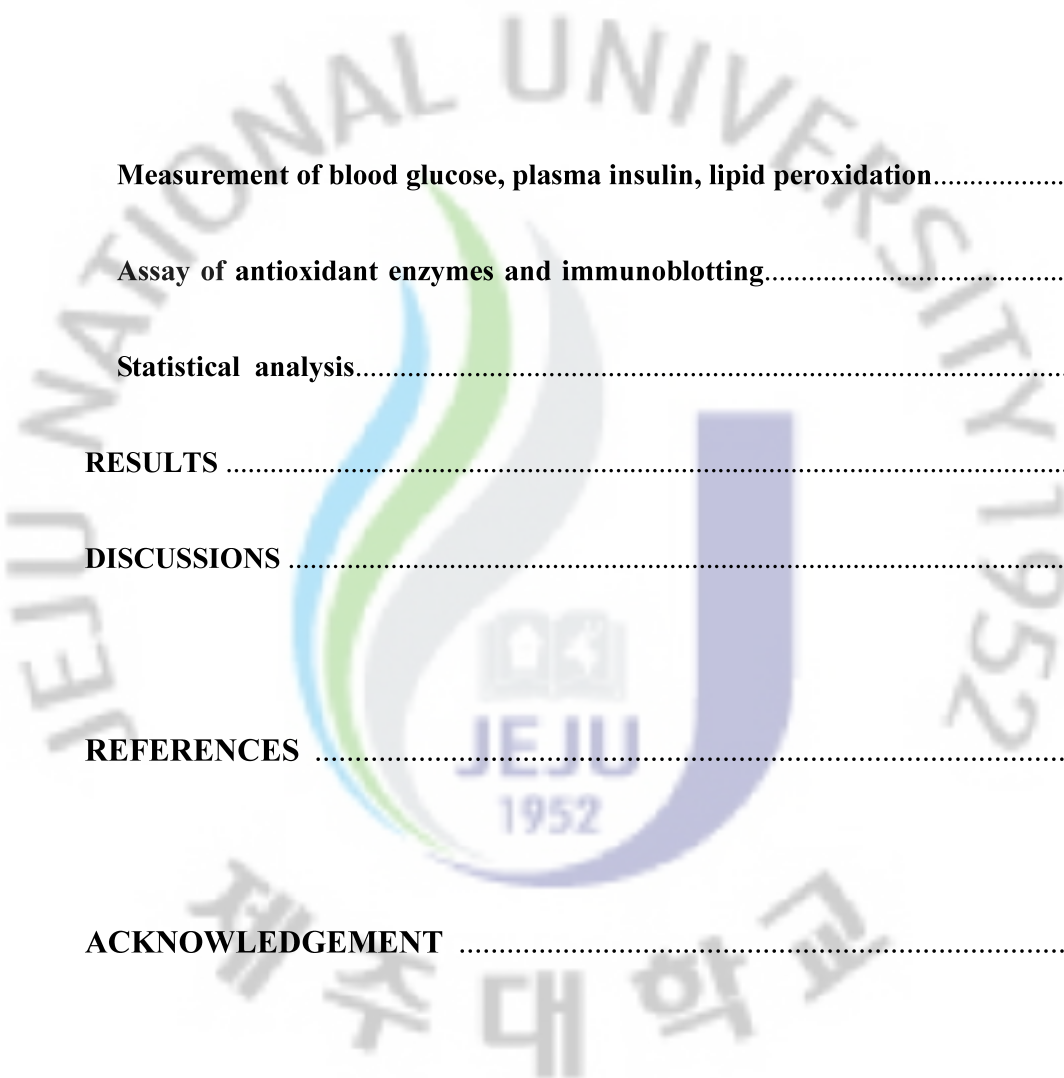
Statistical analysis.....63

RESULTS64

DISCUSSIONS74

Part IV. Octaphlorethol A isolated from *Ishige sinicola* prevents and protects against STZ-induced pancreatic β -cells damage in *in vitro* and *in vivo*

ABSTRACT	81
MATERIALS AND METHODS	83
Materials	83
Cell culture	83
Assay of cell viability	83
Assay of lipid peroxidation	84
Assay of intracellular ROS levels and Image analysis	84
Comet assay	85
Antioxidant enzyme assays	86
Cell cycle analysis	87
Nuclear staining with Hoechst 33342	88
Western blot analysis	88
Glucose stimulated insulin secretion (GSIS)	89
Animals and experimental design	90



Measurement of blood glucose, plasma insulin, lipid peroxidation.....	91
Assay of antioxidant enzymes and immunoblotting.....	93
Statistical analysis.....	93
RESULTS	94
DISCUSSIONS	116
REFERENCES	123
ACKNOWLEDGEMENT	139

국문초록

현대사회의 도시화된 생활환경 (운동부족, 스트레스), 과도한 영양섭취를 일으키는 다양한 인스턴트 식품의 범람과 노동력 위주의 경제활동에서 정보통신의 발달로 인한 사회적 업무환경으로의 전환은 과다한 에너지의 저장으로 인하여 발생하는 대사성질환의 발현을 필연적으로 증가시키고 있다. 복합적 증상으로 나타나는 대사성질환의 원인으로 다양한 요소가 존재하지만 가장 중요한 요소로 받아들여지고 있는 것은 인슐린 저항성이다. 따라서 대사성질환의 발병과 깊은 상관관계를 보여주는 당뇨병 (인슐린 저항성을 특징으로 하는 2형 당뇨병 포함)의 증가추세가 두드러짐에 따라 당뇨병은 현재 전세계적으로 급격하게 증가하는 추세이고 2025년에는 전세계적으로 당뇨병 환자가 약 3억 2천 4백만 명에 이를 것으로 추산하고 있으며 전 인구에 유병율이 8% 이상이며 특히 노인환자에서는 유병율이 크게 증가하고 있다. 이에 따라 세계 당뇨관련 시장은 연평균 12.5%의 성장률로 성장하여 2005년 182억 달러에서 2015년 602억 달러의 시장을 형성할 것으로 전망. 국내의 경우 연평균 12.5%의 성장률로 성장하여 2005년 1,229억 원에서 2015년 4,218억 원의 시장을 형성할 것으로 전망하고 있다. 기존 당뇨병 약제의 경우 약물에 따라, 저혈당, 심장손상, 간손상, 복통, 식욕부진, 체중증가 및 장내 가스 발생 등 심각한 부작용이 나타날 수 있으며, 복용기간이 지속되면 약물의 효능이 감소될 수 있어 시간이 지남에 따라 약물의 종류를 바꾸거나 복용량을 변화시키는 등 많은 문제점을 가지고 있

다.

따라서 부작용이 없고 우수한 효과를 나타내는 당뇨병의 예방 치료물질로서 천연물 유래 소재의 발굴에 대한 연구가 절실하다. 해양생물자원 중 해조류 유래의 다양한 천연물들은 그 구조와 생리활성도의 특이성 면에서 질병 예방 및 치료제 개발을 위한 강력한 신물질의 보고로 떠오르고 있다. 따라서 해조류에 관한 연구는 급속도로 증가하고 있으며 생화학, 의·약학 등의 기초 및 응용연구에도 많이 활용되고 있다. 또한 강력하고 특이한 생리활성을 가진 상당수의 해조류는 의약품, 기능성식품 및 화장품 등으로 개발 및 산업화에 성공하여 새로운 기능성 소재를 탐색하는 분야에서 해조류는 무한한 가능성을 가지고 있다. 이러한 점에서 우리나라의 해양생물 분포 상 중요한 위치를 차지하는 제주 연안의 해조류를 이용하여 항당뇨 소재로서의 활용은 경제 산업적 측면에서 체계적으로 연구할 가치가 있다고 생각된다. 따라서 이 연구에서는 제주연안에 서식하고 있는 갈조류를 대상으로 항당뇨성 물질을 분리하고 기능성 식의약품 소재로서의 개발 가능성을 확인하였다.

제주연안에 서식하고 있는 17종의 갈조류를 대상으로 α -glucosidase 저해활성 및 근육세포에서의 포도당 흡수촉진 효과를 스크리닝한 결과 넓패 (*Ishige sinicola*), 부챗말 (*Padina arborescens*), 큰톱니모자반 (*Sargassum serratifolium*) 그리고 큰잎모자반 (*Sargassum coreanum*)에서 다른 갈조류에 비해 우수한 효과를 나타내는 것을 확인하였고, raw materials 확보와 식용가능여부 등을 고려하여 넓패를 대상으로 활

성물질을 분리하였다. 그 결과 phlorotannin계열의 octaphloretol A (OPA)이라는 잠재적인 항당뇨성 물질을 분리하였다.

분리된 항당뇨성 물질인 OPA의 장내 탄수화물 가수분해 효소인 α -glucosidase와 α -amylase저해 활성을 측정한 결과 시판되는 식후 혈당강하제인 acarbose보다 우수한 저해 활성을 나타내는 것을 확인하였고 *in vivo* 실험을 통한 식후 혈당강하 및 내당능 test에서도 우수한 혈당 강하 효과를 나타냈다. 또한 제 2형 당뇨동물 모델에서도 혈당강하효과 및 인슐린 저항성 개선 작용을 나타냈다. 식후 혈당강하 효과와 더불어 내당능 및 인슐린 저항성개선 효과를 나타냄에 따라 그 작용기전을 구명하기 위해 근육세포에서 포도당 흡수 촉진 효과를 측정하였다. 그 결과 인슐린과 유사한 포도당 흡수 촉진 효과를 나타냈다. 세포 내 포도당 흡수는 insulin dependent pathway와 insulin independent pathway로 이루어진다. Insulin dependent pathway에 있어서 대표적인 단백질인 Akt는 insulin에 의해 활성화 되며, insulin independent한 pathway에 있어서 핵심 단백질이 AMPK로 알려져 있다. 활성화된 Akt와 AMPK는 포도당수송반체인 GLUT4의 translocation을 통해 세포 내로 포도당이 흡수된다. OPA에 의한 포도당 흡수 촉진 효과가 어떠한 pathway로 이루어지는 지 Western blot를 통해 살펴본 결과 OPA는 Akt와 AMPK를 모두 활성화시켰으며 이에 따라 GLUT4가 세포막으로 translocation되어 포도당이 흡수효과가 나타나는 것을 구명하였다.

췌장 베타세포는 인슐린을 분비하는 세포로서 산화적 스트레스나 염증 등과 같은 자극에 의해 세포 손상을 받게 되면 인슐린 분비능이 감소되어 혈당이 상승하게 된다. Streptozotocin으로 유도된 췌장 베타세포의 손상을 OPA가 보호하는지를 *in vitro*와 *in vivo* 상에서 살펴본 결과 streptozotocin 처리한 구에서는 세포 생존률 감소, 세포 내 ROS 증가, DNA 손상과 apoptosis가 증가한 반면 OPA를 처리하였을 때 산화적 스트레스와 apoptosis을 억제하여 세포 생존률 증가 및 우수한 세포 보호효과를 나타냈으며, 인슐린 분비능 또한 상당히 개선시켰음을 확인하였다.

이 모든 결과를 종합해 볼 때, 췌장에서 분리한 OPA는 다양하고 우수한 항당뇨 활성을 가지고 있음을 확인하였으며 그에 따라 OPA는 항당뇨성 물질로서 잠재적인 기능성 식품 및 천연의약 소재로서 충분한 가능성이 있으리라 판단된다.

LIST OF FIGURES

Fig. I . Chemical structures of phlorotannins isolated from brown algae.

Fig. II . Major targeted sites of oral drug classes.

Fig. III . Outline of pathways regulating glucose transport GLUT4 translocation to the plasma membrane in skeletal muscle.

Fig. IV . Overview of the putative sequence of events leading to β -cell death in animal model of type 1 and type 2 diabetes.

Fig. 1-1. The photography of a brown alga *Ishige sinicola*.

Fig. 1-2. α -glucosidase inhibitory effect of 80% MeOH extracts from brown algae.

Experiments were performed in triplicate and the data are expressed as mean \pm SE.

Fig. 1-3. Glucose uptake effect of 80% MeOH extracts from brown algae. Experiments

were performed in triplicate and the data are expressed as mean \pm SE.

Fig. 1-4. α -glucosidase inhibitory (A) and glucose uptake (B) effect of *I. Sinicola* extracts

partitioned by various organic solvents. M, 80% MeOH extract; H, Hexane; C, CHCl₃;

E, EtOAc; B, BuOH. Experiments were performed in triplicate and the data are expressed

as mean \pm SE.

Fig. 1-5. Isolation scheme of octaphloretol A (OPA) from *I. sinicola*.

Fig. 1-6. Proton and Carbon NMR spectrum of octaphloretol A (OPA).

Fig. 1-7. Gradient HMBC and HMQC NMR spectrum of octaphloretol A (OPA).

Fig. 1-8. MS spectrum of octaphloretol A (OPA).

Fig. 1-9. Chemical structure of octaphloretol A (OPA).

Fig. 2-1. Inhibitory effects OPA isolated from *I. sinicola* on α -glucosidase (A) and α -amylase (B). Inhibitory effects were determined using pNPG and pNPM as substrates, respectively, and acarbose was employed as a positive control. Values are expressed as means \pm S.E. in triplicate experiments. ^{a-d}Values with different alphabets are significantly different at $P < 0.05$ as analyzed via Duncan's multiple range test. The final concentration of acarbose is 0.5 mg/ml.

Fig. 2-2. Blood glucose levels after the administration of OPA in streptozotocin-induced diabetic mice (A) and normal mice (B). Control (distilled water), OPA (100 mg/kg), acarbose (100 mg/kg) and metformin (100 mg/kg) were co-administered orally with starch (2 g/kg). Each value is expressed as mean \pm S.D. of six mice ($n=48$). Significantly different from control at $*P < 0.05$.

Fig. 2-3. The effects of the administration of OPA on the glucose tolerance test in streptozotocin-induced diabetic mice (A) and normal mice (B). Control (distilled water), OPA (100 mg/kg), acarbose (100 mg/kg) and metformin (100 mg/kg) intraperitoneally injected with glucose (1 g/kg body weight). The blood glucose concentration was measured at the indicated times and presented as percent of glucose

injection zero time. Each value is expressed as mean \pm S.D. of six mice (n=48). Significantly different from control at *P<0.05.

Fig. 3-1. Cytotoxicity of OPA. Cytotoxicity of OPA was determined using the MTT and LDH method. Each value is expressed as mean \pm S.E. in triplicate experiments.

Fig. 3-2. OPA dose- and time-dependently stimulates glucose uptake in L6 skeletal muscle cells. (A) Cells were starved in serum free (SF) media for 12 h, and incubated for 1 h with increasing of OPA and insulin. (B) Cells were starved for 12 h in SF media followed by incubation with 50 μ g/ml OPA for different time periods up to 12 h. Insulin (100 nM, for 1 h) was used as a positive control. Values are expressed as means \pm S.E. in triplicate experiments. ^{a-d}Values with different alphabets are significantly different at P<0.05 as analyzed via Duncan's multiple range test.

Fig. 3-3. OPA-induced increase of glucose uptake was reduced by wortmannin and compound C. After 12 h starvation, L6 skeletal muscle cells were pretreated with or without 100 nM wortmannin (phosphatidylinositol (PI) 3-kinase inhibitor) and 10 μ M compound C, (AMPK inhibitor) for 30 min, and then treated with 50 μ g/ml OPA for 2 h. Each value is expressed as mean \pm S.E. in triplicate experiments. *P<0.05 vs. control or between two groups as indicated.

Fig. 3-4. Effects of OPA on the insulin signaling pathway in L6 cells. Cells were pretreated with or without 100 nM wortmannin for 30 min, and then treated with the indicated concentrations of OPA and insulin for 2 h and 10 min, respectively. The cell lysates were

analyzed via Western blotting using anti-phosphoIRS-1 (Tyr 612), anti-IRS-1, anti-phosphoAkt (Ser 473) and anti-Akt. Figures are representative of three independent experiments.

Fig. 3-5. Effect of OPA on AMPK signaling pathway. Cells were pretreated with or without 10 μ M compound C for 30 min, and then treated with the indicated concentrations of OPA and insulin for 2 h and 10 min, respectively. The cell lysates were analyzed via Western blotting using anti-phosphoAMPK (Thr 172) and anti-AMPK. Figures are representative of three independent experiments.

Fig. 3-6. Effect of OPA on GLUT4 translocation to the plasma membrane. Cells were pretreated with or without 10 μ M compound C for 30 min, and then treated with the indicated concentrations of OPA and insulin for 2 h and 10 min, respectively. The cell lysates were analyzed via Western blotting using anti-GLUT4. Figures are representative of three independent experiments.

Fig. 3-7. Glucose uptake mechanism of OPA in L6 skeletal muscle cells.

Fig. 4-1. Animals and experimental design.

Fig. 4-2. Effect of OPA on cell viability in STZ treated RINm5F pancreatic β cells. Cells (1×10^5 cells/well) in wells of 96-well plates were preincubated with the indicated

concentrations of OPA for 3 h, and then incubated with STZ for 24 h. Each value is expressed as mean±S.E. ^{a-c}Values with different alphabets are significantly different at p<0.05 as analyzed by Duncan's multiple range test.

Fig. 4-3. Effect of OPA on TBARS generation in STZ treated RINm5F pancreatic β cells.

Cells (1×10^5 cells/well) in wells of 24-well plates were preincubated with the indicated concentrations of OPA for 3 h, and then incubated with STZ for 24 h. Each value is expressed as mean±S.E. ^{a-c}Values with different alphabets are significantly different at p<0.05 as analyzed by Duncan's multiple range test.

Fig. 4-4. Effect of OPA on intracellular ROS generation in STZ treated RINm5F pancreatic β cells. (A) The intracellular ROS generated was detected using flow

cytometry after DCF-DA addition. (B) Images illustrate the increase in green fluorescence intensity of DCF produced by ROS in STZ treated cells as compared to control and lowered fluorescence intensity in STZ treated cells with OPA. A, Control; B, 10 mM STZ; C, 12.5 μ g/ml OPA + STZ; D, 25 μ g/ml OPA + STZ; E, 50 μ g/ml OPA + STZ.

Fig. 4-5. Inhibitory effect of OPA on STZ-induced DNA damages. The damaged cells on

STZ treatment was determined by comet assay. (A) \square , % Fluorescence in tail; \blacklozenge , Inhibitory effect of cell damage. (B) Photomicrographs of DNA damage and migration

observed under OPA. A, Control; B, 10 mM STZ; C, 12.5 $\mu\text{g/ml}$ OPA + STZ; D, 25 $\mu\text{g/ml}$ OPA + STZ; E, 50 $\mu\text{g/ml}$ OPA + STZ. Experiments were performed in triplicate and the data are expressed as mean \pm SE. Statistical evaluation was performed to compare the experimental groups and corresponding control groups. *, $P < 0.05$

Fig. 4-6. Protective effect of OPA on STZ-induced apoptosis in RINm5F pancreatic β cells.

The cells were pretreated with the indicated concentrations of OPA for 3 h, and then incubated with STZ for 24 h. (A) The cells were stained with PI and analyzed by flow cytometry. (B) Apoptotic bodies were stained with Hoechst 33342 solution and then observed under a fluorescent microscope using a blue filter. A, Control; B, 10 mM STZ; C, 12.5 $\mu\text{g/ml}$ OPA + STZ; D, 25 $\mu\text{g/ml}$ OPA + STZ; E, 50 $\mu\text{g/ml}$ OPA + STZ. Each value is expressed as mean \pm S.E. ^{a-e} Values with different alphabets differ significantly at $p < 0.05$ as analyzed via Duncan's multiple range test.

Fig. 4-7. OPA modulated the expression levels of apoptosis-related protein in RINm5F

pancreatic β cells. Cells were pretreated with or without the indicated concentrations of OPA for 3 h, and then treated with the STZ for 24 h. The cell lysates were analyzed via Western blotting using anti-P53, anti-Bax, anti-Bcl-xL, anti-caspase-3, -9 and anti-PARP. Figures are representative of three independent experiments.

Fig. 4-8. Effects of OPA on insulin secretion in STZ-treated RINm5F pancreatic β cells.

Cells (1×10^6) in 10 mm dishes were pretreated with the indicated concentrations of OPA for 3 h, and then incubated with STZ for 24 h. Insulin secretion from RIN-m5F cells in response to glucose (5 and 25 mM) concentration. Each value is expressed as mean \pm S.E.

^{a-c}Values with different alphabets differ significantly at $p < 0.05$ as analyzed by Duncan's multiple range test.

Fig. 4-9. Effects of OPA expression levels of apoptosis-related protein in STZ-treated

mice. The OPA dissolved saline was administered orally into mice, receiving at a dose of 5 mg/kg or 10 mg/kg body weight first at 12 h and then again at 2 h before the administration of STZ. The pancreatic tissue lysates were analyzed via Western blotting using anti-P53, anti-Bax, anti-Bcl-xL and anti-caspase-3. Figures are representative of experiments.

LIST OF TABLES

Table 1-1. The list and polyphenol content of brown algae.

Table 1-2. ^1H and ^{13}C NMR assignments for octaphlorethol A (OPA).

Table 2-1. IC_{50} values of inhibitory effect of OPA on α -glucosidase and α -amylase.

Table 2-2. Area under curve (AUC) of postprandial glucose responses of normal and streptozotocin-induced diabetic mice.

Table 2-3. The effects of the administration of OPA on blood glucose, plasma insulin level, and body weight in C57BL/KsJ-*db/db* mice.

Table 4-1. Effects of OPA on antioxidant enzyme activities in STZ treated RINm5F pancreatic β cells.

Table 4-2. Effects of OPA on the levels of blood glucose, plasma insulin and body weight in STZ-treated mice.

Table 4-3. Effects of OPA on the lipid peroxidation and antioxidant enzyme activities in STZ-treated mice.

INTRODUCTION

Marine organisms are rich sources of structurally diverse bioactive compounds with valuable nutraceutical, pharmaceutical and cosmeceutical potential (Barrow and Shahidi, 2008; Shahidi and Zhong, 2008). Among them, marine algae represent one of the richest sources of marine organisms (Ruperez, 2001; Mayer and Hamann, 2002). Marine algae are classified as unicellular microalgae and macroalgae, which are macroscopic plants of marine benthoses (Ricketts and Calvin, 1962). Macroalgae, also known as seaweed, are distinguished according to the nature of their pigments: brown algae (phaeophyta), red algae (rhodophyta) and green algae (chlorophyta). In Asian countries, several species of seaweed are used as food ingredients and medicine, to provide nutrition and a peculiar taste. Recently, The marine algae have been identified as an under-exploited plant resource and functional food (Nisizawa et al., 1987; Heo et al., 2005a,b). They have also proven to be rich sources of structurally diverse bioactive compounds with valuable pharmaceutical and biomedical potential. In particular, brown algae are plentifully present around Jeju Island, Korea, where these valuable brown algae have various biological compounds, such as xanthophyll, pigments, fucoidans, phycocolloids, phlorotannins, and fucoxanthin (Halliwell and Gutteridge, 1999). Several researches on those kinds of compounds have pointed out a variety of biological benefits including antioxidant, anticoagulant, antihypertention,

antibacterial and antitumor activities (Nagayama et al., 2002; Mayer and Hamann, 2005; Athukorala and Jeon, 2005; Kotake-Nara et al., 2005; Heo et al., 2008).

Polyphenolic compounds are one of the most common classes of secondary metabolites found in terrestrial plants and marine algae. There are fundamental differences in the chemical structures of polyphenols in both terrestrial and marine plants (Shibata et al., 2002).

In general, polyphenols or phenolic compounds have a similar basic structural chemistry including an “aromatic” or “phenolic” ring structure. Phenolic compounds have been associated with antioxidative action in biological systems, acting as scavengers of singlet oxygen and free radicals (Rice-Evans et al., 1995; Jorgensen et al., 1999). The protective effects of plant polyphenols in biological systems are ascribed to their capacity to transfer electrons to free radicals, chelate metal catalysts, activate antioxidant enzymes and inhibit oxidases. Polyphenols are classified broadly into two classes; condensed tannins, which are polymeric flavonoids, and hydrolysable tannins, which are derivatives of gallic acid (Haslam, 1989). Marine brown algae accumulate a variety of phloroglucinol-based polyphenols of low, intermediate and high molecular weights containing both phenyl and phenoxy unit. Phlorotannins, marine algal polyphenols, consisting of phloroglucinol units linked to one another in various ways, occur broadly among the brown and red algae (Singh and Bharate, 2006) (**Fig. 1**). Several studies have demonstrated the variety of biological

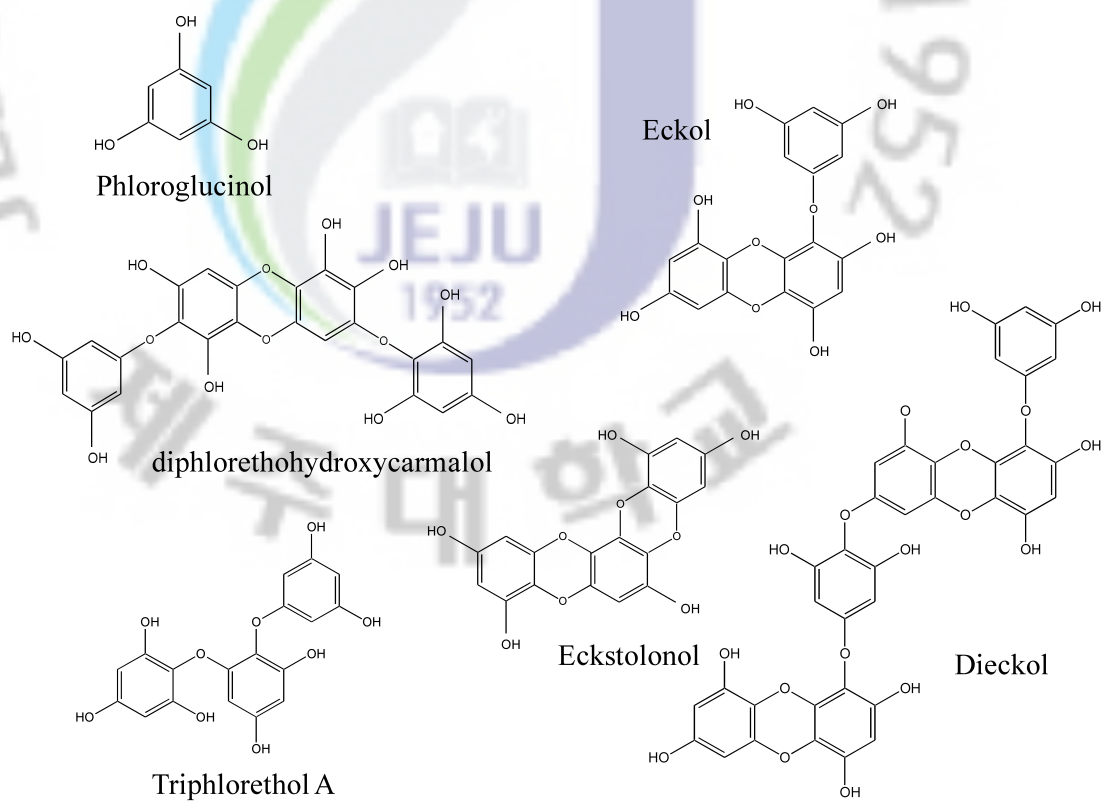


Fig. 1 . Chemical structures of phlorotannins isolated from brown algae.

benefits associated with phlorotannins, including antioxidant, anticoagulant, antibacterial, anti-inflammatory, and anti-cancer activities (Shibata et al., 2002; Mayer and Hamann, 2005; Heo et al., 2008; Kong et al., 2009).

Diabetes mellitus is characterized by abnormal metabolism of glucose, due in part to resistance to the action of insulin in peripheral tissues. The characteristic symptoms are polyuria, polydipsia, and polyuria. Diabetes mellitus is the most serious and chronic disease that is developing with an increasing obesity and aging in the general population over the world. Diabetes mellitus is a complex disorder that is characterized by hyperglycemia. It is largely classified into insulin-dependent diabetes mellitus (type 1 diabetes) and non-insulin-dependent diabetes mellitus (type 2 diabetes). In particular, type 2 diabetes is an increasing worldwide health problem and is the most common type of diabetes (Zimmet et al., 2001). Hyperglycemia plays an important role in the development type 2 diabetes and complications associated with the diseases such as micro-vascular and macro-vascular diseases (Baron, 1998). Therefore, the effective control of blood glucose level is the key to prevent or reverse diabetic complications and improve the quality of the life in diabetic patients (DeFronzo, 1999). Currently available therapies for type 2 diabetes include insulin and various oral antidiabetic drugs such as sulfonylureas, metformin, α -glucosidase inhibitors, and thiazolidinediones (**Fig. II**). However, these therapies have either limited efficacy or



Fig. II. Major targeted sites of oral drug classes.

significant mechanism based side effects like hypoglycemia, flatulence, body weight gain of enhancement of gastrointestinal problems.

The control of postprandial hyperglycemia has been shown to be important in the treatment of diabetes and the prevention of cardiovascular complications. One of the therapeutic approaches adopted thus far to ameliorate postprandial hyperglycemia involves the retardation of glucose absorption via the inhibition of carbohydrate-hydrolyzing enzymes including α -glucosidase and α -amylase, in the digestive organs (Bhandari et al., 2008). The powerful synthetic α -glucosidase and α -amylase inhibitors, such as acarbose, miglitol, and voglibose, function directly in reducing the sharp increases in glucose levels that occur immediately after food uptake (Saito et al., 1998; Sels et al., 1999; Stand et al., 1999). However, the continuous use of those synthetic agents should be limited because those agents may induce side effects such as flatulence, abdominal cramps, vomiting, and diarrhea (Hanefeld, 1998). Additionally, there have been some reports describing an increased incidence of renal tumors, serious hepatic injury, and acute hepatitis (Diaz-Gutierrez et al., 1998; Charpentier et al., 2000). Therefore, a number of studies have been conducted in the search for naturally derived α -glucosidase and α -amylase inhibitors that induce no deleterious side effects (Matsui et al., 2007; Kim et al., 2008; Heo et al., 2009a).

Metabolic detuning is involved in the morbidity of Type 2 diabetes mellitus and insulin

resistance (Moller, 2001), and is also associated with cardiovascular diseases and other complications (Keen et al., 1999). Management of glycemic control within the normal level reduces the acute and chronic complications associated with diabetes and promotes long-term health (Klein et al., 1996; UK Prospective Diabetes Study Group, 1998). Insulin resistance, defined as the inability of cells or tissues to respond to physiological concentrations of insulin, is a major defect underlying the development of type 2 diabetes and is a central component of the metabolic syndrome, a constellation of abnormalities including obesity, hypertension, glucose intolerance, and dyslipidemia (Hotamisligil, 2006; Moller and Flier, 1992). Skeletal muscle, a key insulin sensitive tissue, has a paramount role in energy balance and is the principal site for postprandial glucose utilization and disposal. In skeletal muscle insulin stimulates glucose uptake primarily by increasing translocation and redistribution of the glucose transporter-4 (GLUT4) from internal membrane to the plasma membrane (Stephens and Pilch, 1995; Zaid et al., 2008). Under insulin resistance, translocation of insulin sensitive GLUT4 is impaired resulting in consequent defect in the insulin-stimulated glucose uptake, a rate-limiting step for glucose disposal (Petersen and Shulman, 2006).

The insulin signaling pathway (**Fig. III**) leading to increased muscle glucose uptake involves binding of insulin to its receptor, phosphorylation of downstream insulin receptor

substrates (IRS) and activation of phosphatidylinositol-3 kinase (PI3-K) and Akt which promotes GLUT4 glucose transporter translocation from an intracellular pool to the plasma membrane (Taniguchi et al., 2006; Dugani et al., 2008). AMP-activated protein kinase (AMPK) is a heterotrimeric ser/thr kinase that functions as a cellular energy sensor that becomes activated when the cellular AMP/ATP ratio is increased (Towler and Hardie, 2007) and in recent years has become an attractive pharmacological target for the treatment of insulin resistance and type 2 diabetes. In skeletal muscle, AMPK is activated by exercise/contraction (Musi and Goodyear, 2003), metformin (Zhou et al., 2001; Fryer et al., 2002), and thiazolidinediones (Fryer et al., 2002) resulting in an increase in glucose uptake.

Since insulin resistance is a major metabolic abnormality of type 2 diabetes mellitus, there has been considerable interest in insulin-sensitizing agents to counteract insulin resistance for the treatment of this disease (Moller, 2001). Current therapeutics for diabetes are often associated with undesirable side effects and in many cases the precise mechanism of action remains to be completely clarified (Campbell, 2009). Therapeutic approaches with natural products investigate for searching safe, effective and relatively inexpensive new remedies for diabetes mellitus and associated metabolic disorders (Moller, 2001; Tan et al., 2008). Additionally, the use of natural products for the treatment of metabolic diseases has not been explored in depth despite the fact that a number of modern oral hypoglycemic agents such as

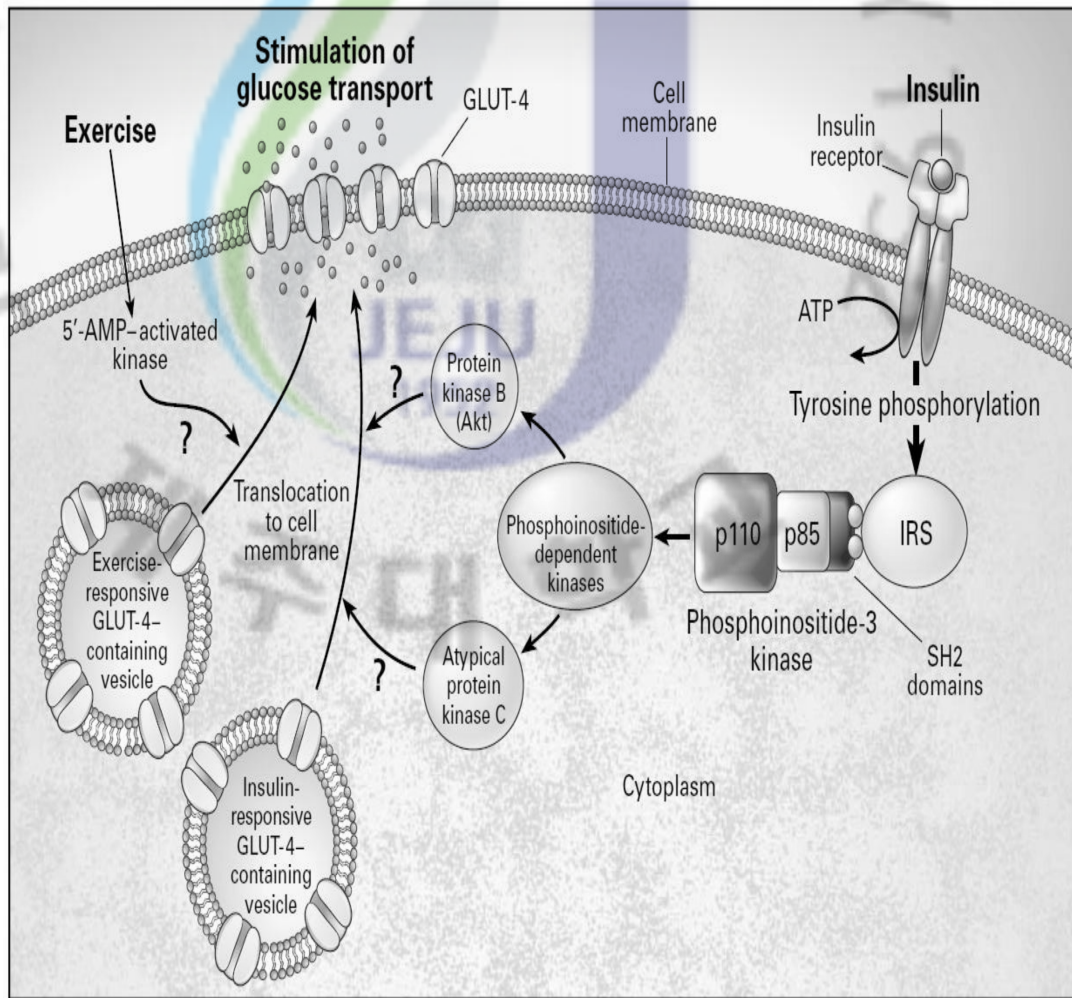


Fig. III. Outline of pathways regulating glucose transport GLUT4 translocation to the plasma membrane in skeletal muscle.

metformin are derivatives of natural products.

The two main forms of diabetes are type 1 and type 2 diabetes. Both types are characterized by progressive β -cell failure. In type 1 diabetes, this is typically caused by an autoimmune assault against the β -cells, inducing progressive β -cell death. The pathogenesis of type 2 diabetes is more variable, comprising different degrees of β -cell failure relative to varying degrees of insulin resistance (**Fig. IV**).

In type 1 diabetes, β -cell mass is reduced by 70–80% at the time of diagnosis. Because of the variable degrees of insulinitis and absence of detectable β -cell necrosis, it was suggested that β -cell loss occurs slowly over years (Kloppel et al., 1985). These pathology findings are in line with the progressive decline in first-phase insulin secretion in antibody-positive individuals, long before the development of overt diabetes (Srikanta et al., 1983). It was later shown that β -cell apoptosis causes a gradual β -cell depletion in rodent models of type 1 diabetes (Eizirik and Mandrup-Poulsen, 2001). In type 2 diabetic subjects, initial pathological studies suggested a β -cell loss of 25–50% (Kloppel et al., 1985; Clark et al., 1988), but this was debated by others (Guiot et al., 2001). A progressive decrease of β -cell function leads to glucose intolerance, which is followed by type 2 diabetes that inexorably aggravates with time (UK Prospective Diabetes Study Group, 1995).

Pancreatic β cell dysfunction performs a crucial function in the pathogenesis of type 2

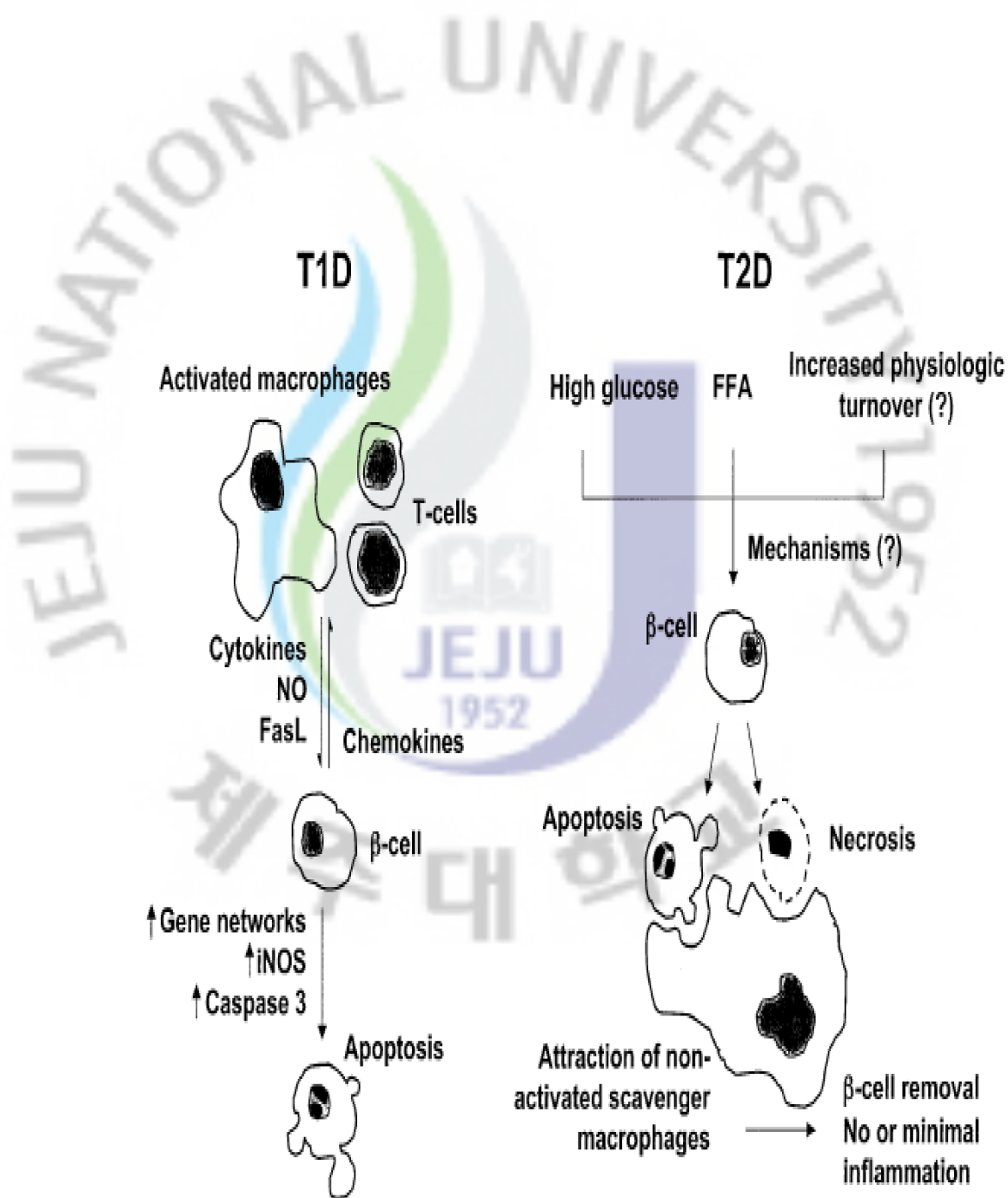


Fig. IV. Overview of the putative sequence of events leading to β -cell death in animal model of type 1 and type 2 diabetes.

diabetes. Although the exact mechanism underlying β cell destruction remains unknown, it has been suggested that the oxidative stress induced by high glucose is one of the major factors contributing to the destruction of pancreatic β cells (Rashied et al., 2010). Several studies have demonstrated that chronic exposure of β cells to high glucose results in β cell dysfunction and apoptosis (Kaneto et al., 2005; Rashid et al., 2010). Under high glucose levels, mitochondria produce excessive amounts of reactive oxygen species (ROS) as they utilize alternative glucose-metabolizing pathways prone to induction of oxidative stress (Robertson, 2004). In addition to increasing the production of ROS by mitochondria, glucose is known to induce an increase in ROS generated by NADPH oxidase in the cell membrane. The results of several studies suggest that antioxidants can prevent the pathological damage induced by the hyperglycemia-induced oxidative stress associated with diabetes (Yokozawa et al., 2007; Lee et al., 2010a). Thus, in order to reduce the risk of pathological damage such as diabetes, it is important to find ways to attenuate the oxidative stress induced by hyperglycemia. There is a great deal of interest in identifying antioxidant compounds that do not cause side effects or exhibit toxicity. The phlorotannins, which constitute one of the most diverse and widespread groups of natural compounds, are probably the most abundant natural phenolics found in marine algae. These compounds exhibit a broad spectrum of chemical and biological activities, including antioxidant properties (Kang et al., 2003; Ahn et

al., 2007; Heo et al., 2009b).

As previously mentioned, currently available drugs for type 2 diabetes have a number of limitations, such as adverse effects and high rates of secondary failure. Therefore, recently, there has been a growing interest in alternative therapies and in the therapeutic use of natural products for diabetes, especially those derived from herbs (Chang et al., 2006; Jung et al., 2007). This is because plant sources are usually considered to be less toxic with fewer side effects than synthetic ones. Marine algae are known to provide an abundance of bioactive compounds with great pharmaceutical foods and biomedical potential.

In previous studies (Heo et al., 2009a; Lee et al., 2010a,b), we isolated dieckol and diphlorethohydroxycarmalol, a type of phlorotannin from the brown algae *Ecklonia cava* and *Ishige okamurae* of Jeju Island, Korea, and demonstrated its anti-diabetic activities in *in vitro* and *in vivo*. However, anti-diabetic effect of marine algae of Jeju Island remains poorly investigated. Therefore, in this study, we tried to screen active compounds from 17 species of brown algae and evaluated anti-diabetic effects of the active compounds which can be as possible nutraceuticals or functional foods for improvement of type 2 diabetes.



Part I .

Screening of α -glucosidase inhibitory and glucose uptake effects of brown seaweeds and isolation of potential anti- diabetic compounds

Part I .

Screening of α -glucosidase inhibitory and glucose uptake effects of brown seaweeds and isolation of potential anti-diabetic compounds

1. ABSTRACT

Anti-diabetic activities of 17 species of the brown algae collected from Jeju Island area were measured by α -glucosidase inhibitory and glucose uptake. A variety of methanol extracts of brown algae showed anti-diabetic activity. Among them, *Ishige sinicola*, *Padina arborescens*, *Sargassum serratifolium* and *Sargassum coreanum* extracts exhibited strong activities both α -glucosidase inhibitory and glucose uptake. For the development of functional food and medical drug materials, reflecting on edibility and collection of raw materials, we selected *I. sinicola*. Therefore, further experiment used *I. sinicola*. Ethyl acetate (EtOAc) fractions of *I. sinicola* extracts showed higher anti-diabetic activities than the other organic solvent fractions. Therefore, the fractions of *I. sinicola* extracts were selected for use in further isolation octaphloretol A (OPA). OPA was isolated from the methanolic extract from *I. sinicola*. This structure was elucidated based on NMR spectroscopic data.

2. MATERIALS AND METHODS

2.1. General experimental procedures

The UV and FT-IR spectra were recorded on a Pharmacia Biotech Ultrospec 3000 UV/Visible spectrometer and a SHIMAZU 8400s FT-IR spectrometer, respectively. NMR spectra were recorded on a Varian INOVA 400 MHz spectrometer. DMSO was used as a solvent for the NMR experiments, and the solvent signals were used as an internal reference. ESI and HREI mass spectra acquired using Finnigan Navigator 30086 and JMS-700 MSTATION high resolution mass spectrometer, respectively. The Preparative HPLC was carried out on a DIONEX prep-HPLC system and Chromeleon software using C₁₈ column (uBondapak RP-18, 19×300 mm, 10 μm, Waters Co.). The HPLC was carried out on a YoungLin Instrument HPLC system equipped with a YoungLin acme 9000 UV/VIS detector and Autochrome software using C₁₈ column (Waters Spherisorb® DOS-2 RP-18, 4.6×250 mm, 5 μm, Waters Co.).

2.2. Materials

Seventeen species of brown algae were collected along the coast of Jeju Island, Korea, between March 2009 and December 2010 (**Table 1-1**). The samples were washed three times with tap water to remove salt, sand, and epiphytes attached to the surface, then carefully

rinsed with fresh water, and maintained in a medical refrigerator at -20°C . Therefore, the frozen samples were lyophilized and homogenized with a grinder prior to extraction.

2.3. Extraction procedure of 80% methanolic extracts from brown algae

The brown algae samples were pulverized into powder using a grinder. The algae powder (1 g) was extracted with 80% methanol (100 ml) at a room temperature for 24 h and filtrated. After filtration, the methanolic extracts were evaporated to dryness under vacuum. This extracts were used for further biological study.

2.4. Inhibition assay for α -glucosidase activity

The α -glucosidase inhibitory assay was done by the chromogenic method described by Watanabe et al. (1997) using a readily available yeast enzyme. Briefly, yeast α -glucosidase (0.7 U, Sigma) was dissolved in 100 mM phosphate buffer (pH 7.0) containing 2 g/l bovine serum albumin and 0.2 g/l NaN_3 and used as an enzyme solution. 5 mM p-Nitrophenyl- α -D-glucopyranoside in the same buffer (pH 7.0) was used as a substrate solution. The 50 μl of enzyme solution and 10 μl of sample dissolved in dimethylsulfoxide were mixed in a microtiter plate and measured absorbance at 405 nm at zero time. After incubation for 5 min, substrate solution (50 μl) was added and incubated for another 5 min at room temperature.

Table 1-1. The list and polyphenol content of brown algae.

No.	Scientific name (Korean name)	Polyphenol content (mg/g)
BS1	<i>Dictyota coriacea</i> (참가죽그물바탕말)	10.35
BS2	<i>Sargassum thunbergii</i> (지충이)	23.94
BS3	<i>Myelophycus caespitosus</i> (바위수염)	40.23
BS4	<i>Ishige sinicola</i> (넓괘)	42.82
BS5	<i>Padina arborescens</i> (부챗말)	44.52
BS6	<i>Hizikia fusiforme</i> (돛)	13.35
BS7	<i>Undaria pinnatifida</i> (미역)	14.53
BS8	<i>Sargassum serratifolium</i> (큰톱니모자반)	38.52
BS9	<i>Sargassum horneri</i> (괘쟁이모자반)	25.11
BS10	<i>Sargassum hemiphyllum</i> (작잎모자반)	11.35
BS11	<i>Sargassum piluiferum</i> (구슬모자반)	13.94
BS12	<i>Sargassum patens</i> (짱발이모자반)	25.29
BS13	<i>Sargassum tortile</i> (파배기모자반)	22.35
BS14	<i>Sargassum macrocarpum</i> (큰열매모자반)	14.53
BS15	<i>Myagropsis myagroides</i> (외톨개모자반)	15.70
BS16	<i>Undariopsis peterseniana</i> (넓미역)	13.12
BS17	<i>Sargassum coreanum</i> (큰잎모자반)	67.93

The increase in the absorbance from zero time was measured. Percent inhibitory activity was expressed as 100 minus relative absorbance difference (%) of test compounds to absorbance change of the control where test solution was replaced by carrier solvent.

2.5. Cell culture

Rat myoblast L6 cells were maintained in high glucose-DMEM supplemented with 10% heat-inactivated FBS, penicillin (100 U/ml) and streptomycin (100 µg/ml). Cultures were maintained at 37°C in 5 % CO₂ incubator. For differentiation, the cells were seeded in appropriate culture plates, and after sub-confluence (about 80%), the medium was changed to DMEM containing 2% horse serum for 7 days, with medium changes every day. All experiments were performed in differentiated L6 myotubes after 7 days.

2.6. Glucose uptake assay

L6 cells were seeded in a 24-well plate. After differentiation, the cells were starved in serum-free low glucose DMEM for 12 h, and then washed with PBS and incubated with fresh serum-free low glucose DMEM. After that, the cells were treated without or with 100 µg/ml of samples for 3 h. Glucose uptake was measured by glucose concentration in the media solution using glucose oxidase assay kit (Asan Pharmaceutical corp., Korea).

2.7. Extraction and isolation of octaphlorethol A (OPA)

The dried *Ishige sinicola* (Fig. 1-1) powder was extracted three times with 80% aqueous MeOH, and filtered. The filtrate evaporated at 40 °C to obtain the MeOH extract, which was dissolved in water, then partitioned with EtOAc. The EtOAc extract was fractionated by silica column chromatography with stepwise elution of CHCl₃-MeOH mixture (50:1-0:1) to afford separated active fractions. A combined active fraction was further subjected to prep-HPLC, and then finally purified by reversed-phase HPLC to give novel compound octaphlorethol A (OPA) (Fig. 1-10).

Octaphlorethol A (OPA): brownish yellow amorphous powder, ¹H NMR (400 MHz, DMSO-*d*₆) and ¹³C NMR (100 MHz, DMSO-*d*₆), see Table 1-2; ESI-MS *m/z* 992.19 [M-2H]²⁻ (C₄₈H₃₄O₂₅: 994.14389).

2.8. Statistical analysis

The data are presented as mean ± standard error (SE). Statistical comparison was performed via the SPSS package for Windows (Version 14). P-values of less than 0.05 were considered to be significant.

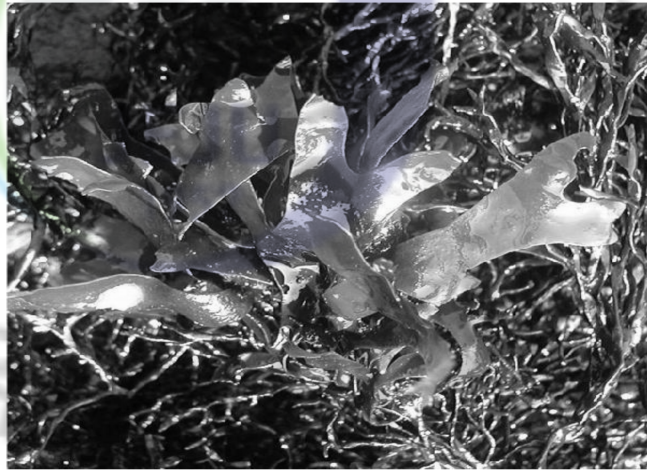


Fig. 1-1. The photography of a brown alga *Ishige sinicola*.

3. RESULTS AND DISCUSSIONS

Currently available drugs for type 2 diabetes have a number of limitations, such as adverse effects and high rates of secondary failure. Therefore, recently, there has been a growing interest in alternative therapies and in the therapeutic use of natural products for diabetes, especially those derived from herbs (Chang et al., 2006; Jung et al., 2007). This is because plant sources are usually considered to be less toxic with fewer side effects than synthetic ones. Marine algae are known to provide an abundance of bioactive compounds with great pharmaceutical foods and biomedical potential.

In previous studies (Heo et al., 2009a; Lee et al., 2010a,b), we isolated dieckol and diphlorethohydroxycarmalol, a type of phlorotannin isolated from the brown algae *Ecklonia cava* and *Ishige okamurae* of Jeju Island, Korea, and demonstrated its anti-diabetic activities in *in vitro* and *in vivo*. However, anti-diabetic effect of marine algae of Jeju Island remains poorly investigated. Therefore, in this study, we tried to screen active compounds from 17 species of brown algae and evaluated anti-diabetic effects of the active compounds which can be as possible nutraceuticals or functional foods for improvement of type 2 diabetes.

α -Glucosidase is one of the glucosidases located within the brush-border surface membranes of intestinal cells, and is a key enzyme in carbohydrate digestion (Lebovitz, 1997). Similarly, α -amylase catalyzes the hydrolysis of α -1,4-glucosidic linkages of starch,

glycogen, and a variety of oligosaccharides, and α -glucosidase further degrades the disaccharides into simpler sugars, which are readily available for intestinal absorption. The inhibition of their activity in the human digestive tract, is regarded as an effective method for the control of diabetes by diminishing the absorption of glucose decomposed from starch by these enzymes (Hara and Honda, 1990). The inhibitory effect of α -glucosidase by brown algae extracts was presented in **Fig. 1-2**. It was observed that *Sargassum coreanum* (BS17) extract showed the highest α -glucosidase inhibitory effect (86.77%), and *Myelophycus caespitosus* (BS3), *Ishige sinicola* (BS4), *Padina arborescens* (BS5), and *Sargassum serratifolium* (BS8) extracts also had 68.28, 77.66, 82.28, and 78.98% α -glucosidase inhibitory effects, respectively. A relationship between polyphenolic compound and α -glucosidase inhibitory effect in marine algae has been reported (Kim et al., 2008; Heo et al., 2009a; Lee et al., 2010a). Polyphenolic compounds such as tannins from terrestrial plants and phlorotannins from marine algae associate with a variety of proteins to form complexes. The results of several recent studies have demonstrated that the hydroxyl groups in polyphenolic compounds may, therefore, perform a crucial function in promoting inhibitory activity (Stern et al., 1996; Kim et al., 2008). Also, this study showed that brown algae with

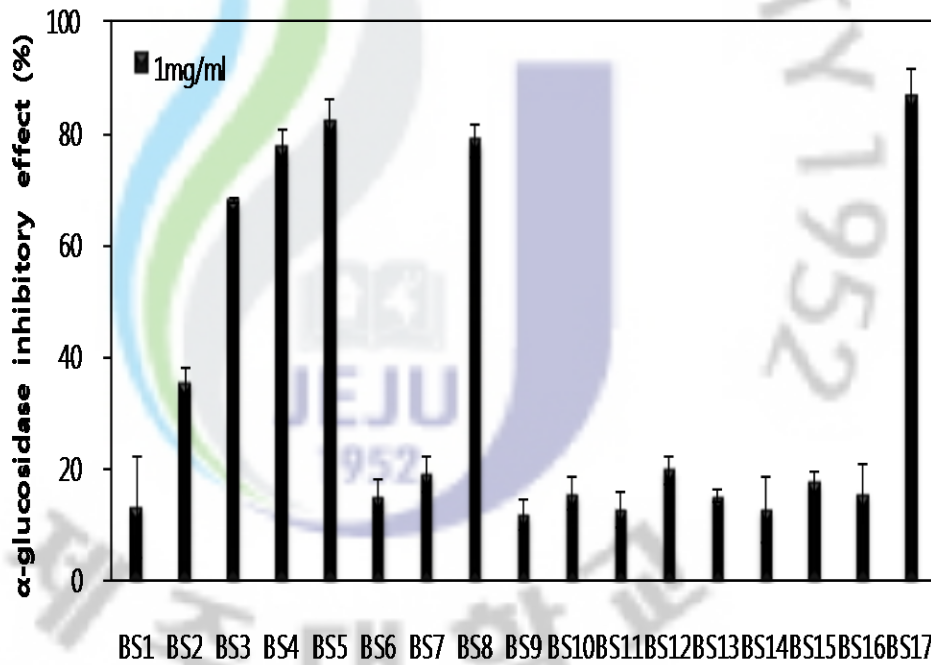


Fig. 1-2. α -glucosidase inhibitory effect of 80% MeOH extracts from brown algae.

Experiments were performed in triplicate and the data are expressed as mean \pm SE.

high amount polyphenol displayed higher % α -glucosidase inhibitory effect (**Table 1-1** and **Fig. 1-2**).

Skeletal muscle has been identified as the major tissue in glucose metabolism, accounting for nearly 75% of whole-body insulin-stimulated glucose uptake (DeFronzo et al., 1981). Insulin-stimulated glucose uptake in skeletal muscle is critical for reducing blood glucose levels. Failure of glucose uptake due to decreased insulin sensitivity leads to the development of type 2 diabetes. The effect of glucose uptake by brown algae extracts was presented in **Fig. 1-3**. It was observed that extracts of *Ishige sinicola* (BS4), *Padina arborescens* (BS5), *Sargassum serratifolium* (BS8) and *Sargassum coreanum* (BS17) exhibited higher effects of glucose uptake. Several reports have recently described the ability to glucose uptake effect on marine algae (Cherng and Shih, 2006; Kang et al., 2008). These researches indicated that marine algae could be used to potential antidiabetes and pharmaceutical industries.

In this study, we are screened anti-diabetic effects of brown algae extracted by 80% methanol to find antidiabetic compounds from brown algae. Among these results, *I. sinicola*, *P. arborescens*, *S. serratifolium* and *S. coreanum* showed relatively higher effects both α -glucosidase inhibitory and glucose uptake than the other brown algae. For the development of functional food and medical drug materials, reflecting on edibility and collection of raw

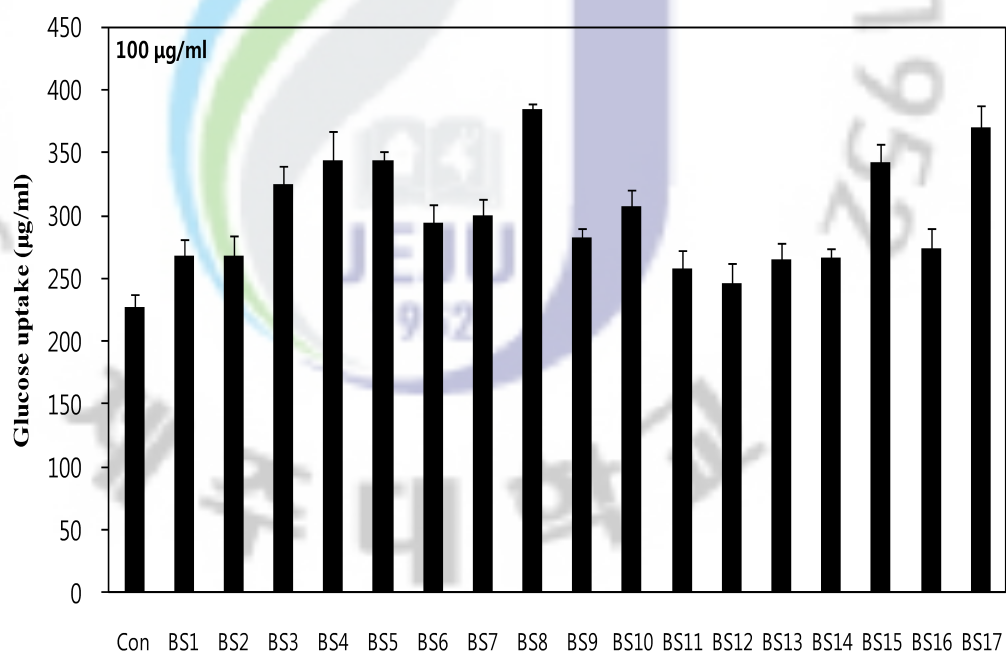


Fig. 1-3. Glucose uptake effect of 80% MeOH extracts from brown algae.

Experiments were performed in triplicate and the data are expressed as mean \pm SE.

materials, we selected *I. sinicola*. Therefore, *I. sinicola* was partitioned with hexane, CHCl₃, EtOAc and BuOH to find bioactive compounds and the anti-diabetic effects were investigated. The anti-diabetic effects of the organic solvent fractions on α -glucosidase inhibitory and glucose uptake were shown in **Fig. 1-4**. The 80% methanol extracts were successfully partitioned according to their polarity. It was observed that EtOAc fraction exhibited the highest effects both α -glucosidase inhibitory and glucose uptake compared to the other organic solvent fractions. Therefore, the fractions of *I. sinicola* extracts were selected for use in further isolation antidiabetic compounds.

As the EtOAc extract showed prominent anti-diabetic effects, the active compound of this extract was fractionated by silica gel open column chromatography and prep-HPLC, and then finally novel active compound were purified by reversed-phase HPLC (**Fig. 1-5**). Octaphlorethol A (OPA) was isolated as a brownish yellow amorphous powder, and its molecular formula deduced as C₄₈H₃₄O₂₅ based on NMR (**Table 1-2 and Fig. 1-6, 7**) and ESI-MS analyses (M-2H²⁺, *m/z*: 994.14389) (**Fig. 1-8**). The OPA was then used in further experiments regarding on antidiabetic agent and nutraceuticals

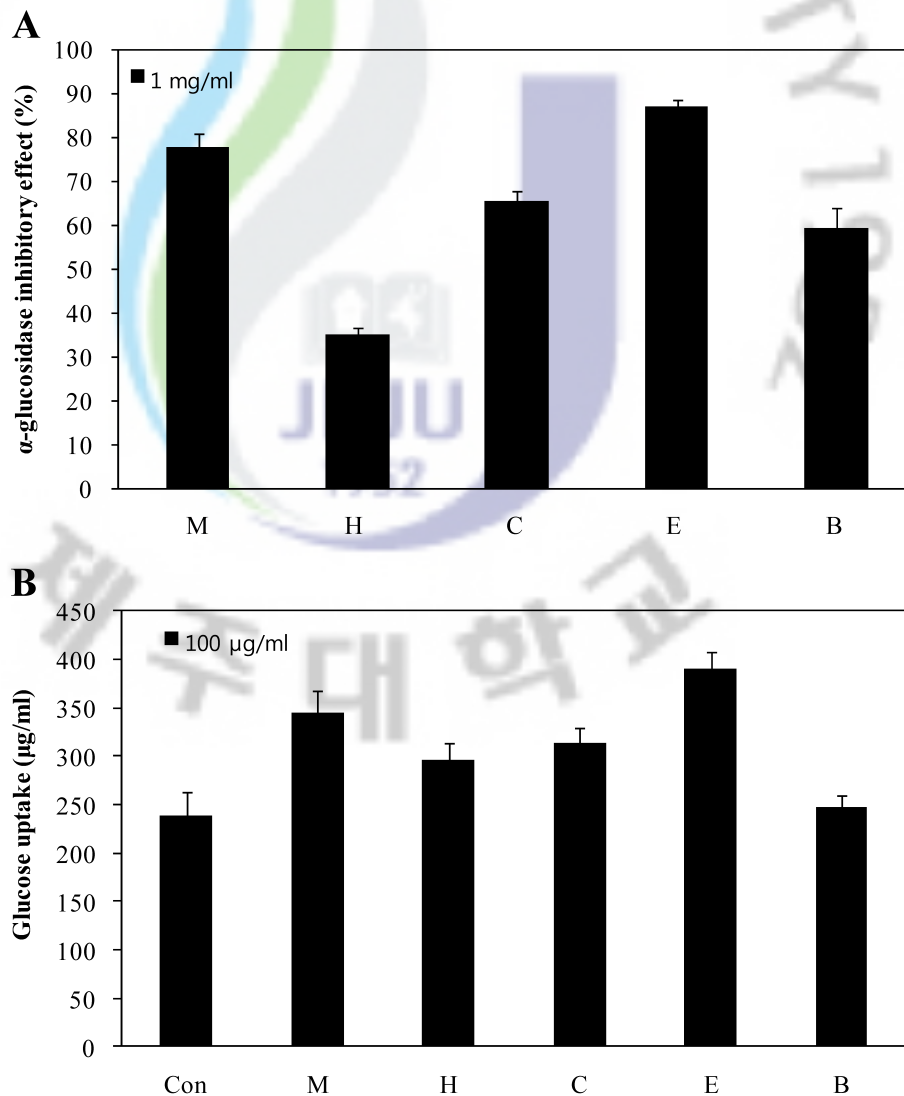


Fig. 1-4. α -glucosidase inhibitory (A) and glucose uptake (B) effect of *I. Sinicola* extracts partitioned by various organic solvents. M, 80% MeOH extract; H, Hexane; C, CHCl₃; E, EtOAc; B, BuOH. Experiments were performed in triplicate and the data are expressed as mean \pm SE.

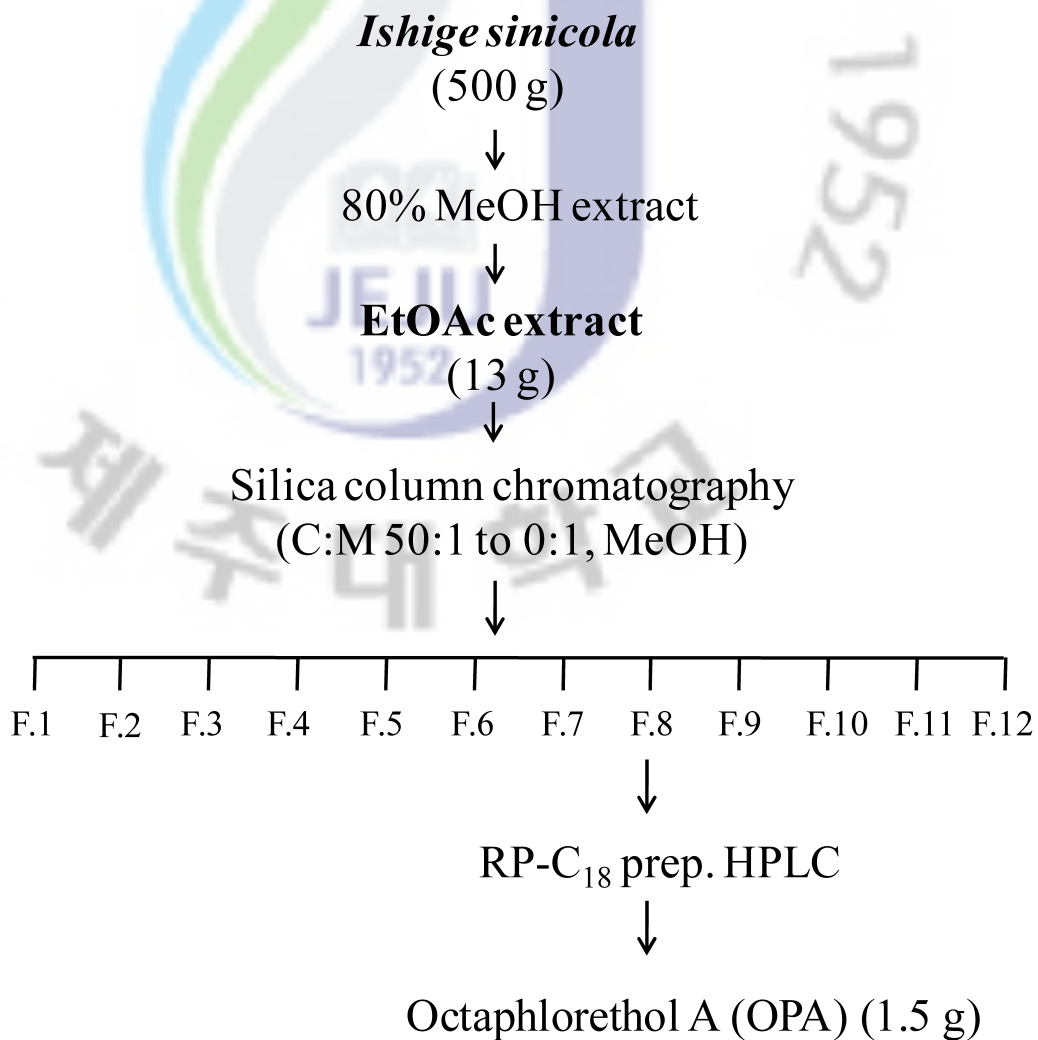


Fig. 1-5. Isolation scheme of octaphlorethol A (OPA) from *I. sinicola*.

Table 1-2. ^1H and ^{13}C NMR assignments for octaphlorethol A (OPA).

Position	^{13}C	^1H (mult. $J=\text{Hz}$)
1	93.9	5.58 (0.21H, d, $J=2.76$)
2	94.0	5.60 (0.48H, s)
3	94.1	5.68 (0.23H)
4	94.6	5.72 (0.2H)
5	94.8	5.81 (0.15H, t)
6	122.0	5.95 (0.27H, d, $J=1.84$)
7	123.3	6.16 (1H, d, $J=1.6$)
8	123.4	
9	123.5	
10	150.8	
11	151.1	
12	152.6	
13	152.7	
14	152.8	
15	152.9	
16	154.0	
17	154.1	
18	154.5	
19	156.1	
20	156.2	
22	158.6	
23	161.0	

* 400 MHz for ^1H and 100 MHz for ^{13}C

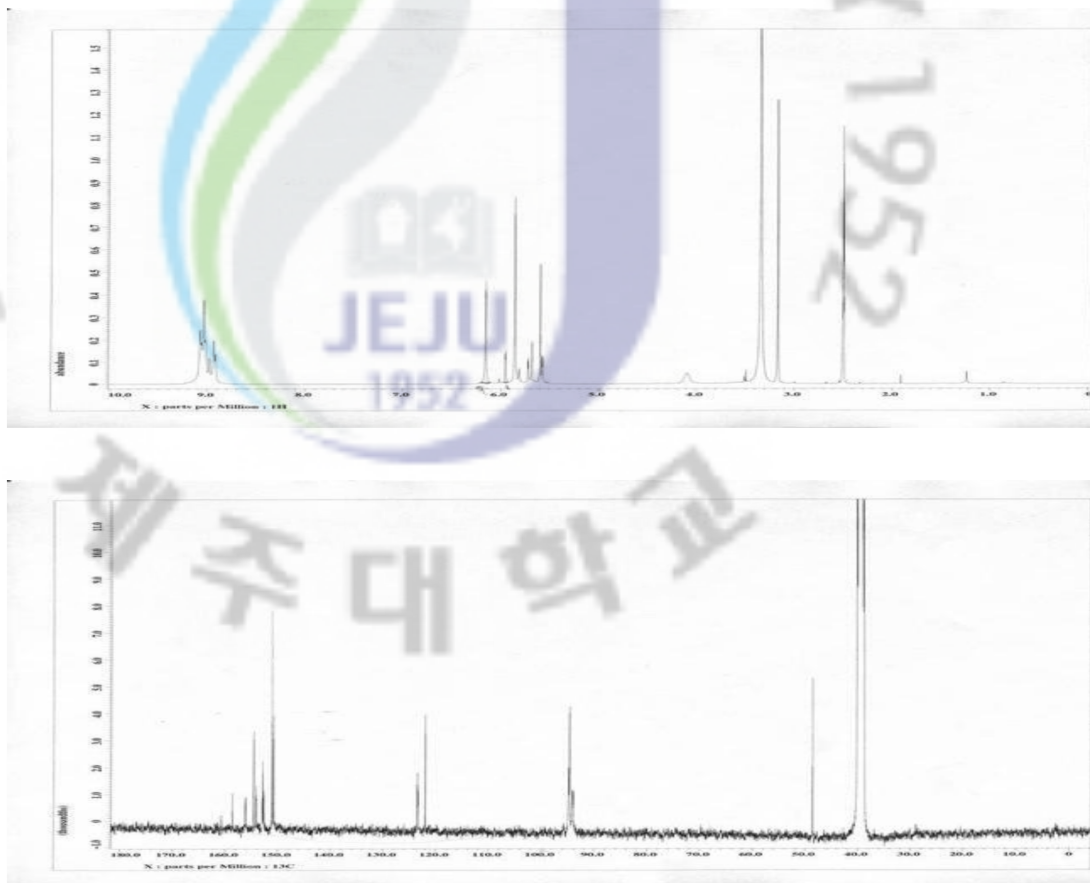


Fig. 1-6. Proton and Carbon NMR spectrum of octaphloretol A (OPA).

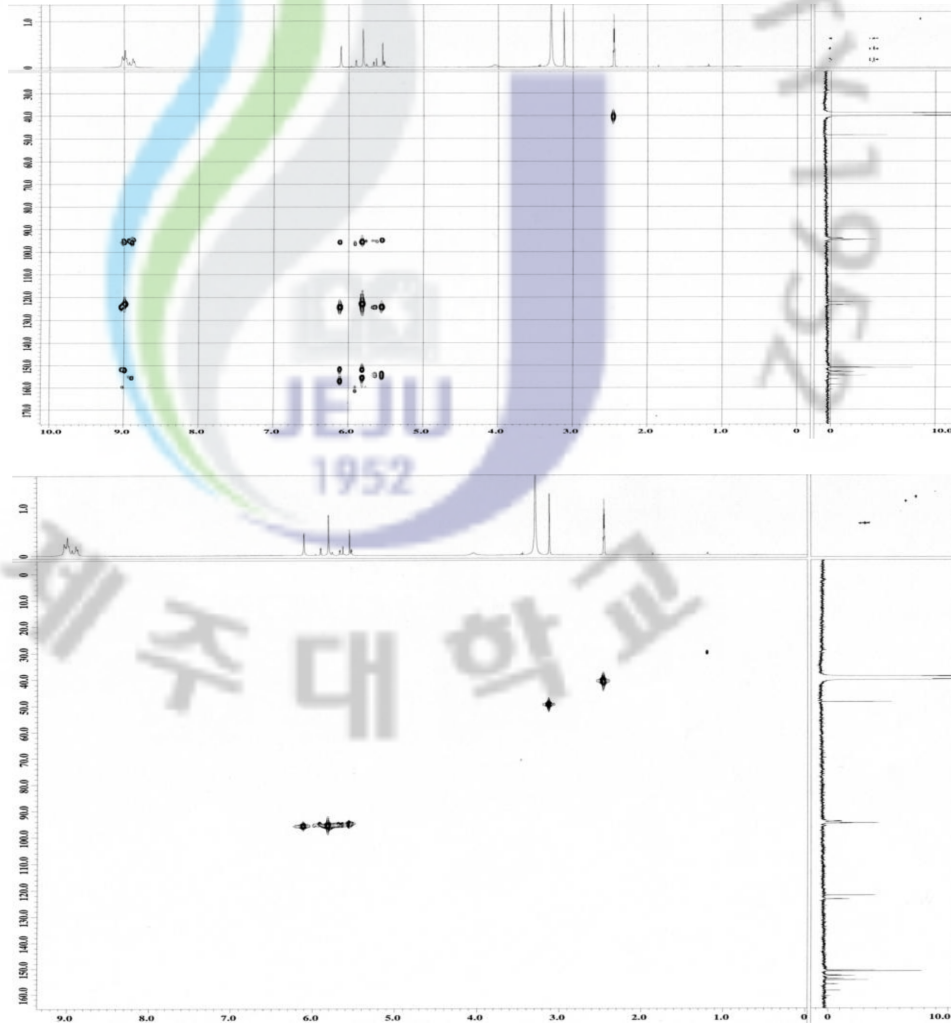


Fig. 1-7. Gradient HMBC and HMQC NMR spectrum of octaphloretol A (OPA).

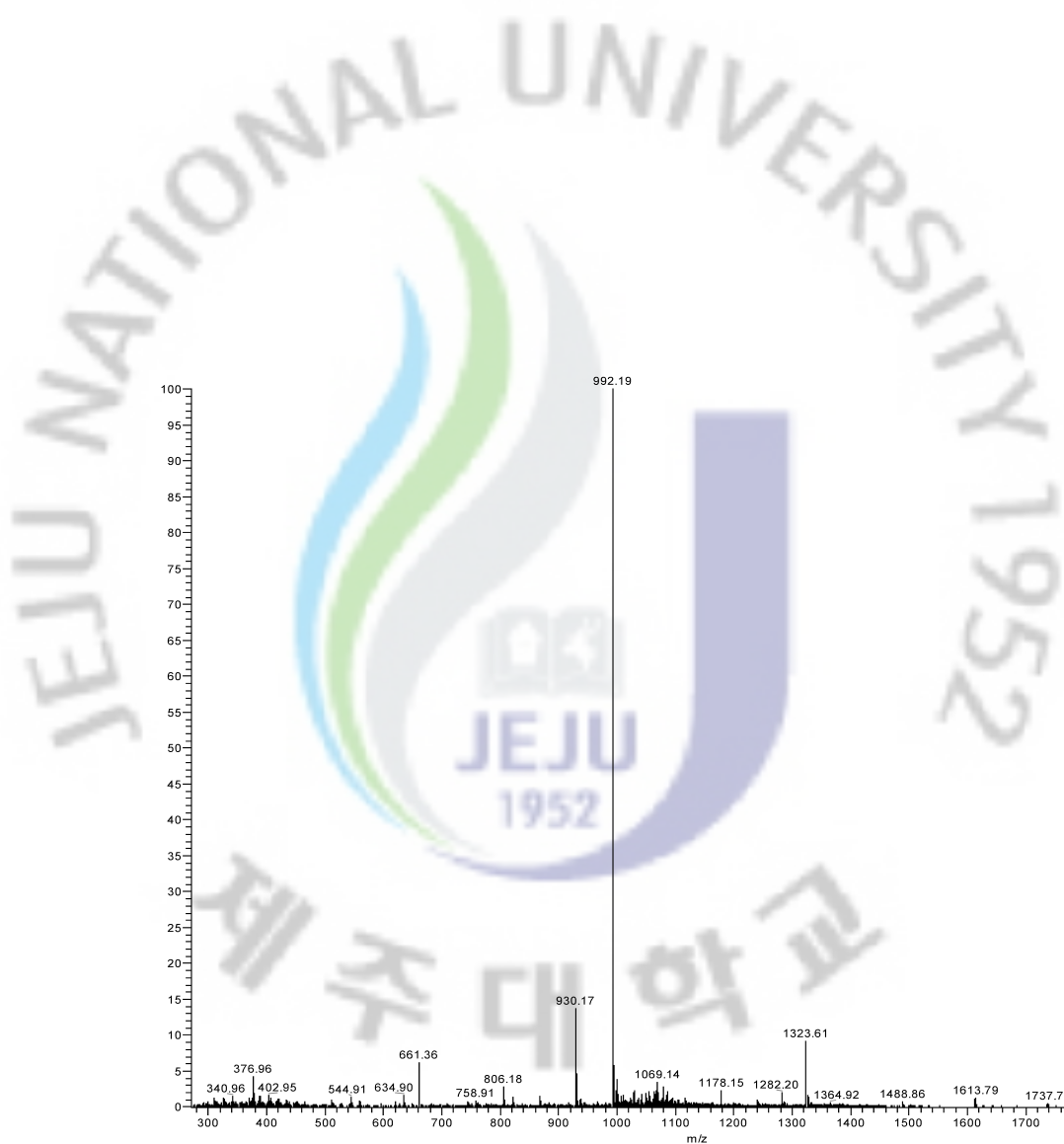
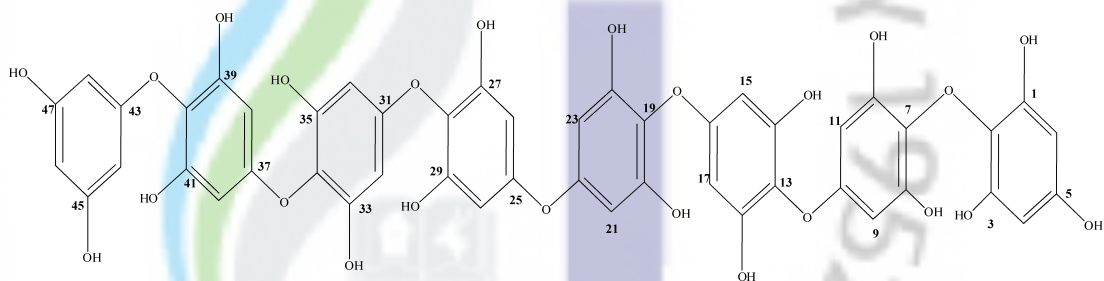


Fig. 1-8. MS spectrum of octaphloretol A (OPA).



2-(4-(4-(4-(4-(4-(4-(3,5-dihydroxyphenoxy)-3,5-dihydroxyphenoxy)-3,5-dihydroxyphenoxy)-3,5-dihydroxyphenoxy)-2,6-dihydroxyphenoxy)-2,6-dihydroxyphenoxy)-2,6-dihydroxyphenoxy)benzene-1,3,5-triol

Fig. 1-9. Chemical structure of octaphloretol A (OPA).



Part II.

Octaphlorethol A isolated from *Ishige sinicola* inhibits α -glucosidase and α -amylase *in vitro* and alleviates hyperglycemia in diabetic mice

Part II.

Octaphlorethol A isolated from *Ishige sinicola* inhibits α -glucosidase and α -amylase *in vitro* and alleviates hyperglycemia in diabetic mice

1. ABSTRACT

This study was designed to investigate whether octaphlorethol A (OPA) may inhibit α -glucosidase and α -amylase activities, and alleviate hyperglycemia in diabetic mice. OPA isolated from *Ishige sinicola*, a brown algae, evidenced prominent inhibitory effect against α -glucosidase and α -amylase. The IC_{50} values of OPA against α -glucosidase and α -amylase were 0.11 and 0.34 mg/ml, respectively, which evidenced the higher activities than that of acarbose. The increase of postprandial blood glucose levels were significantly suppressed in the OPA administered group than those in the streptozotocin-induced diabetic or normal mice. Also, the area under curve (AUC) was significantly reduced via OPA administration (907 versus 1034 mg·h/dl) in the diabetic mice as well as it delays absorption of dietary carbohydrates. Moreover, an intraperitoneal glucose tolerance test (IPGTT) was evaluated to determine the effects of OPA administration on glucose tolerance. In that result, the blood glucose levels of the OPA administered mice was significantly lower than the control group

and it was almost similar to that of metformin administered mice. Finally, the anti-diabetic effects of OPA was investigated in C57BL/KsJ-*db/db* (*db/db*), type 2 diabetic mice. The administration of OPA significantly lowered the blood glucose levels and plasma insulin levels compared to the control *db/db* mice. These results suggest that OPA might be developed into medicinal preparations, nutraceuticals, or functional foods for diabetes, and may also be applied in other therapeutic fields.

2. MATERIAL AND METHODS

2.1. Materials

α -glucosidase, p-Nitrophenyl- α -D-glucopyranoside, porcine pancreatic amylase, p-Nitrophenyl- α -D-maltopentoglycoside, streptozotocin, acarbose and metformin were obtained from Sigma Chemical Co. (St. Louis, Mo, USA). All others chemicals and reagents used were of analytical grade and obtained from commercial sources.

2.2. Inhibitory effect of OPA on α -glucosidase and α -amylase *in vitro*

The α -glucosidase inhibitory assay was done by the chromogenic method described by Watanabe et al. (1997) using a readily available yeast enzyme. Briefly, yeast α -glucosidase (0.7 U) was dissolved in 100 mM phosphate buffer (pH 7.0) containing 2 g/l bovine serum albumin and 0.2 g/l NaN_3 and used as an enzyme solution. 5 mM p-Nitrophenyl- α -D-glucopyranoside in the same buffer (pH 7.0) was used as a substrate solution. The 50 μl of enzyme solution and 10 μl of sample dissolved in dimethylsulfoxide were mixed in a microtiter plate and measured absorbance at 405 nm at zero time. After incubation for 5 min, substrate solution (50 μl) was added and incubated for another 5 min at room temperature. The increase in the absorbance from zero time was measured. The α -amylase inhibitory activity was assayed in the same way as described for α -glucosidase inhibitory assay except

the using of porcine pancreatic amylase (100 U) and blocked p-Nitrophenyl- α -D-maltopentoglycoside as enzyme and substrate, respectively. Percent inhibitory activity was expressed as 100 minus relative absorbance difference (%) of test compounds to absorbance change of the control where test solution was replaced by carrier solvent.

2.3. Experimental animals

Male ICR mice (4 weeks of age; purchased from Joong Ang Lab Animal Co., Korea) were used. All animals were housed individually in a light- (12 h on/12 h off) and temperature-controlled room with food and water available ad libitum. The animals were maintained with pelleted food, while tap water was available ad libitum. After an adjustment period of approximately 2 weeks, diabetes was induced by intraperitoneal injection of streptozotocin (150 mg/kg i.p.) dissolved in a freshly prepared citrate buffer (0.1 M, pH 4.5). Tail bleeds were performed and animals with a blood glucose concentration above 300 mg/dl were considered to be diabetic.

2.4. Measurement of postprandial blood glucose level

Normal mice and streptozotocin-induced diabetic mice fasted overnight were randomly divided into four groups. Fasted animals were deprived of food for at least 12 h but allowed

free access to water. After overnight fasting, the mice were administered orally soluble starch (2 g/kg body weight) alone or with OPA (100 mg/kg body weight) or acarbose (100 mg/kg body weight) and metformin (100 mg/kg body weight). Blood samples were taken from the tail vein at 0, 30, 60, 90, and 120 min (Kim, 2004). Blood glucose was measured using a glucometer (Roche Diagnostics GmbH, Germany). Areas under the curve (AUC) were calculated using the trapezoidal rule.

2.5. Intraperitoneal glucose tolerance test (IPGTT)

An intraperitoneal glucose tolerance test (IPGTT) was performed in the same way as described for postprandial blood glucose level assay except the using of intraperitoneally injected glucose. Following an overnight fast, the mice were injected intraperitoneally glucose (1 g/kg body weight) alone or with OPA (100 mg/kg body weight) or acarbose (100 mg/kg body weight) and metformin (100 mg/kg body weight). The blood glucose levels were determined in tail blood samples 0, 30, 60, 90, and 120 min after the glucose administration.

2.6. Type 2 diabetic mice and experimental design

Male C57BL/KsJ-*db/db* (*db/db*) mice (4 weeks of age; purchased from Joong Ang Lab Animal Co., Korea) were used. All animals were housed individually in a light- (12h on/12h

off) and temperature-controlled room with food and water available ad libitum. The animals were maintained with pelleted food, while tap water was available ad libitum. After an adjustment period of approximately 4 weeks. To determine the effects of OPA, mice were divided into the following groups; 1) non-treated normal group, 2) OPA (2.5 mg/kg B.W) group, 3) OPA (5 mg/kg B.W), and treated with OPA by intraperitoneal injection once per day for 2 weeks. During the experiment, body weight and blood glucose levels were measured every two days. The levels of plasma insulin were determined using radioimmunoassay with enzyme-linked immunosorbent assay ELISA kit (Linco Research Inc, Billerica, MA, USA).

2.7. Statistical analysis

The data are presented as mean \pm standard error (SE). Statistical comparison was performed via the SPSS package for Windows (Version 14). P-values of less than 0.05 were considered to be significant.

3. RESULT

3.1. Inhibitory effect of OPA on α -glucosidase and α -amylase *in vitro*

The inhibitory effect of OPA against α -glucosidase was determined using p-Nitrophenyl- α -glucopyranoside (pNPG) as a substrate. OPA inhibited α -glucosidase activity in a dose-dependent manner as 35.6, 54.2, 70.9, and 83.4% at the concentrations of 0.0625, 0.125, 0.25, and 0.5 mg/ml, respectively (**Fig. 2-1A**). Moreover, the OPA evidenced more effective than that of acarbose even at the low concentration (0.25 mg/ml). The α -amylase inhibitory effect of OPA was also illustrated using p-Nitrophenyl- α -maltopenotoglycoside (pNPM) as a substrate. Both activities were compared with a commercial inhibitor, acarbose. The inhibitory effect of OPA against α -amylase was dose-dependent and the increment was 16.55, 32.49, 48.78, and 61.92% at the concentrations of 0.0625, 0.125, 0.25, and 0.5 mg/ml, respectively (**Fig. 2-1B**). IC_{50} values of OPA against α -glucosidase and α -amylase were 0.11 and 0.34 mg/ml, respectively, which were evidenced stronger inhibitory effect than was observed with acarbose (**Table 2-1**).

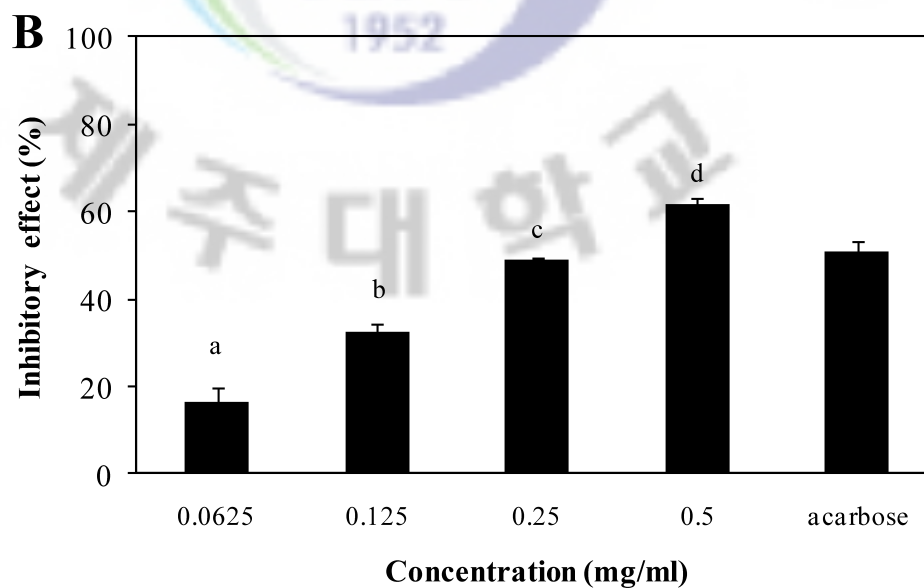
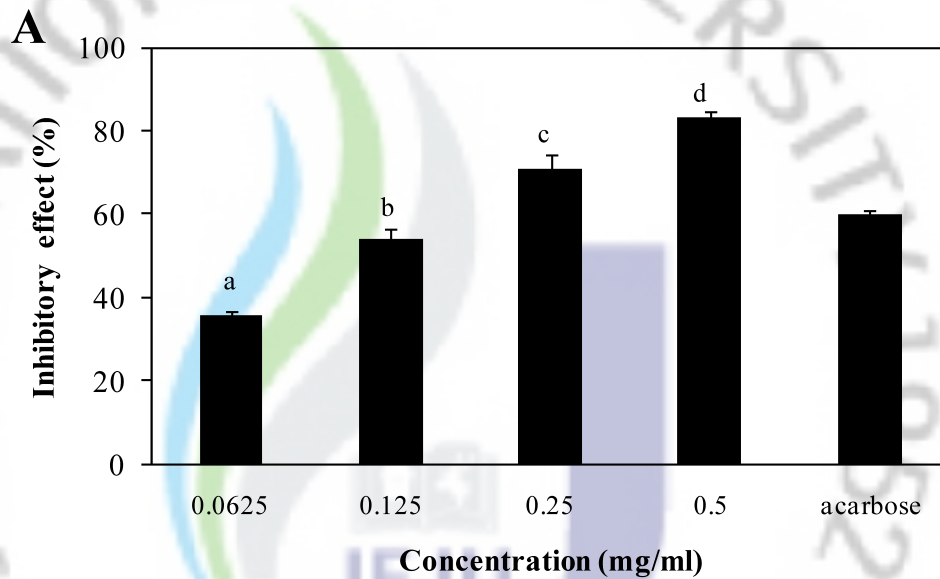


Fig. 2-1. Inhibitory effects OPA isolated from *I. sinicola* on α -glucosidase (A) and α -amylase (B). Inhibitory effects were determined using pNPG and pNPM as substrates, respectively, and acarbose was employed as a positive control. Values are expressed as means \pm S.E. in triplicate experiments. ^{a-d}Values with different alphabets are significantly different at $P < 0.05$ as analyzed via Duncan's multiple range test. The final concentration of acarbose is 0.5 mg/ml.

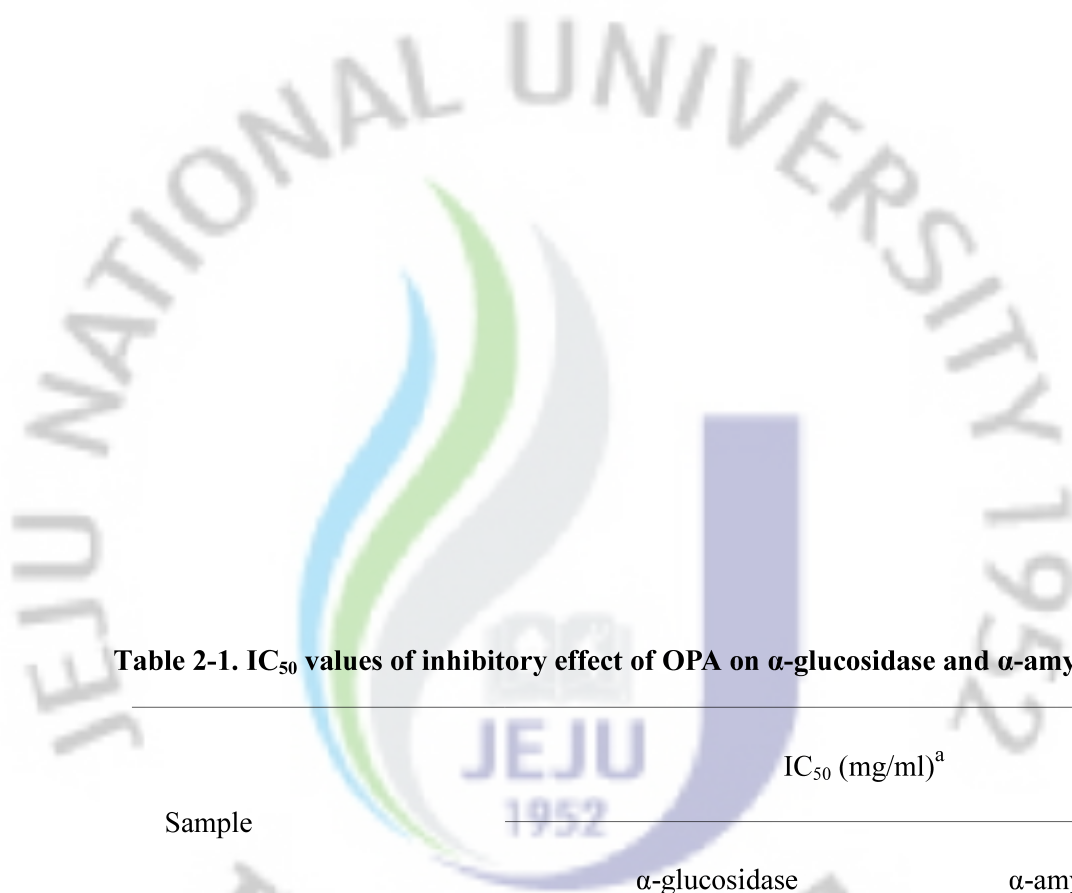


Table 2-1. IC₅₀ values of inhibitory effect of OPA on α -glucosidase and α -amylase.

Sample	IC ₅₀ (mg/ml) ^a	
	α -glucosidase	α -amylase
Acarbose	0.19±0.03	0.47±0.07
OPA	0.11±0.05*	0.34±0.06*

^a IC₅₀ value is the concentration of sample required for 50% inhibition. Each value is expressed as mean ± S.E. in triplicate experiments. Significantly different from control at *P<0.05.

3.2. Effect of OPA on postprandial blood glucose level *in vivo*

The effect of OPA on blood glucose level after a meal was investigated in streptozotocin-induced diabetic and normal mice. Postprandial blood glucose level of the administered OPA were lower than those of the control in diabetic mice (**Fig. 2-2A**). The blood glucose level increased until 37% at 30 min after a meal, and decreased thereafter. However, the increase in postprandial blood glucose level was significantly suppressed when the mice was fed after the administration of OPA as 14, 11, 6, and 2% at 30, 60, 90, and 120 min, respectively. The postprandial blood glucose level was also significantly decreased when the normal mice were orally administered with starch together with OPA (**Fig. 2-2B**). In normal mice, OPA significantly suppressed the postprandial hyperglycemia caused by starch. In addition, the blood glucose level of the OPA administered group was significantly lower than those of both the streptozotocin-induced diabetic and the normal mice administered with metformin and it was almost similar to that of acarbose administered mice. The area under curve (AUC) for glucose response of OPA administered group (907 ± 83.5 mg·h/dl) was significantly lower than that of the control group (1034 ± 135.8 mg·h/dl) and similar to the acarbose group (901 ± 70.7 mg·h/dl) in the diabetic mice (**Table 2-2**). The AUC in normal mice corroborated the hyperglycemia effect of OPA.

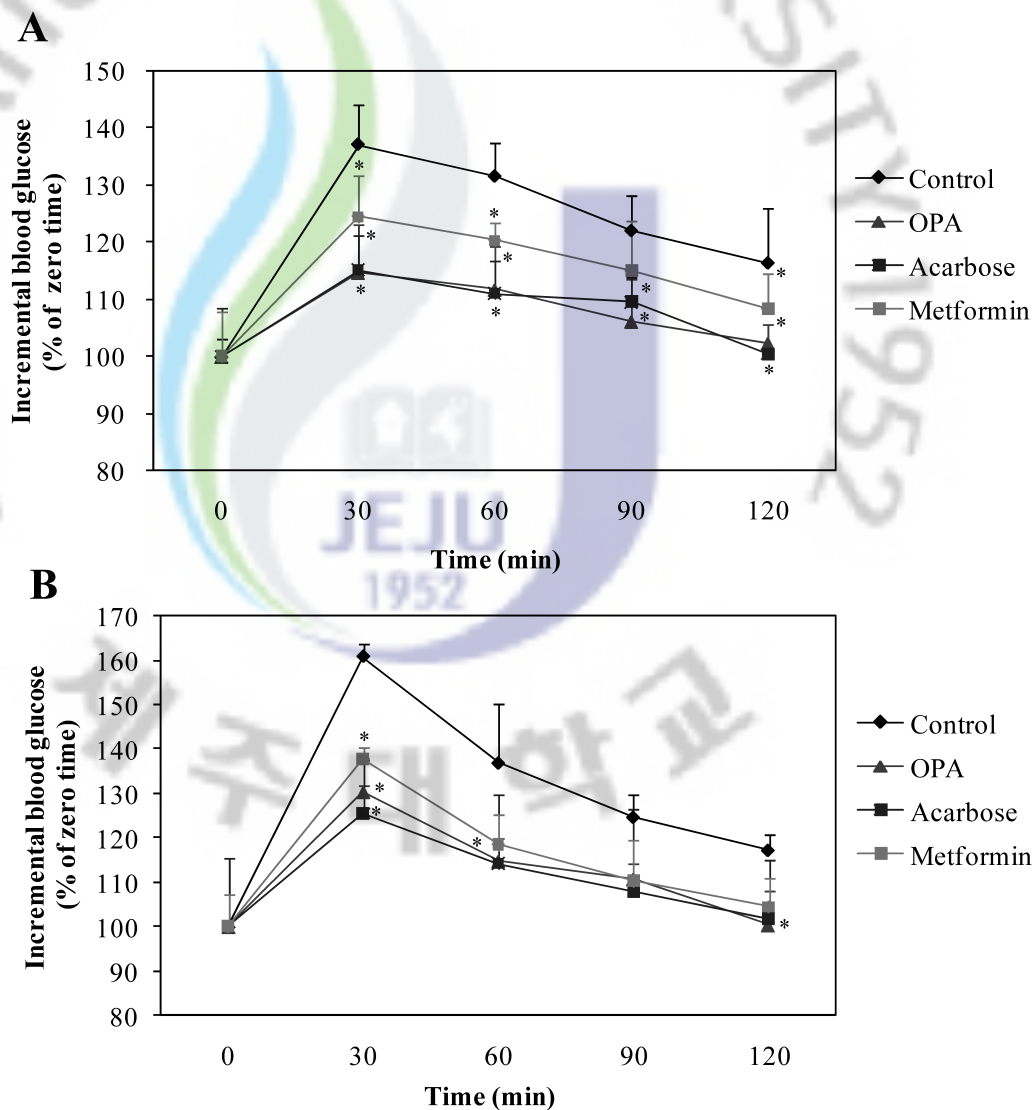


Fig. 2-2. Blood glucose levels after the administration of OPA in streptozotocin-induced diabetic mice (A) and normal mice (B). Control (distilled water), OPA (100 mg/kg), acarbose (100 mg/kg) and metformin (100 mg/kg) were co-administered orally with starch (2 g/kg). Each value is expressed as mean \pm S.D. of six mice (n=48). Significantly different from control at *P<0.05.

Table 2-2. Area under curve (AUC) of postprandial glucose responses of normal and streptozotocin-induced diabetic mice.^a

Group ¹⁾	AUC (mg·h/dl)	
	Normal mice	Diabetic mice
Control	392.9±43.8 ^a	1034.8±135.8 ^a
OPA	325.1±25.5 ^{cd}	907.8±83.5 ^c
Acarbose	307.9±26.9 ^d	901.7±70.7 ^c
Metformin	344.4±35.3 ^b	921.0±99.5 ^b

¹⁾ Control (distilled water), OPA (100 mg/kg), acarbose (100 mg/kg) and metformin (100 mg/kg) were co-administered orally with starch (2 g/kg body weight). Each value is expressed as mean ± S.E. of six mice (n=48). ^{a-d}Values with different alphabets are significantly different at P<0.05 as analyzed via Duncan's multiple range test.

3.3. Intraperitoneal glucose tolerance test (IPGTT)

The effect of OPA on blood glucose level after glucose injection was investigated in streptozotocin-induced diabetic and normal mice. The administration of OPA improved the glucose tolerance in the streptozotocin-induced diabetic and normal mice (**Fig. 2-3A and B**).

When the mice were first injected with glucose, the rate of increase in the blood glucose level was the same for four groups during the first 30 min, after that it became significantly lower the OPA and metformin administered groups compared to the control and acarbose group.

3.4. The effects of the administration of OPA on the levels of blood glucose, plasma insulin, and body weight in C57BL/KsJ-db/db mice

The blood glucose level, plasma insulin level, and body weight were presented in **Table 2-3**. The administration of OPA tended to lower the blood glucose and plasma insulin levels compared to the control *db/db* mice at two weeks of the experimental period. At the start of the study, the body weights of control and OPA administered *db/db* mice groups did not differ significantly. The body weight of control *db/db* mice groups increased during the two week period. At the end of the study, the mice in OPA administered *db/db* mice had a significantly lower body weight as compared to the control *db/db* mice.

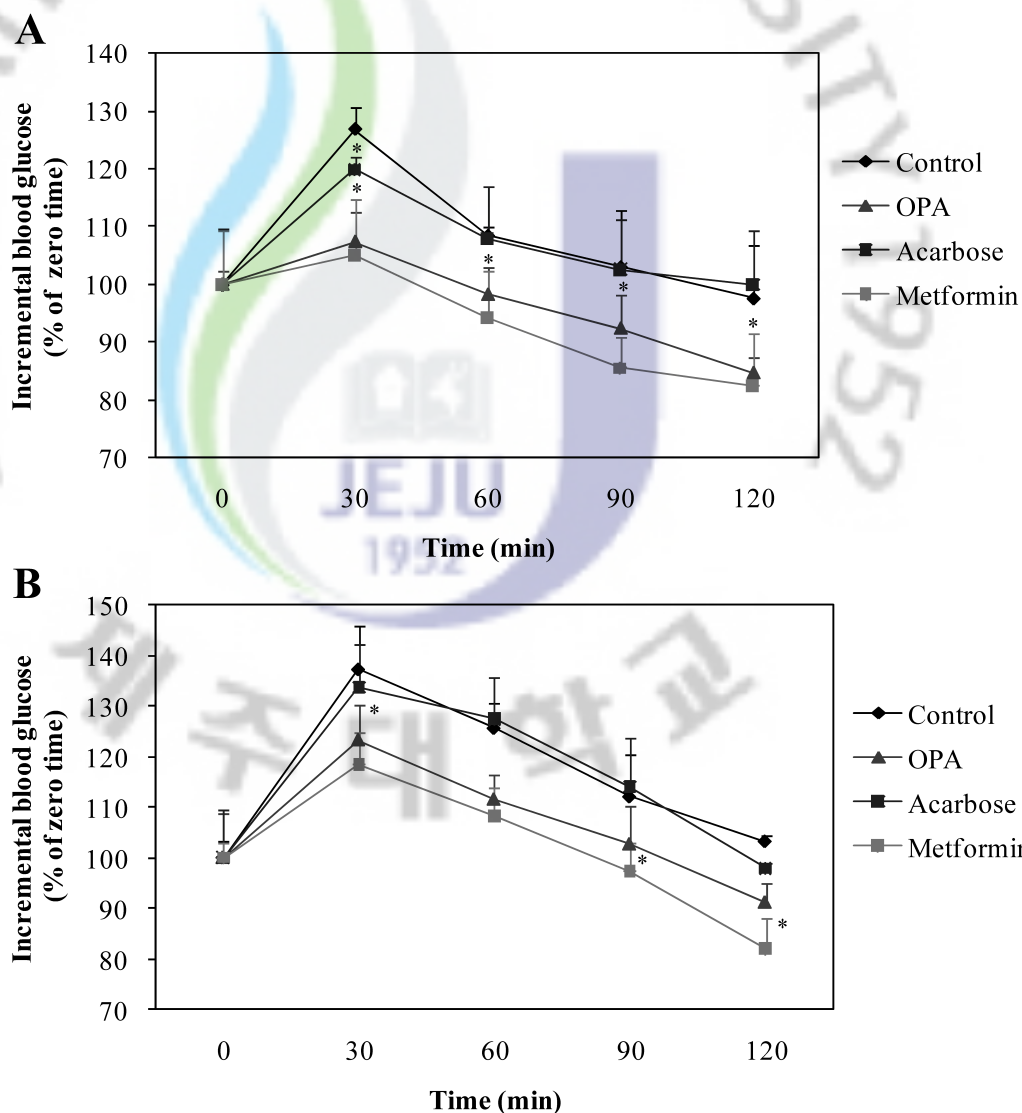


Fig. 2-3. The effects of the administration of OPA on the glucose tolerance test in streptozotocin-induced diabetic mice (A) and normal mice (B). Control (distilled water), OPA (100 mg/kg), acarbose (100 mg/kg) and metformin (100 mg/kg) intraperitoneally injected with glucose (1 g/kg body weight). The blood glucose concentration was measured at the indicated times and presented as percent of glucose injection zero time. Each value is expressed as mean \pm S.D. of six mice (n=48). Significantly different from control at *P<0.05.

Table 2-3. The effects of the administration of OPA on blood glucose, plasma insulin level, and body weight in C57BL/KsJ-*db/db* mice¹.

	<i>db/db</i> ²	<i>db/db</i> -OPA-2.5 ³	<i>db/db</i> -OPA-5 ⁴
Blood glucose (mg/dl)			
Initial	249.20±60.53	305.75±77.52	297.75±77.20
Final	320.40±93.65	206.14±92.84	147.23±64.57
Plasma insulin (ng/ml)	9.7±1.45	7.3±1.03	4.9±0.30
Body weight (g)			
Initial	54.37±1.87	54.30±1.57	51.18±1.82
Final	55.95±2.34	49.33±2.33	47.78±1.38

The OPA dissolved saline was administered OPA by intraperitoneal injection once per day for 2 weeks .

¹ Means ± SE (n = 5).

² C57BL/KsJ-*db/db* mice.

³ C57BL/KsJ-*db/db* mice administered with OPA 2.5 mg/kg B.W.

⁴ C57BL/KsJ-*db/db* mice administered with OPA 5 mg/kg B.W.

4. Discussion

A sudden increase in blood glucose levels, which causes hyperglycemia in type 2 diabetes patients, occurs as the result of the hydrolysis of starch by pancreatic α -amylase and glucose uptake due to intestinal α -glucosidases (Gray, 1995). An effective strategy for the management of type 2 diabetes patients involved the profound inhibition of intestinal α -glucosidases and the mild inhibition of pancreatic α -amylase (Krentz and Bailey, 2005). Several natural resources have been evaluated for their ability to suppress the production of glucose from carbohydrates in the gut or glucose absorption from the intestine (Matsui et al., 2007). α -Glucosidase is one of the glucosidases located within the brush-border surface membranes of intestinal cells, and is a key enzyme in carbohydrate digestion (Lebovitz, 1997). Similarly, α -amylase catalyzes the hydrolysis of α -1,4-glucosidic linkages of starch, glycogen, and a variety of oligosaccharides, and α -glucosidase further degrades the disaccharides into simpler sugars, which are readily available for intestinal absorption. The inhibition of their activity in the human digestive tract, is regarded as an effective method for the control of diabetes by diminishing the absorption of glucose decomposed from starch by these enzymes (Hara and Honda, 1990). Therefore, effective and nontoxic inhibitors of α -glucosidase and α -amylase have long been sought.

In this study, we evaluated the inhibitory effects of OPA against α -glucosidase and α -amylase to elucidate the possible use of OPA as an anti-hyperglycemic agent. OPA exhibited stronger inhibitory activity against both α -glucosidase and α -amylase than that of the commercial carbohydrate digestive enzyme inhibitor, acarbose, which evidenced no cytotoxicity. Kim et al. (2008) reported that bromophenols isolated from the red alga, *Grateloupia elliptica*, have the potential to prevent diabetes mellitus because of their high α -glucosidase inhibitory activity. Polyphenolic compounds such as tannins from terrestrial plants and phlorotannins from marine algae associate with a variety of proteins to form complexes. The results of several recent studies have demonstrated that the hydroxyl groups in polyphenolic compounds may, therefore, perform a crucial function in promoting inhibitory activity (Stern et al., 1996; Kim et al., 2008). OPA, a type of phlorotannin, was the marine algal polyphenolic compound isolated from *I. sinicola*. Thus, OPA should bind to the active or binding sites of the enzymes, resulting in the inhibition of enzyme activity.

It has been previously established that postprandial hyperglycemia performs a critically important function in the development of type 2 diabetes and complications associated with cardiovascular diseases (Baron, 1998). Therefore, the control of postprandial hyperglycemia has been regarded as important in the treatment of diabetes and the prevention of cardiovascular complications. In this study, we determined the anti-hyperglycemic effect of

OPA in streptozotocin-induced diabetic and normal mice after consuming of starch. The increase in postprandial blood glucose levels was suppressed significantly in both streptozotocin-induced diabetic and normal mice which were treated with OPA. This result demonstrates that OPA may delay the absorption of dietary carbohydrates, resulting in the suppression of an increase in postprandial blood glucose level. Inoue et al. (1997) reported that the medication, which flattens peak postprandial blood glucose, reduces the AUC of the blood glucose response curve. In this study, OPA was shown to reduce both the blood glucose level at the peak time point and the AUC. Postprandial hyperglycemia is also involved in a variety of metabolic disorders and other diseases, including virus-based diseases and cancer (Dennis et al., 1987; Gruters et al., 1987). Glycosidase inhibitors are important tools for studying the mechanisms of actions on glycosidases, and are also prospective therapeutic agents for certain degenerative diseases (Winchester and Fleet, 1992). In this study, we determined the improvement effect of glucose tolerance of OPA in streptozotocin-induced diabetic and normal mice after injection of glucose. The present study observed that the administration of OPA can improve blood glucose levels and impaired glucose tolerance in streptozotocin-induced diabetic and normal mice and it was almost similar to that of metformin administered mice. Metformin has been reported to enhance insulin action, thereby improving glucose tolerance and reducing hyperinsulinemia

in animals and humans with type 2 diabetes. Accordingly, the improvement of glucose tolerance suggest that OPA may enhance insulin sensitivity.

Many synthetic compounds have already been employed in efforts to develop a treatment for diabetes. However, they have, generally, been associated with marked toxic or undesirable side effects (Hanefeld, 1998; Li et al., 2005). Therefore, marine algae are currently recognized as good candidate sources for naturally-derived anti-diabetic compounds. Previously, we evaluated the effects of diphlorethohydroxycarmalol and dieckol isolated from brown algae, *Ishige okamurae* and *Ecklonia cava*, on postprandial hyperglycemia in an *in vivo* test, and also assessed the prominent effects of diphlorethohydroxycarmalol in both streptozotocin-induced diabetic mice and normal mice (Heo et al., 2009; Lee et al., 2010). Cherng and Shih (2006) and Kang et al. (2008) also noted that *Chlorella* and *Petalonia* exerted anti-diabetic effects via both insulin-like and insulin-sensitizing activities on *in vivo* tests. The findings of this study showed that OPA may prove useful as an effective natural anti-diabetic compound.

In conclusion, OPA exerts a profound inhibitory effect against α -glucosidase and α -amylase, which may eventually provide a method for generating a carbon source, such as starch, in the fermentation process. Also, OPA may delay the absorption of dietary carbohydrates in the intestine, resulting in the suppression of increased blood glucose levels after a meal. Further,

the administration of OPA improved the glucose level and plasma insulin level in the C57BL/KsJ-*db/db* (*db/db*), type 2 diabetic mice. Thus, we suggested that OPA might be developed into medicinal preparations, nutraceuticals, or functional foods for diabetes, and may also be applied in other therapeutic fields.

The background features a large, faint watermark of the Jeju National University logo. The logo is circular, with the text "JEJU NATIONAL UNIVERSITY" at the top and "1952" at the bottom. In the center, there is a stylized flame or leaf shape composed of blue, green, and grey elements, with a purple vertical bar to its right.

Part III.

Octaphlorethol A isolated from *Ishige sinicola* stimulates glucose uptake in skeletal muscle cells by activating Akt and AMPK pathway

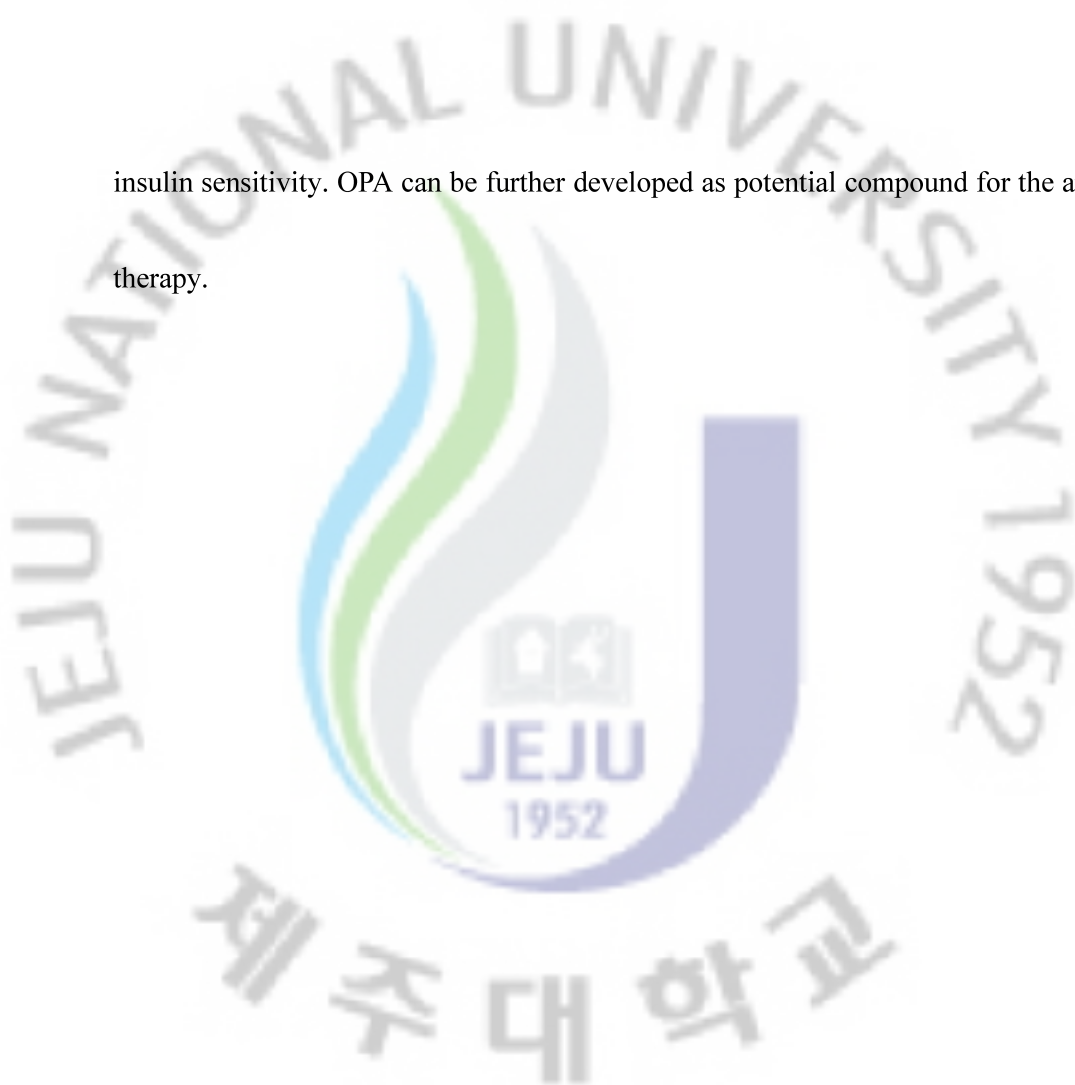
Part III.

Octaphloretol A isolated from *Ishige sinicola* stimulates glucose uptake in skeletal muscle cells by activating Akt and AMPK pathway

1. ABSTRACT

In the present study, we reported the glucose uptake effects of octaphloretol A (OPA) isolated from *Ishige sinicola*, on skeletal muscle cells. OPA dose-dependently increased glucose uptake in differentiated L6 rat myoblast cells compared to control. Inhibitor of phosphatidylinositol 3-kinase (PI3K) by wortmannin pretreating the cells with wortmannin potently reduced OPA-stimulated glucose uptake, also inhibition of AMP-activated protein kinase (AMPK) by compound C exhibited significant inhibitory effect on OPA-mediated glucose uptake. Western blotting analyses revealed that OPA increased the phosphorylation level of Akt and AMPK and such enhancement can be specifically inhibited by wortmannin and compound C. In addition, we demonstrated that glucose transporter GLUT4 translocation to plasma membrane was increased by OPA. In summary, PI3K/Akt and AMPK activation was involved in the effects of OPA on glucose transport activation and

insulin sensitivity. OPA can be further developed as potential compound for the anti-diabetic therapy.



2. MATERIALS AND METHODS

2.1. Materials

The rat myoblast cell line L6 was purchased from the Korean Cell Line Bank (KCLB; Seoul, KOREA). DMEM (Dulbecco's modified Eagle's medium), wortmannin, and compound C were purchased from Sigma (St. Louis, MO, USA). Antibodies against insulin receptor substrate-1 (IRS-1), AMP-activated protein kinase (AMPK), phospho-AMPK (Thr 172), Protein kinase B (Akt), phospho-Akt (Ser 473), β -actin, and glucose transporter 4 (GLUT4) were from Cell Signaling Technology (Bedford, Massachusetts, USA). Phospho-IRS-1 (Tyr 612), and second IgG HRP-linked antibodies were from Santa Cruz Biotechnology (Santa Cruz, CA, USA). The other chemicals and reagents used were of analytical grade.

2.2. Cell culture

Rat myoblast L6 cells were maintained in high glucose-DMEM supplemented with 10% heat-inactivated FBS, penicillin (100 U/ml) and streptomycin (100 μ g/ml). Cultures were maintained at 37°C in 5 % CO₂ incubator. For differentiation, the cells were seeded in appropriate culture plates, and after sub-confluence (about 80%), the medium was changed to DMEM containing 2% horse serum for 7 days, with medium changes every day. All

experiments were performed in differentiated L6 myotubes after 7 days.

2.3. MTT assay

The cytotoxicity of OPA against the L6 cells were determined by a colorimetric MTT assay. Cells were seeded in a 24-well plate. After 24 h, the cells were treated with various concentrations (6.25, 12.5, 25, 50, and 100 $\mu\text{g/ml}$) of the OPA. The cells were then incubated for an additional 24 h at 37°C. MTT stock solution (100 μl ; 2 mg/ml in PBS) was then added to each well. After incubating for 4 h, the plate was centrifuged at 2,000 rpm for 10 min and the supernatant was aspirated. The formazan crystals in each well were dissolved in DMSO. The amount of purple formazan was determined by measuring the absorbance at 540 nm.

2.4. LDH Cytotoxicity Assay

L6 cells plated in 24-well plates were pre-incubated and then treated with various concentrations (6.25, 12.5, 25, 50, and 100 $\mu\text{g/ml}$) of the OPA at 37°C for 24 h. The medium was carefully removed from each well, and the LDH activity in the medium was determined using an LDH cytotoxicity detection kit. Briefly, 100 μl of reaction mixture were added to each well, and the reaction was incubated for 30 min at room temperature in the dark. The absorbance of each well was measured at 490 nm using a UV spectrophotometer.

2.5. Glucose uptake assay

L6 cells were seeded in a 24-well plate. After differentiation, the cells were starved in serum-free low glucose DMEM for 12 h, and then washed with PBS and incubated with fresh serum-free low glucose DMEM. After that, the cells were treated with insulin (100 nM) for 1h, or the indicated concentrations (to determine the dose response of L6 myotubes to OPA) and times (to determine the time response of L6 myotubes to OPA) of OPA. Glucose uptake was measured by glucose concentration in the media solution using glucose oxidase assay kit (Asan Pharmaceutical corp., Korea).

In some experiments, 100 nM of Wortmannin (PI3-kinase inhibitor) and 10 μ M of Compound C (AMPK inhibitor) were added 30 min before the OPA treatment.

2.6. Western blot analysis

L6 myotubes were grown 100 mm dishes and were starved in serum-free low glucose DMEM for 12 h prior to treatment with the indicated agents. Following treatment the media were aspirated and the cells were washed twice in ice-cold PBS. The cells were lysed in NucBuster™ Protein Extraction Kit (Novagen, San Diego, CA, USA) for 10 min and then centrifuged at 16,000 rpm for 5 min at 4°C. The protein concentrations were determined by using BCA™ protein assay kit. The lysate containing 50 μ g of protein were subjected to

electrophoresis on 7.5% sodium dodecyl sulfate-polyacrylamide gel, and the gel was transferred onto a nitrocellulose membrane. The membranes was blocked in 5% bovine serum albumin (BSA) in TBST (25 mM Tris-HCl, 137 mM NaCl, 0.1% Tween 20, pH 7.4) for 2 h. The primary antibodies were used at a 1:500 dilution. Membranes incubated with the primary antibodies at 4°C for overnight. Then the membranes were washed with TTBT and then incubated with the secondary antibodies used at 1:2000 dilution. Signals were developed using an ECL western blotting detection kit and exposed to X-ray films.

2.7. Plasma membrane fractionation and immunoblot analysis

L6 myotubes were treated with the indicated agents and harvested. The cell lysates were prepared with lysis buffer [250 mM sucrose, 20 mM HEPES (pH 7.4), 10 mM KCl, 1.5 mM MgCl₂, 1 mM EDTA, 1 mM EGTA, 1 mM dithiothreitol (DTT), and protease inhibitors (1 mM PMSF, 25 µg/ml aprotinin, and 25 µg/ml leupeptin)] and kept on ice for 10 min. The cell lysate were ultracentrifuged at 22,000 rpm for 1 h at 4°C. The pellet was resuspended in a lysis buffer and kept on ice for 10 min and then centrifuged at 8,000 rpm for 5 min at 4°C to obtain plasma membrane fraction from the middle layer of the supernatant. Immunoblot analyses of GLUT4 described in the method to 2.6.

2.8. Statistical analysis

The data are presented as mean \pm standard error (SE). Statistical comparison was performed via the SPSS package for Windows (Version 14). P-values of less than 0.05 were considered to be significant.

3. RESULTS

3.1. Cytotoxicity of OPA

Cytotoxicity of OPA was evaluated using the MTT and LDH assay in various concentrations (6.25, 12.5, 25, 50, and 100 $\mu\text{g/ml}$). In that results, OPA did not show cytotoxicity up to 100 $\mu\text{g/ml}$ compared with control (**Fig. 3-1**). This result showed that 50 $\mu\text{g/ml}$ of OPA did not influence on the cytotoxicity of L6 cells. Thus, the concentrations were used in subsequent experiments.

3.2. OPA stimulates glucose uptake in skeletal muscle cells

In order to determine the role of OPA did not shown cytotoxicity up to 100 $\mu\text{g/ml}$ compared with control in glucose metabolism of muscle cells, the effect of OPA on glucose uptake was investigated in L6 skeletal muscle cells. It was found that OPA dose-dependently stimulated glucose uptake as shown in **Fig. 3-2A**, and the effect of OPA (50 $\mu\text{g/ml}$) was comparable to that of insulin, which indicates that OPA may have metabolic effects in skeletal muscle cells. We next investigated the time-effect of OPA on L6 skeletal muscle cells, and the cells were maintained in serum-free media OPA (50 $\mu\text{g/ml}$) for the indicated times. Activation induced by OPA reached a peak after 2h and gradually decreased until 12 h (**Fig. 3-2B**). Thus, I carried out the consequent OPA treatments at this time point and this concentration.

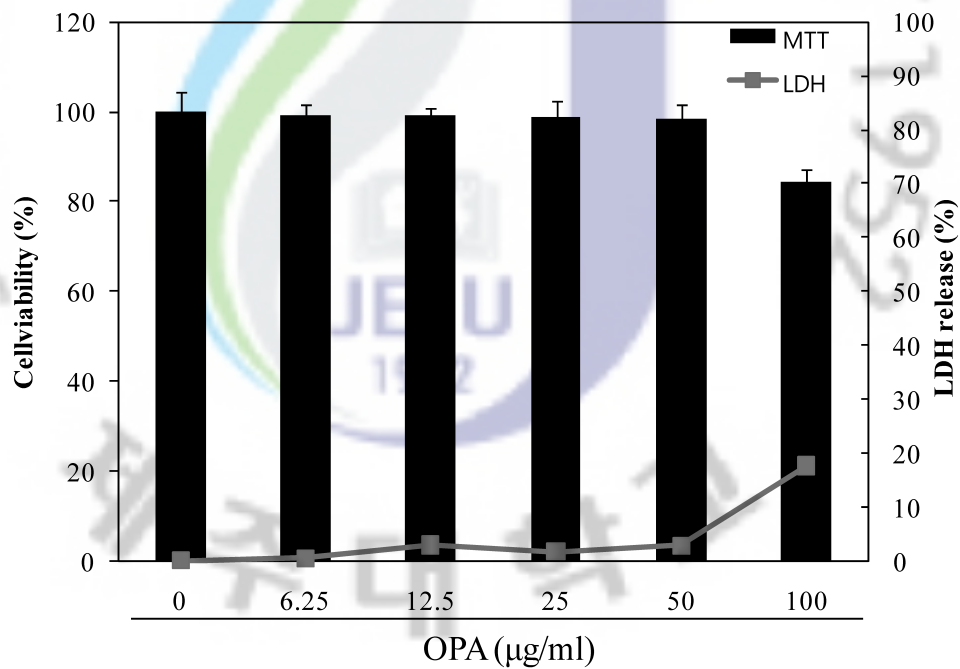


Fig. 3-1. Cytotoxicity of OPA. Cytotoxicity of OPA was determined using the MTT and LDH method. Each value is expressed as mean \pm S.E. in triplicate experiments.

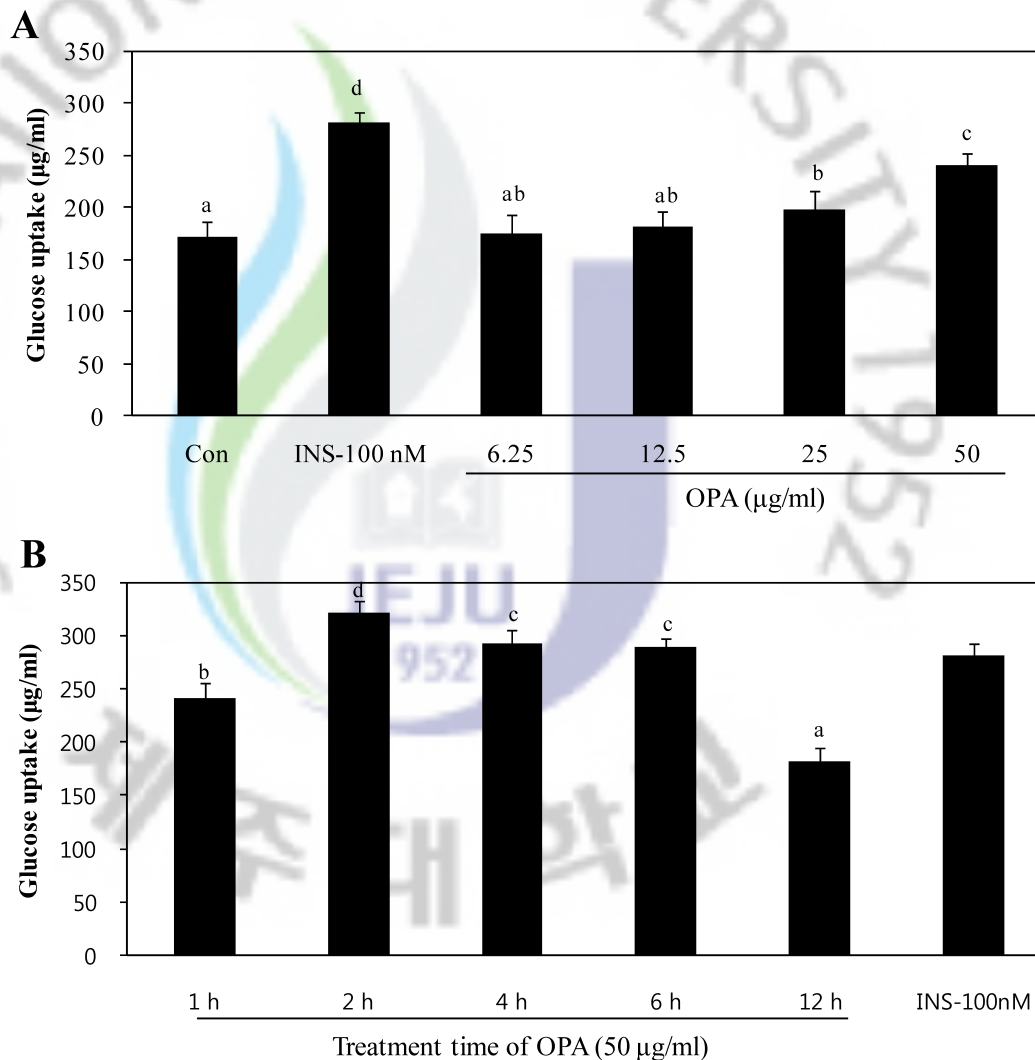


Fig. 3-2. OPA dose- and time-dependently stimulates glucose uptake in L6 skeletal muscle cells. (A) Cells were starved in serum free (SF) media for 12 h, and incubated for 1 h with increasing of OPA and insulin. (B) Cells were starved for 12 h in SF media followed by incubation with 50 µg/ml OPA for different time periods up to 12 h. Insulin (100 nM, for 1 h) was used as a positive control. Values are expressed as means ± S.E. in triplicate experiments. ^{a-d}Values with different alphabets are significantly different at $P < 0.05$ as analyzed via Duncan's multiple range test.

3.3. OPA-induced increase of glucose uptake was dependent of PI-3 kinase (Akt) and AMPK activation

To look into which pathway may be involved in the effect of OPA on glucose uptake in L6 cells, L6 cells were pretreated with wortmannin, an inhibitor of phosphatidylinositol (PI) 3-kinase and compound C, a selective AMPK inhibitor. As shown in **Fig. 3-3**, wortmannin and compound C exhibited significant inhibition on glucose uptake stimulated by OPA (50 µg/ml). The results indicate that OPA-induced increase in the glucose uptake may involve phosphatidylinositol (PI) 3-kinase (Akt) and AMPK activation.

3.4. Effect of OPA on insulin-mediated signaling pathway

Western blotting analysis was then carried out to further investigate insulin-mediated signaling pathway in OPA action. After L6 cells were treated with OPA for 2 h, the phosphorylation levels of IRS-1 and Akt were determined. Tyrosine phosphorylation of IRS-1 was induced by insulin, and treatment of OPA treatment significantly increased the level of phosphorylated IRS-1 (**Fig. 3-4**). In accord with the activation of phosphorylated IRS-1, phosphorylated Akt also increased significantly by treatment of OPA. As shown in **Fig. 3-4**, the increase in the phosphorylation of Akt was inhibited by pretreatment of wortmannin, an inhibitor of phosphatidylinositol (PI) 3-kinase. These results indicate that OPA strongly

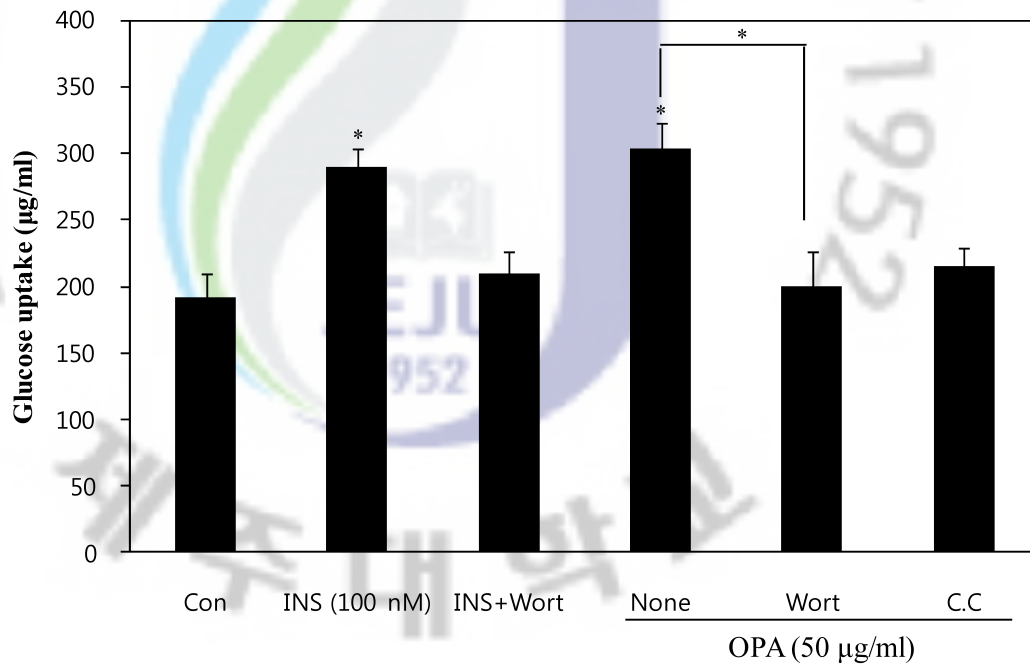


Fig. 3-3. OPA-induced increase of glucose uptake was reduced by wortmannin and compound C. After 12 h starvation, L6 skeletal muscle cells were pretreated with or without 100 nM wortmannin (phosphatidylinositol (PI) 3-kinase inhibitor) and 10 µM compound C, (AMPK inhibitor) for 30 min, and then treated with 50 µg/ml OPA for 2 h. Each value is expressed as mean ± S.E. in triplicate experiments. *P<0.05 vs. control or between two groups as indicated.

enhances insulin signaling, and the increase in phosphorylated IRS-1 and Akt may play an important role in this process.

3.5. Effect of OPA on AMPK signaling pathway

To look into the roles of OPA in AMPK signaling pathway, we investigated the effects of OPA on AMPK activation. We found that treatment of OPA induced increase in AMPK phosphorylation in L6 cells (**Fig. 3-5**). However, the increase in phosphorylation of AMPK was inhibited by pretreatment of compound C, a selective AMPK inhibitor for 30 min before treatment of OPA (**Fig. 3-5**). This result, together with above results, strongly indicates that OPA plays a metabolic role in skeletal muscle cells through the AMPK pathway.

3.6. Effect of OPA on GLUT4 translocation to the plasma membrane

I next examined the effect of OPA on the insulin-mediated and AMPK signaling pathway that leads to the translocation of glucose transport 4 (GLUT4) to the plasma membrane and increases the uptake of glucose. After L6 myotubes cells were treated with OPA for 2 h, the translocation of GLUT4 was determined. As seen in **Fig. 3-6**, GLUT4 translocation to the plasma membrane of L6 myotubes cells were markedly increased by treatment of OPA. However, increased translocation of GLUT4 to the plasma membrane of OPA-treated L6

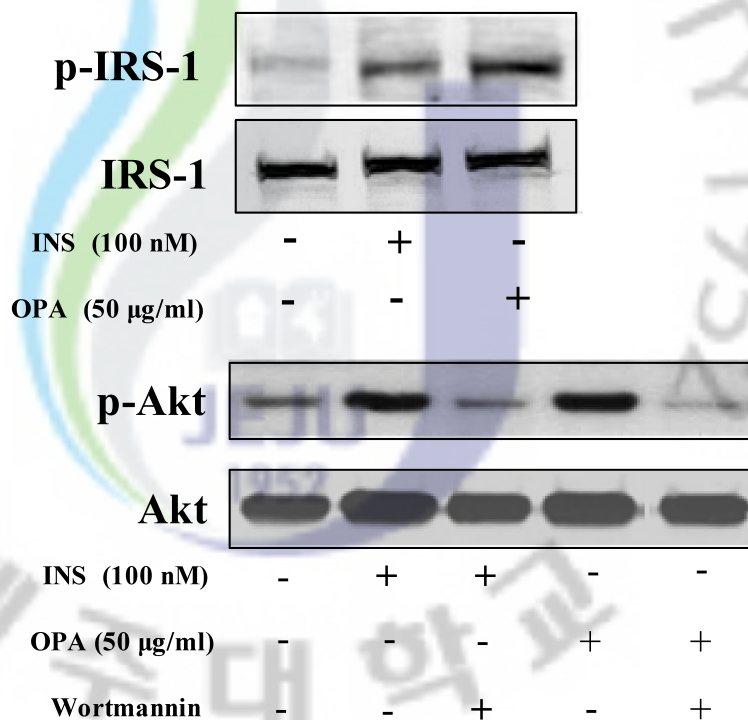


Fig. 3-4. Effects of OPA on the insulin signaling pathway in L6 cells. Cells were pretreated with or without 100 nM wortmannin for 30 min, and then treated with the indicated concentrations of OPA and insulin for 2 h and 10 min, respectively. The cell lysates were analyzed via Western blotting using anti-phosphoIRS-1 (Tyr 612), anti-IRS-1, anti-phosphoAkt (Ser 473) and anti-Akt. Figures are representative of three independent experiments.

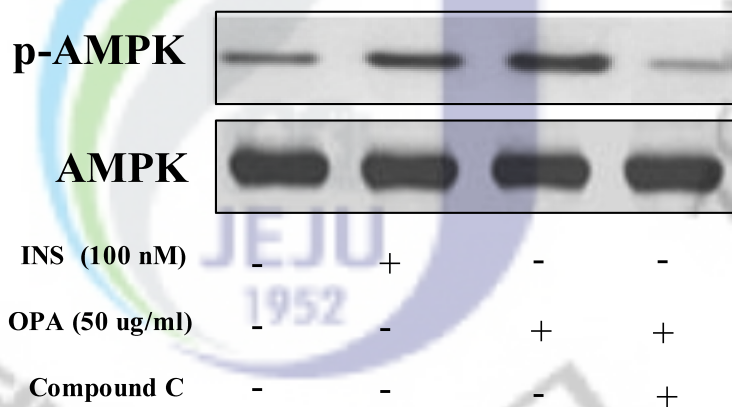


Fig. 3-5. Effect of OPA on AMPK signaling pathway. Cells were pretreated with or without 10 μ M compound C for 30 min, and then treated with the indicated concentrations of OPA and insulin for 2 h and 10 min, respectively. The cell lysates were analyzed via Western blotting using anti-phosphoAMPK (Thr 172) and anti-AMPK. Figures are representative of three independent experiments.

myotubes cells were almost completely abolished by wortmannin and compound C pretreatment. These results suggest that OPA stimulated increase in GLUT4 translocation to the plasma membrane possibly via activating PI3K/Akt and AMPK pathway.

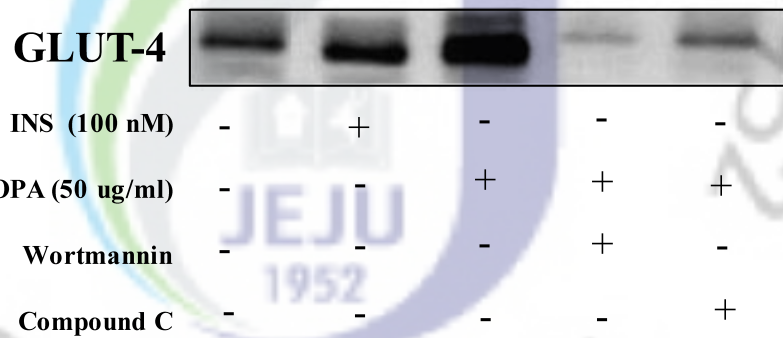


Fig. 3-6. Effect of OPA on GLUT4 translocation to the plasma membrane. Cells were pretreated with or without 10 μ M compound C for 30 min, and then treated with the indicated concentrations of OPA and insulin for 2 h and 10 min, respectively. The cell lysates were analyzed via Western blotting using anti-GLUT4. Figures are representative of three independent experiments.

4. Discussion

Diabetes mellitus is the most serious and chronic disease that is developing with an increasing obesity and aging in the general population over the world. Diabetes mellitus is a complex disorder that is characterized by hyperglycemia. It is largely classified into insulin-dependent diabetes mellitus (type 1 diabetes) and non-insulin-dependent diabetes mellitus (type 2 diabetes). In particular, type 2 diabetes is an increasing worldwide health problem and is the most common type of diabetes (Zimmet et al., 2001). Hyperglycemia plays an important role in the development type 2 diabetes and complications associated with the diseases such as micro-vascular and macro-vascular diseases (Baron, 1998). Therefore, the effective control of blood glucose level is the key to prevent or reverse diabetic complications and improve the quality of the life in diabetic patients (DeFronzo, 1999).

Currently available drugs for type 2 diabetes have a number of limitations, such as adverse effects and high rates of secondary failure. Therefore, recently, there has been a growing interest in alternative therapies and in the therapeutic use of natural products for diabetes, especially those derived from herbs (Chang et al., 2006; Jung et al., 2007). This is because plant sources are usually considered to be less toxic with fewer side effects than synthetic ones. Marine algae are known to provide an abundance of bioactive compounds with great pharmaceutical foods and biomedical potential. However, anti-diabetic effect of marine

algae on glucose metabolism remains poorly investigated.

Skeletal muscle has been identified as the major tissue in glucose metabolism, accounting for nearly 75% of whole-body insulin-stimulated glucose uptake (DeFronzo et al., 1981).

Insulin-stimulated glucose uptake in skeletal muscle is critical for reducing blood glucose levels. Failure of glucose uptake due to decreased insulin sensitivity leads to the development of type 2 diabetes. In skeletal muscle, glucose transport can be activated by at least two major mechanisms. In the present study, we try to find out whether OPA has an effect on glucose uptake in skeletal muscle cells. In our study, OPA alone could stimulate glucose uptake in skeletal muscle cell. In addition, to clarify that OPA exerts the glucose uptake via insulin signaling pathway or AMPK, we examined several molecules involved in insulin and AMPK signal pathway.

One is the insulin signaling pathway via PI3-kinase activity. PI3-kinase is a key molecular switch, that mediates glucose transport by insulin and leads to several metabolic effects (Okada et al., 1994). Indeed, PI3-kinase activity accelerates glucose uptake via the phosphorylation leading to the translocation of glucose transporter 4 (GLUT4) to the plasma membrane (Wang et al., 1999). Our data in L6 myotubes shows a significant increase in glucose uptake by OPA in the absence of insulin via PI3K/Akt pathway. Using wortmannin, a selective PI3K/Akt inhibitor, we demonstrated a significant reduction in OPA-stimulated

glucose uptake providing support of the notion that PI3K/Akt pathway is a mediator of the OPA effects on glucose uptake.

The mammalian AMPK is a trimeric enzyme and represents a metabolite-sensing protein kinase. AMPK is known to play a major role in energy homeostasis in ATP-depleting metabolic states such as ischemia, hypoxia, heart shock, oxidative stress, and especially exercise (Harder et al., 2001; Raj and Dentino, 2002). Once activated under such condition, it accelerates ATP-generating catabolic pathway including glucose uptake and fatty acid oxidation through direct regulation of key metabolic enzymes (Sheetz and King, 2002). In recent papers, it has been reported that AMPK serves as a key metabolic sensor through cellular regulation of insulin-independent glucose uptake and glycogen metabolism as described previously (Ozcan et al., 2004; Hotamisligil, 2006). From this, AMPK is emerging as a potentially interesting target for the treatment of diabetes (Nakatani et al., 2005), especially because it could play a principal role in exercised-induced adaptation of skeletal muscle (Ozawa et al., 2005), type 2 diabetes, obesity and the metabolic syndrome. Present study showed a significant increase in AMPK phosphorylation by OPA. And also, the OPA-mediated activation of AMPK is abolished by pretreatment of compound C, highly-selective AMPK inhibitor. Therefore, these results indicate that AMPK is a principal factor in OPA-stimulated glucose uptake.

Furthermore, GLUT4 translocation to the plasma membrane of L6 myotubes cells were markedly increased by treatment of OPA. In addition, increased translocation of GLUT4 to the plasma membrane of OPA-treated L6 myotubes cells were almost completely abolished by wortmannin and compound C pretreatment. Therefore, these results suggest that OPA stimulated increase in GLUT4 translocation to the plasma membrane possibly via activating PI3K/Akt and AMPK pathway. Hyperglycemic-hyperinsulinemic clamp analyses of human type 2 diabetic patients show that insulin resistance in muscle is caused by a defect in glucose transport. The principal glucose transporter in muscle is glucose transporter 4 (GLUT4), which is the primary mediator both of basal and insulin-stimulated glucose transport in muscle. Thus, the effects of OPA in activating GLUT4 expression are reflected in an increased ability of the muscle cells to transport glucose.

In consequence, these results demonstrate that OPA improve glucose uptake via activating PI3K/Akt and AMPK pathway in skeletal muscles (**Fig. 3-7**). Especially, the skeletal muscle has a major role in the regulation of energy balance (Ozcan et al., 2006) and is the primary tissue for glucose uptake and disposal. Indeed, the glucose uptake, by skeletal muscle, accounts for >70% of the glucose removal from the serum in humans (Cormont et al., 1993). With this, it is considered an important target tissue for type 2 diabetes (Sheetz and King, 2002).

In conclusion, OPA increases glucose uptake through activating PI3K/Akt and AMPK pathway, a novel target for treatment of type 2 diabetes and we can find a new possibility of OPA as a antidiabetic compound.



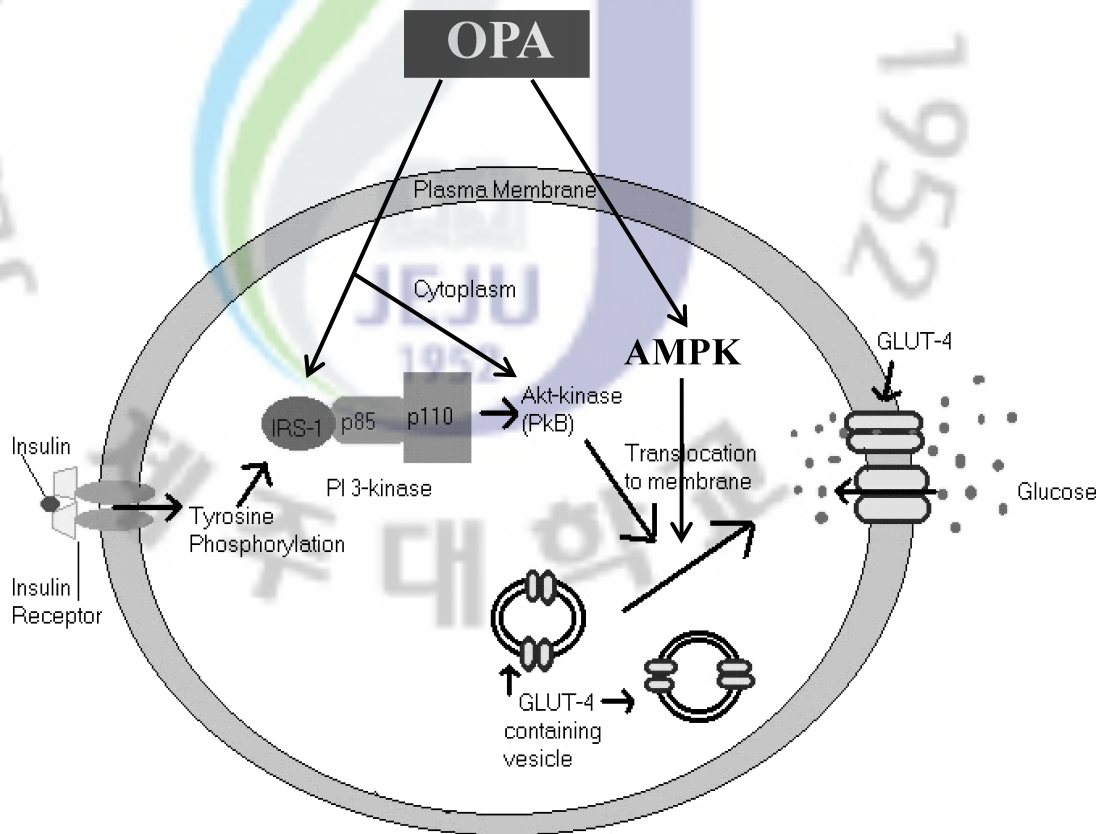


Fig. 3-7. Glucose uptake mechanism of OPA in L6 skeletal muscle cells.



Part IV.

Octaphlorethol A isolated from *Ishige sinicola* prevents and protects against STZ-induced pancreatic beta-cell damage in *in vitro* and *in vivo*

Part IV.

Octaphlorethol A isolated from *Ishige sinicola* prevents and protects against STZ-induced pancreatic β -cells damage in *in vitro* and *in vivo*

1 ABSTRACT

Pancreatic β cells are very sensitive to oxidative stress and this might play an important role in β cell death in diabetes. The protective effect of octaphlorethol A (OPA), one of phlorotannin polyphenol compounds purified from *Ishige sinicola* (*I. sinicola*) against streptozotocin (STZ)-induced pancreatic β cells damage was investigated using RINm5F pancreatic β cells and STZ-induced diabetes. Pretreatment of OPA increased the viability of STZ-treated RINm5F pancreatic β cells at concentration 12.5 or 50 $\mu\text{g/ml}$. Furthermore, pretreatment with OPA dose-dependently reduced thiobarbituric acid reactive substances (TBARS), intracellular reactive oxygen species (ROS) generation and DNA damage in STZ treated RINm5F pancreatic β cells. Also, OPA pretreatment increased activities of antioxidant enzymes including catalase (CAT), superoxide dismutase (SOD) and glutathione peroxidase (GSH-px) in STZ treated RINm5F pancreatic β cells. In addition, OPA inhibited

the STZ-induced apoptosis, which is detected using flow cytometry and western blot assays. Moreover, OPA pretreatment improved the secretory responsiveness following stimulation with glucose. These results indicate that OPA protects against STZ-induced pancreatic β cells damage via reducing ROS-induced oxidative stress and apoptosis. Additionally, the protective effect of OPA was further demonstrated by restoration of pancreatic β cells damage in STZ-induced diabetic mice. The protective effects of OPA in STZ-induced diabetic mice were essentially the same as those observed when RINm5F cells were used. The diabetogenic effects of STZ were completely prevented when mice were pretreated with OPA. The anti-diabetogenic effects of OPA were also mediated by reducing of oxidative stress and apoptosis. Collectively, these results indicate that OPA may have therapeutic value in preventing β cells damage.

2. MATERIAL AND METHODS

2.1. Materials

RPMI 1640 medium, fetal bovine serum (FBS) penicillin–streptomycin and trypsin–EDTA were purchased from Gibco/BRL (Burlington, Ont, Canada). 3-(4,5-Dimethylthiazol-2-yl)-2,5-diphenyltetrazolium bromide (MTT), RNase A, propidium iodide (PI), dimethyl sulfoxide (DMSO), streptozotocin, 2',7'-dichlorodi-hydrofluorescein diacetate (DCF-DA), and Hoechst 33342 were purchased from Sigma (St. Louis, MO, USA). Antibodies against P53, Bax, Bcl-xL, cleaved caspase-3, -9, PARP and β -actin were purchased from Cell Signaling Technology (Bedford, Massachusetts, USA). The other chemicals and reagents used were of analytical grade.

2.2. Cell culture

RINm5F pancreatic β cells were cultured in RPMI 1640 medium, supplemented with 10% fetal bovine serum (FBS), streptomycin (100 μ g/ml) and penicillin (100 units/ml) at 37°C in an humidified atmosphere containing 5% CO₂.

2.3. Assay of cell viability

Cell viability was assessed by a colorimetric MTT assay, which is based on the conversion of MTT to MTT-formazan by mitochondrial enzymes, as described previously (Fautz et al.,

1991). Cells (1×10^5 cells/well) in wells of 96-well plates were preincubated with the indicated concentrations of OPA for 3 h, and then incubated with STZ for 24 h. Thereafter, a 100 μ l of MTT solution (1 mg/ml) was added to each well of 96-well culture plate, incubated for 4 h at 37°C and the medium containing MTT was removed. The incorporated formazan crystals in the viable cells were solubilized with 100 μ l dimethyl sulfoxide and the absorbance at 540 nm of each well was read using a microplate reader.

2.4. Assay of lipid peroxidation

Lipid peroxidation was measured by thiobarbituric acid reactive substances (TBARS) production (Fraga et al., 1988). Cells (1×10^5 cells/well) in wells of 24-well plates were preincubated with the indicated concentrations of OPA for 3 h, and then incubated with STZ for 24 h. The cells were then washed with cold PBS and homogenized. The TBARS concentrations were determined using TBARS assay kit (ZeptoMetrix, New York, USA). TBARS values were then expressed as equivalent nmoles of malondialdehyde (MDA).

2.5. Assay of intracellular ROS levels and Image analysis

The DCF-DA method was used to detect the intracellular ROS levels (Rosenkranz et al., 1992). DCF-DA diffuses into cells where it is hydrolyzed by intracellular esterase to polar

2',7'-dichloro-dihydrofluorescein. This non-fluorescent fluorescein analog gets trapped inside the cells and is oxidized by intracellular oxidants to yield the highly fluorescent, 2',7'-dichloro-fluorescein. The cells were treated with OPA at 12.5, 25, and 50 $\mu\text{g}/\text{ml}$ followed by application of STZ at 10 mM 3 h later. The cells were incubated for an additional 24 h at 37°C. After the addition of 10 μM of the DCF-DA solution, the fluorescence of 2',7'-dichlorofluorescein was detected using a FACSCalibur flow cytometer (Becton Dickinson, San Jose, CA, USA). For image analysis of the production of intracellular ROS, the cells were seeded in coverslip loaded 6 well plates at 1×10^5 cells/well. Sixteen hours after plating, the cells were treated with OPA and 3 h later, STZ at 10 mM. After changing media, 10 μM of DCF-DA was added in the well and incubated for an additional 30 min at 37°C. After washing with PBS, the stained cells were then observed under a fluorescence microscope equipped with a CoolSNAP-Pro color digital camera to examine the degree of ROS generation.

2.6. Comet assay

A comet assay was performed to assess cell oxidative DNA damage (Ahn et al., 2007). The cell pellet (1×10^5 cells) was mixed with 100 μl of 0.7% low melting point agarose (LMPA), and added to 1.0% normal melting point agarose (NMPA)-coated slides. After keeping them

for 10 min at 4°C, the slides were covered with another 100 µl of 0.7% LMPA and kept for 40 min at 4°C for solidification of the agarose. And the slides were immersed in lysis solution (2.5 M NaCl, 100 µM EDTA, 10 mM Tris, 1% sodium laurylsarcosine and 1% Triton X-100) for 1 h at 4°C. The slides were unwinded and applied for electrophoresis with the electric current of 25 V/300 mA for 20 min. Then, the slides were neutralized in 0.4 M Tris buffer (pH 7.5) for 10 min two times and dehydrated with 70% ethanol. The percentage of fluorescence in the DNA tail of each cell (tail intensity, TI; 50 cells from each of two replicate slides) on the ethidium bromide stained slides were measured by image analysis (Kinetic Imaging, Komet 5.0, UK) and fluorescence microscope (LEICA DMLB, Germany).

2.7. Antioxidant enzyme assays

Cells (1×10^6 cells) in 10 mm dishes were preincubated with the indicated concentrations of OPA for 3 h, and then incubated with STZ for 24 h. The medium was removed and the cells were washed twice with PBS. One milliliter of 50 mM potassium phosphate buffer with 1 mM EDTA (pH 7.0) was added and cells were scraped. The cells were homogenized in NucBuster™ Protein Extraction Kit (Novagen, San Diego, CA, USA) for 10 min and then centrifuged at 16,000 rpm for 5 min at 4°C. Cell supernatants were used for antioxidant enzyme activities. The protein concentrations were determined by using BCA™ protein

assay kit. Superoxide dismutase (SOD), catalase (CAT), and glutathione peroxidase (GSH-px) activities were determined using chemical kits. Briefly, the determination of SOD activity (SOD assay kit-WST, Dojindo Molecular Technologies, Inc., Rockville, MD, USA) was based on the production of O_2^- anions by the xanthine/xanthine oxidase system. The determination of CAT activity (Catalase assay kit, Cayman Chemical, Ann Arbor, MI, USA) was based on the reaction of the enzyme with methanol in the presence of an optimal concentration of H_2O_2 . GSH-px activity (Glutathione peroxidase assay kit, Sigma, St. Louis, MO, USA) was estimated by the analysis of GSH in the enzymatic reaction.

2.8. Cell cycle analysis

Cell cycle analysis was performed to determine the proportion of apoptotic sub- G_1 hypodiploid cells (Nicoletti et al., 1991). The cells were placed in a 6-well plate at a concentration of 1×10^5 cells/ml. Sixteen hours after seeding, the cells were pretreated with the indicated concentrations of OPA for 3 h, and then incubated with STZ for 24 h. After 24 h, the cells were harvested at the indicated time and fixed in 1 ml of 70% ethanol for 30 min at $4^\circ C$. The cells were washed twice with PBS and incubated in the dark in 1 ml of PBS containing 100 μg PI and 100 μg RNase A for 30 min at $37^\circ C$. Flow cytometric analysis was performed with a FACSCalibur flow cytometer (Becton Dickinson, San Jose, CA, USA).

The effect on cell cycle was determined by changes in the percentage of cell distribution at each phase of the cell cycle and assessed by histograms generated by the computer program Cell Quest and Mod-Fit (Wang et al., 1993).

2.9. Nuclear staining with Hoechst 33342

The nuclear morphology of cells was studied by using cell-permeable DNA dye Hoechst 33342. Cells having homogeneously stained nuclei were considered to be viable, whereas the presence of chromatin condensation and/or fragmentation was indicative of apoptosis (Gschwind and Huber, 1995; Lizard et al., 1995). The cells were placed in 24-well plate at a concentration of 1×10^5 cells/ml. Sixteen hours after seeding, the cells were pretreated with the indicated concentrations of OPA for 3 h, and then incubated with STZ for 24 h. Then, Hoechst 33342, a DNA specific fluorescent dye was added into the culture medium at final concentration of 10 $\mu\text{g/ml}$, and plate was incubated for another 10 min at 37°C. The stained cells were then observed under a fluorescence microscope equipped with a CoolSNAP-Pro color digital camera to examine the degree of nuclear condensation.

2.10. Western blot analysis

Cells (1×10^6 cells/ml) in 10 mm dishes were pretreated with the indicated concentrations of

OPA for 3 h, and then incubated with STZ for 24 h. The cells were lysed in NucBuster™ Protein Extraction Kit (Novagen, San Diego, CA, USA) for 10 min and then centrifuged at 16,000 rpm for 5 min at 4°C. The protein concentrations were determined by using BCA™ protein assay kit. The lysate containing 50 µg of protein were subjected to electrophoresis on 12% sodium dodecyl sulfate-polyacrylamide gel, and the gel was transferred onto a nitrocellulose membrane. The membranes was blocked in 5% bovine serum albumin (BSA) in TBST (25 mM Tris-HCl, 137 mM NaCl, 0.1% Tween 20, pH 7.4) for 2 h. The primary antibodies were used at a 1:500 dilution. Membranes incubated with the primary antibodies at 4°C for overnight. Then the membranes were washed with TTBT and then incubated with the secondary antibodies used at 1:3000 dilution. Signals were developed using an ECL western blotting detection kit and exposed to X-ray films.

2.11. Glucose stimulated insulin secretion (GSIS)

Cells (1×10^6) in 10 mm dishes were pretreated with the indicated concentrations of OPA for 3 h, and then incubated with STZ for 24 h. Thereafter, the medium was carefully removed and the cells were washed with PBS, and replaced with fresh medium containing 3 mM glucose and 2% FBS. After 5 h of incubation, the cells were stimulated with Krebs-Ringer buffer (119 mM NaCl, 4.75 mM KCl, 2.54 mM CaCl_2 , 1.2 mM MgSO_4 , 1.2 mM

KH₂PO₄, 5 mM NaHCO₃, 20 mM HEPES, pH 7.4) containing 5 mM or 25 mM glucose for 60 min at 37°C, and then the medium was collected for detection of insulin secretion using methods previously described (Green et al., 2009). Insulin secretion was determined by Rat/Mouse Insulin ELISA kit (Millipore, Billerica, MA, USA).

2.12. Animals and experimental design

Male ICR mice (4 weeks of age; purchased from Joong Ang Lab Animal Co., Korea) were used. All animals were housed individually in a light- (12h on/12h off) and temperature-controlled room with food and water available ad libitum. The animals were maintained with pelleted food, while tap water was available ad libitum. After an adjustment period of approximately 2 weeks, diabetes was induced by intraperitoneal injection of streptozotocin (150 mg/kg i.p.) dissolved in a freshly prepared citrate buffer (0.1 M, pH 4.5). All STZ injections were administered within 5 min of treatment preparation. The OPA dissolved saline was administered orally into mice, receiving at a dose of 5 mg/kg or 10 mg/kg body weight first at 12 h and then again at 2 h before the administration of STZ (**Fig. 4-1**). To determine the effects of OPA, mice were divided into the following groups; 1) non-treated normal group, 2) STZ group, 3) OPA (5 mg/kg B.W) + STZ group, and 4) OPA (10 mg/kg B.W) + STZ group (n=6 for each group). The day on which the first STZ injection was

administered is defined as day 1. Control animals received citrate buffer alone. At the end of the experimental period, the mice were euthanized by decapitation without anesthesia and trunk blood was collected for biochemical. Later the animals were sacrificed and pancreas was removed, cleaned and washed in ice-cold normal saline for biochemical study. The mice were all treated in accordance with Jeju National University guidelines for the care and use of laboratory animals.

2.13. Measurement of blood glucose, plasma insulin, lipid peroxidation

Every day after 12 h fasting, the blood glucose concentration was monitored in the venous blood from the tail vein using a glucometer (Roche Diagnostics GmbH, Mannheim, Germany). Blood samples were collected into tubes. After centrifugation at $1000 \times g$ for 15 min at 4°C , the plasma was carefully removed from the sample. The levels of plasma insulin were determined using radioimmunoassay with enzyme-linked immunosorbent assay ELISA kit (Linco Research Inc, Billerica, MA, USA). Lipid peroxidation was measured by thiobarbituric acid reactive substances (TBARS) production (Fraga et al., 1988). The removed pancreas homogenized in chilled PBS using a Potter Elvehjem homogenizer and use uncentrifuged whole homogenate for analysis. The TBARS concentrations were determined using TBARS assay kit (ZeptoMetrix, New York, USA). TBARS values were

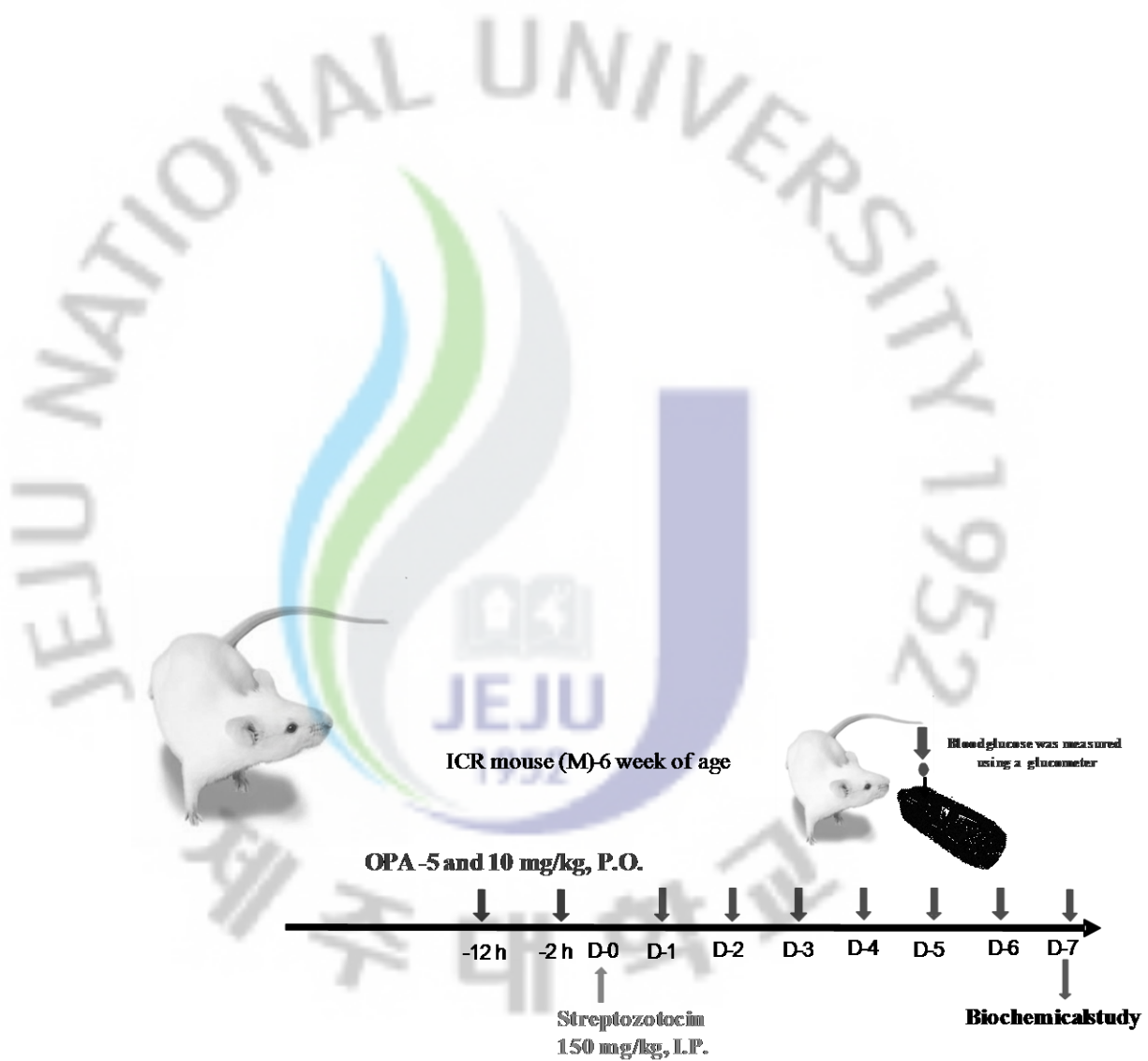


Fig. 4-1. Animals and experimental design.

then expressed as equivalent nmoles of malondialdehyde (MDA).

2.14. Assay of antioxidant enzymes and immunoblotting

The removed pancreas homogenized in PRO-PREP™ Protein Extraction solution (iNtRON Biotechnology, Korea) for 30 min on ice. Then centrifuged at 13,000 rpm at 4°C for 5 min, and transfer supernatants to a fresh tube. The protein concentrations were determined by using BCA™ protein assay kit. Analyses of Antioxidant enzymes activities and immunoblot were described in section 2-7, 10 under method part.

2.15. Statistical analysis

The data are presented as mean \pm standard error (SE). Statistical comparison was performed via the SPSS package for Windows (Version 14). P-values of less than 0.05 were considered to be significant.

3. RESULTS

3.1. Cell viability

Fig. 4-2 shows the effects of OPA on cell viability in RINm5F pancreatic β cells treated with STZ as determined via an MTT assay. When RINm5F pancreatic β cells were treated with STZ only for 24 h, cell viability was reduced significantly. Cell viability was reduced to 50.09% in STZ-treated RINm5F pancreatic β cells, but, OPA protected against the cellular damage induced by STZ in a dose-dependent manner. In particular, pretreatment with 50 $\mu\text{g/ml}$ of OPA along with high glucose treatment resulted in a significant increase in cell viability to 82.65%.

3.2. Lipid peroxidation

As shown in **Fig. 4-3**, the effect of OPA on lipid peroxidation in STZ-treated RINm5F pancreatic β cells was determined by measuring TBARS, a lipid peroxidation product. When RINm5F pancreatic β cells were treated with STZ only for 24 h, TBARS was significantly increased compared to the control. Pretreatment with 50 $\mu\text{g/ml}$ of OPA along with STZ significantly inhibited TBARS formation, indicating protection against lipid peroxidation.

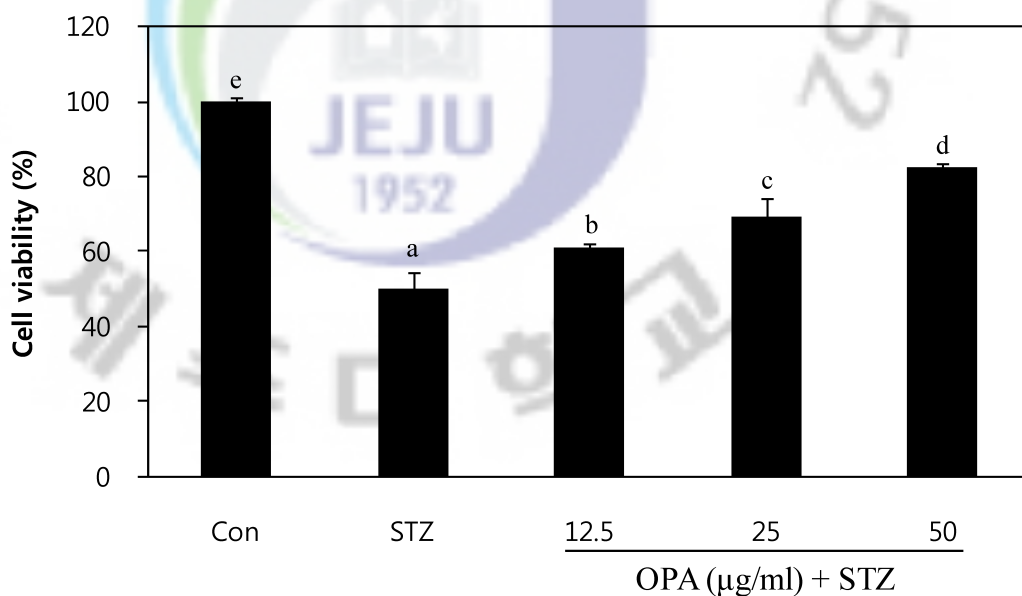


Fig. 4-2. Effect of OPA on cell viability in STZ treated RINm5F pancreatic β cells. Cells (1×10^5 cells/well) in wells of 96-well plates were preincubated with the indicated concentrations of OPA for 3 h, and then incubated with STZ for 24 h. Each value is expressed as mean \pm S.E. ^{a-c}Values with different alphabets are significantly different at $p < 0.05$ as analyzed by Duncan's multiple range test.

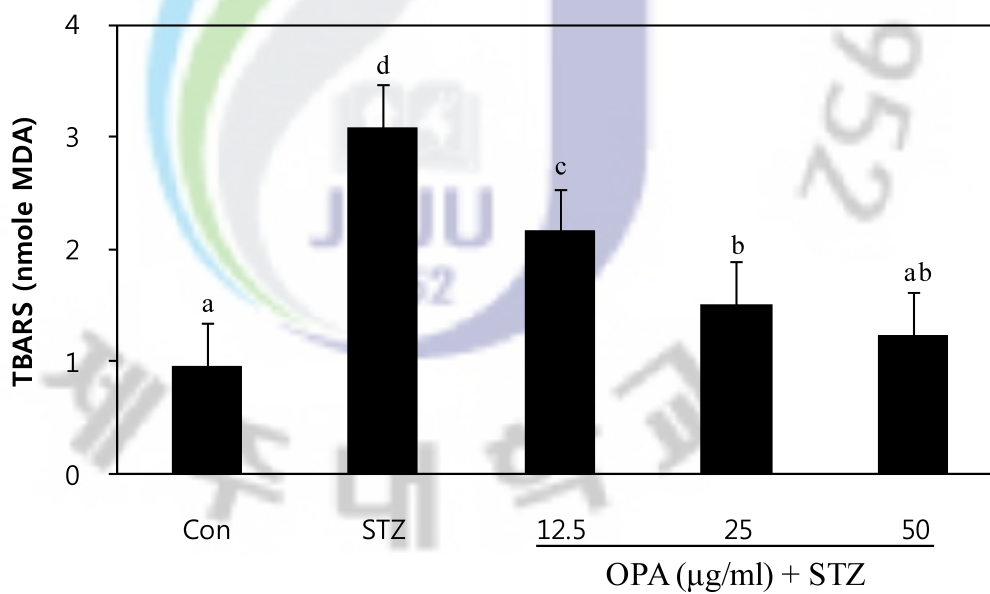


Fig. 4-3. Effect of OPA on TBARS generation in STZ treated RINm5F pancreatic β cells. Cells (1×10^5 cells/well) in wells of 24-well plates were preincubated with the indicated concentrations of OPA for 3 h, and then incubated with STZ for 24 h. Each value is expressed as mean \pm S.E. ^{a-c}Values with different alphabets are significantly different at $p < 0.05$ as analyzed by Duncan's multiple range test.

When the cells were treated with 50 $\mu\text{g/ml}$ of OPA, TBARS was reduced significantly, by 1.24 nmol MDA.

3.3. Intracellular ROS generation

As demonstrated in **Fig. 4-4A**, the effects of OPA on intracellular ROS generation in RINm5F pancreatic β cells treated with STZ determined using flow cytometry. Fluorescence intensity values displayed level of ROS detected by DCF-DA fluorescence dye. The fluorescence intensity value in RINm5F pancreatic β cells increased significantly after treatment with STZ as compared with control, which contained no sample or STZ. When RINm5F pancreatic β cells were exposed with STZ, fluorescence intensity values significantly increased to 201. However, OPA pretreatment dose-dependently reduced the fluorescence intensity values in the cells induced by treatment with STZ. In particular, pretreatment with 50 $\mu\text{g/ml}$ of OPA resulted in a significant reduction in fluorescence intensity values to 167. OPA significantly reduced the elevated ROS levels induced by STZ. In addition, the fluorescence intensity of DCF-DA staining using fluorescence microscope was enhanced in the STZ treated RINm5F pancreatic β cells as shown in **Fig. 4-4B**. OPA reduced the green fluorescence intensity upon STZ treatment, thus reflecting a reduction in ROS generation. These data suggest that OPA possessed ROS scavenging activity.

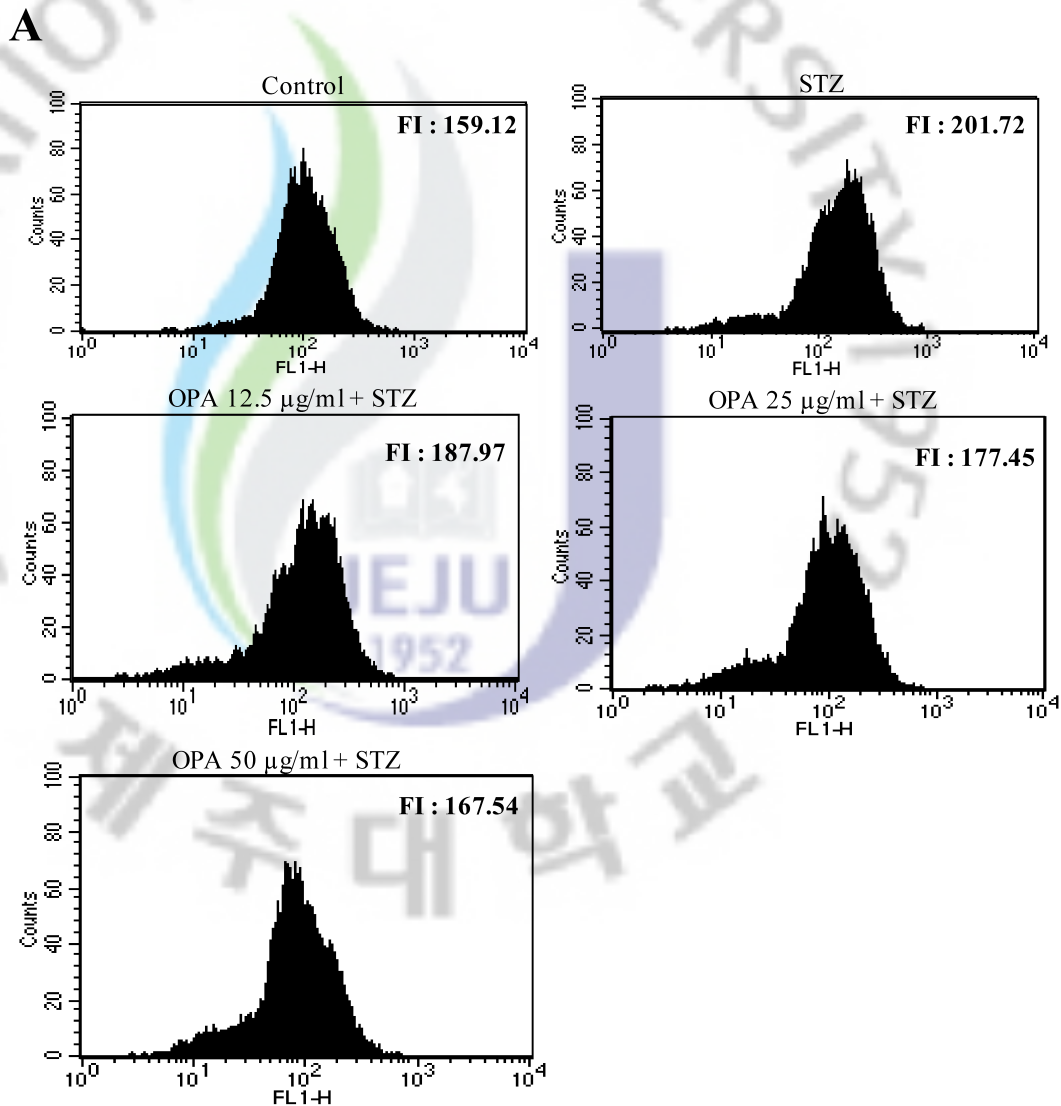


Fig. 4-4. Effect of OPA on intracellular ROS generation in STZ treated RINm5F pancreatic β cells. (A) The intracellular ROS generated was detected using flow cytometry after DCF-DA addition. (B) Images illustrate the increase in green fluorescence intensity of DCF produced by ROS in STZ treated cells as compared to control and lowered fluorescence intensity in STZ treated cells with OPA. A, Control; B, 10 mM STZ; C, 12.5 μ g/ml OPA + STZ; D, 25 μ g/ml OPA + STZ; E, 50 μ g/ml OPA + STZ.

B

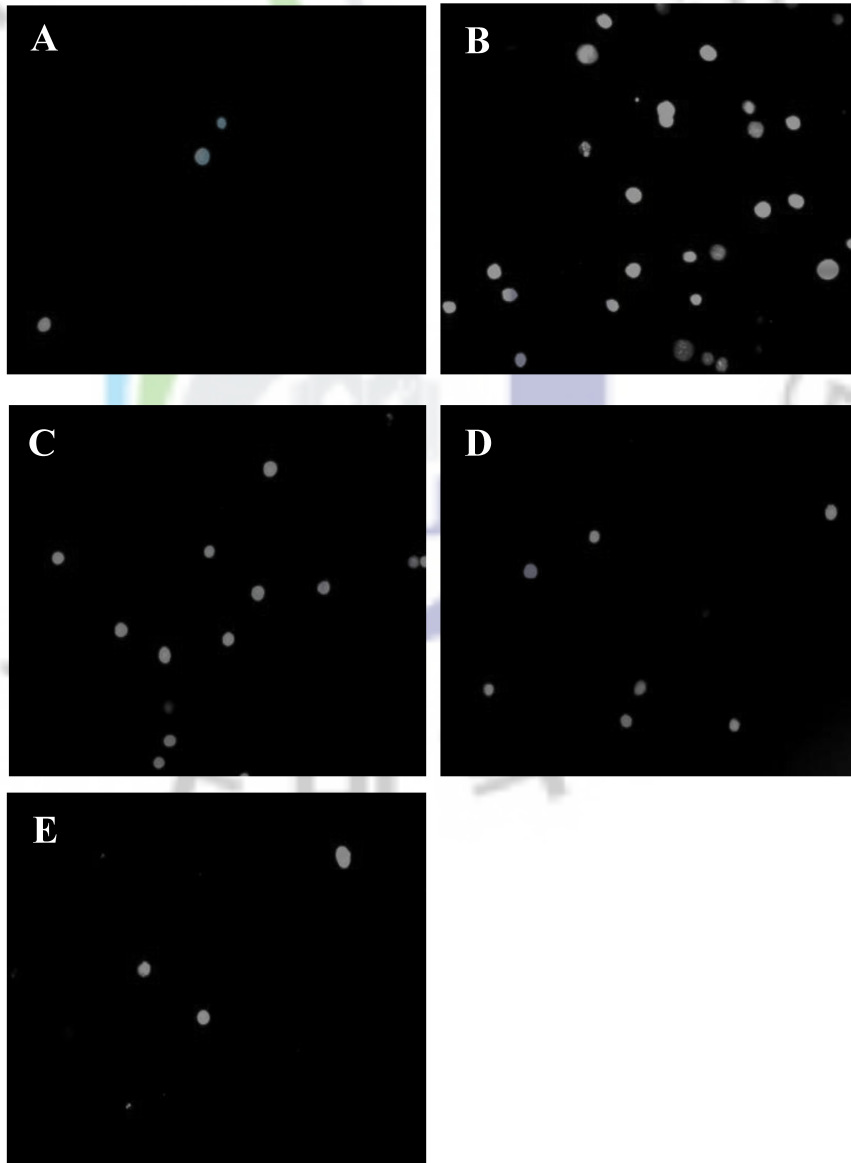


Fig. 4-4. Continued.

3.4. Inhibitory effects of DNA damage

The abilities of OPA to inhibit cellular DNA damage in STZ treated cells were investigated.

Damage to cellular DNA induced by STZ exposure was detected using an alkaline comet

assay. The exposure of cells to STZ increased the comet parameters of tail length and

percentage of DNA in the cell tails. When cells were exposed to STZ, the DNA percentage

in the tail increased 41% as shown in **Fig. 4-5A** and **B**. However, OPA pretreatment dose-dependently reduced the cellular DNA damage in the cells induced by treatment with STZ.

In particular, pretreatment with 50 µg/ml of OPA resulted in a significant reduction in the tail length to 11%, which indicated a protective effect of OPA on STZ induced DNA damage.

3.5. Antioxidant enzymes activity

Cells are protected from activated oxygen species by endogenous antioxidant enzymes

including superoxide dismutase (SOD), catalase (CAT), and glutathione peroxidase (GSH-

px). The effects of OPA on antioxidant enzyme activities in STZ-treated RINm5F pancreatic

β cells are shown in **Table 4-1**. Only treatment for 24 h with STZ significantly attenuated the

SOD activity of RINm5F pancreatic β cells. The pretreatment of RINm5F pancreatic β cells

with OPA increased SOD activity in the STZ-treated cells. Before the cells were treated with

50 µg/ml of OPA, SOD activity was significantly increased to 86.09%. The STZ treatment

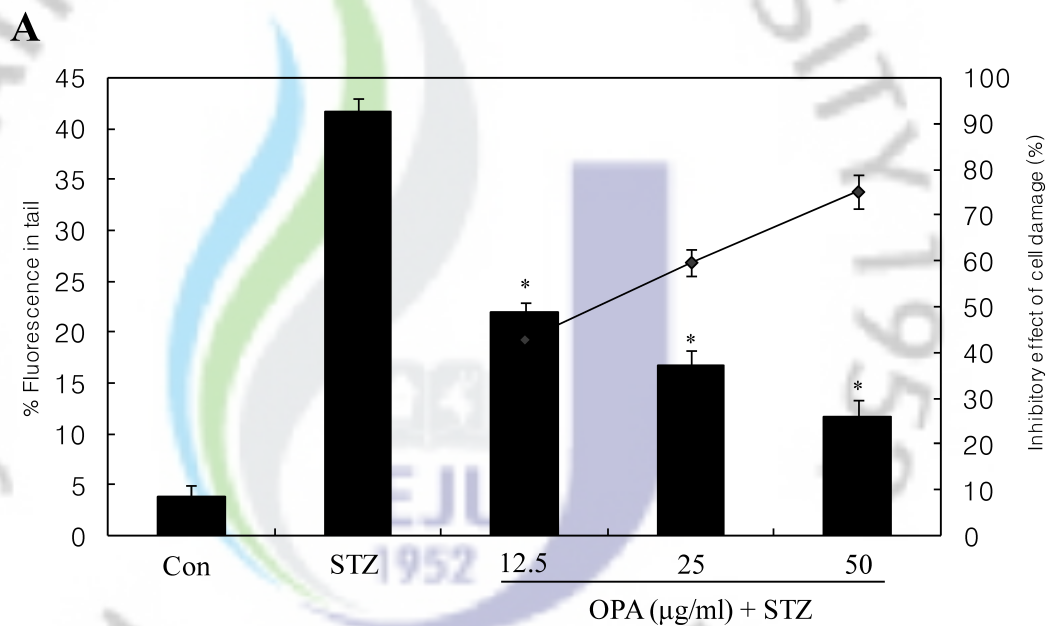


Fig. 4-5. Inhibitory effect of OPA on STZ-induced DNA damages. The damaged cells on STZ treatment was determined by comet assay. (A) □, % Fluorescence in tail; ◆, Inhibitory effect of cell damage. (B) Photomicrographs of DNA damage and migration observed under OPA. A, Control; B, 10 mM STZ; C, 12.5 µg/ml OPA + STZ; D, 25 µg/ml OPA + STZ; E, 50 µg/ml OPA + STZ. Experiments were performed in triplicate and the data are expressed as mean ±SE. Statistical evaluation was performed to compare the experimental groups and corresponding control groups. *, P<0.05

B

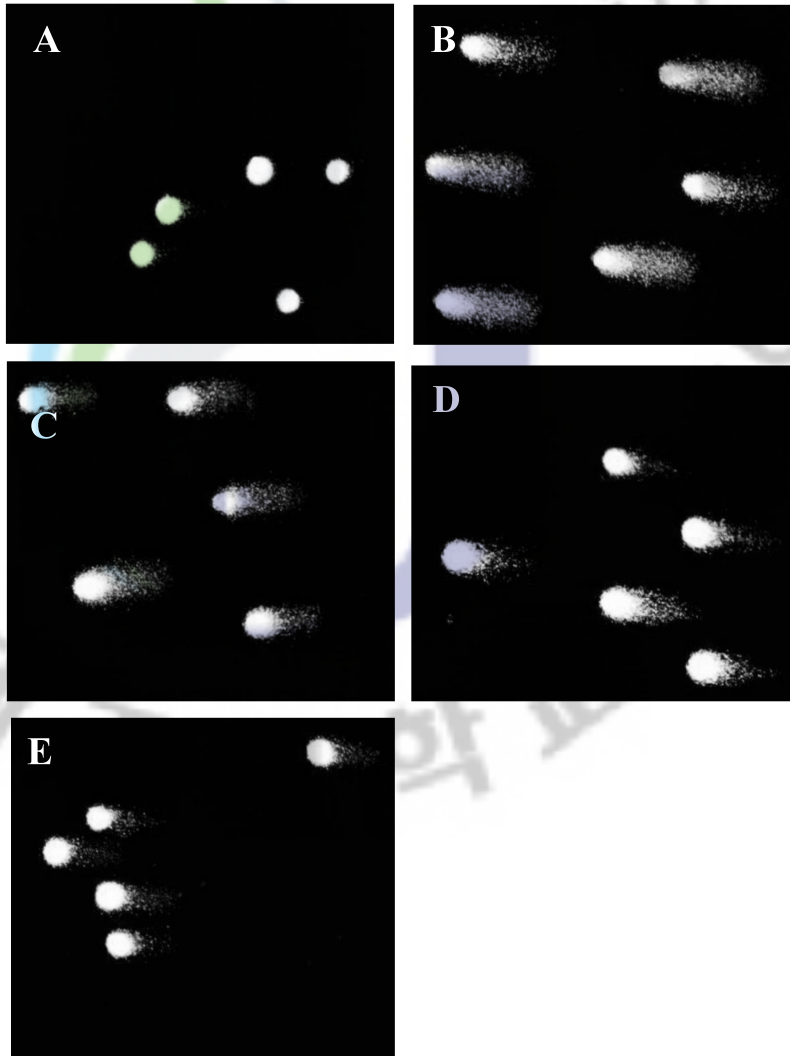


Fig. 4-5. Continued.

reduced CAT activity relative to that measured in the control. OPA pretreatment increased CAT activity in a dose-dependent manner. The treatment of RINm5F pancreatic β cells with OPA increased CAT activity in the STZ-treated cells. Before the cells were treated with 50 $\mu\text{g}/\text{ml}$ of OPA, CAT activity was increased significantly to 1.06 $\mu\text{mole}/\text{mg}$ protein. GSH-px activity in RINm5F pancreatic β cells treated with STZ was significantly reduced in comparison to the control. Preretreatment of STZ-treated RINm5F pancreatic β cells with OPA resulted in an increase of GSH-px activity, as shown by the measured GSH-px activity of 3.41 $\mu\text{mole}/\text{mg}$ protein at a dosage of 50 $\mu\text{g}/\text{ml}$.

3.6. Protective effects of apoptosis

By flow cytometry analysis with PI staining, **Fig. 4-6A** shows, when RINm5F pancreatic β cells were treated with STZ, the proportion of cells with sub-G1 DNA content to 35.69% increased compared to the control. However, OPA pretreatment dose-dependently reduced the sub-G1 DNA contents in the cells induced by the treatment with STZ. In particular, pretreatment with 50 $\mu\text{g}/\text{ml}$ of OPA resulted in a significant reduction in sub-G1 DNA contents. In addition protective effect of apoptosis by OPA was further studied by Hoechst 33342 staining assay. Apoptotic cell death was confirmed by apoptotic body and nuclear condensation as detected by Hoechst 33342 staining assay. The control, without the OPA and

Table 4-1. Effects of OPA on antioxidant enzyme activities in STZ treated RINm5F pancreatic β cells.

	Con	OPA ($\mu\text{g/ml}$) + STZ			
		0	12.5	25	50
SOD activity (%)	90.72 \pm 7.79 ^d	55.36 \pm 3.32 ^a	74.93 \pm 8.30 ^b	80.51 \pm 7.36 ^c	86.09 \pm 7.50 ^d
CAT ($\mu\text{mole/mg protein/min}$)	1.08 \pm 0.05 ^d	0.39 \pm 0.02 ^a	0.79 \pm 0.03 ^b	0.90 \pm 0.03 ^c	1.06 \pm 0.04 ^d
GSH-px ($\mu\text{mole/mg protein}$)	3.81 \pm 0.08 ^c	1.33 \pm 0.03 ^a	2.57 \pm 0.06 ^b	2.73 \pm 0.07 ^{bc}	3.41 \pm 0.09 ^c

Cells (1×10^6 cells) in 10 mm dishes were preincubated with the indicated concentrations of OPA for 3 h, and then incubated with STZ for 24 h. SOD, Super oxide dismutase activity; CAT, Catalase activity; GSH-px, Glutathione peroxidase activity. Each value is expressed as mean \pm S.E. ^{a-d} Values with different alphabets differ significantly at $p < 0.05$ as analyzed via Duncan's multiple range test.

STZ showed clear image and exhibited no apoptotic body. However, obvious cell damage was observed in the cells treated with STZ (**Fig. 4-6B**). Cells pre-treated with OPA at difference concentration (**Fig. 4-6B**) dramatically reduced nuclear condensation and apoptotic bodies. These data indicate that OPA may have notable apoptosis inhibition activity against RINm5F pancreatic β cells.

3.7. OPA modulated the expression levels of apoptosis-related protein in RINm5F pancreatic β cells

To determine whether OPA induces expression of proteins related to STZ-induced apoptosis, OPA concentrations of 25 and 50 $\mu\text{g/ml}$ were pretreated to RINm5F pancreatic β cells. As shown in **Fig. 4-7**, the level of the P53 and Bax pro-apoptotic protein expression was clearly higher in STZ-treated cells than in control cells. However, the expression level by the pretreatment of OPA was reduced markedly. In addition, expression of anti-apoptosis related protein such as Bcl-xL tends to decrease in STZ-treated cells. On the other hand, the cells pretreated with OPA showed higher Bcl-xL expression than the STZ-treated cells. Furthermore, expression levels of the active form of cleaved caspase-3, -9 and PARP were increased significantly in RINm5F pancreatic β cells treated with STZ. However, the

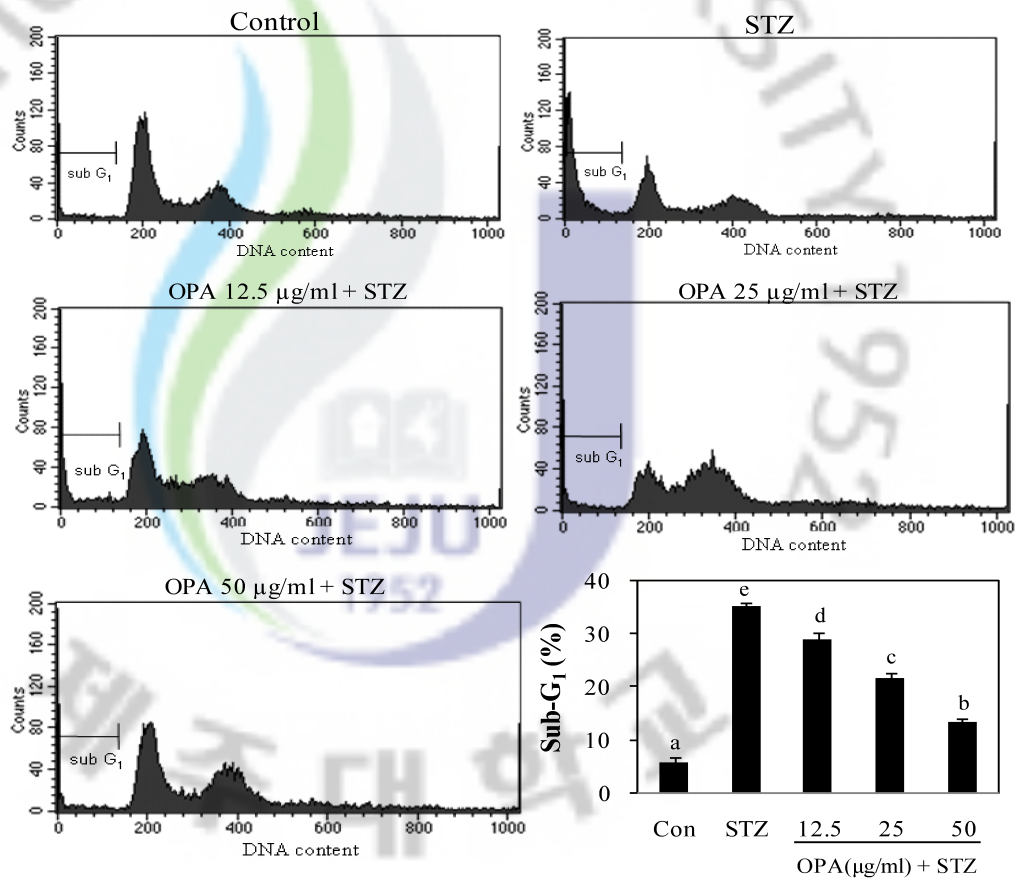
A

Fig. 4-6. Protective effect of OPA on STZ-induced apoptosis in RINm5F pancreatic β cells. The cells were pretreated with the indicated concentrations of OPA for 3 h, and then incubated with STZ for 24 h. (A) The cells were stained with PI and analyzed by flow cytometry. (B) Apoptotic bodies were stained with Hoechst 33342 solution and then observed under a fluorescent microscope using a blue filter. A, Control; B, 10 mM STZ; C, 12.5 μ g/ml OPA + STZ; D, 25 μ g/ml OPA + STZ; E, 50 μ g/ml OPA + STZ. Each value is expressed as mean \pm S.E. ^{a-e} Values with different alphabets differ significantly at $p < 0.05$ as analyzed via Duncan's multiple range test.

B

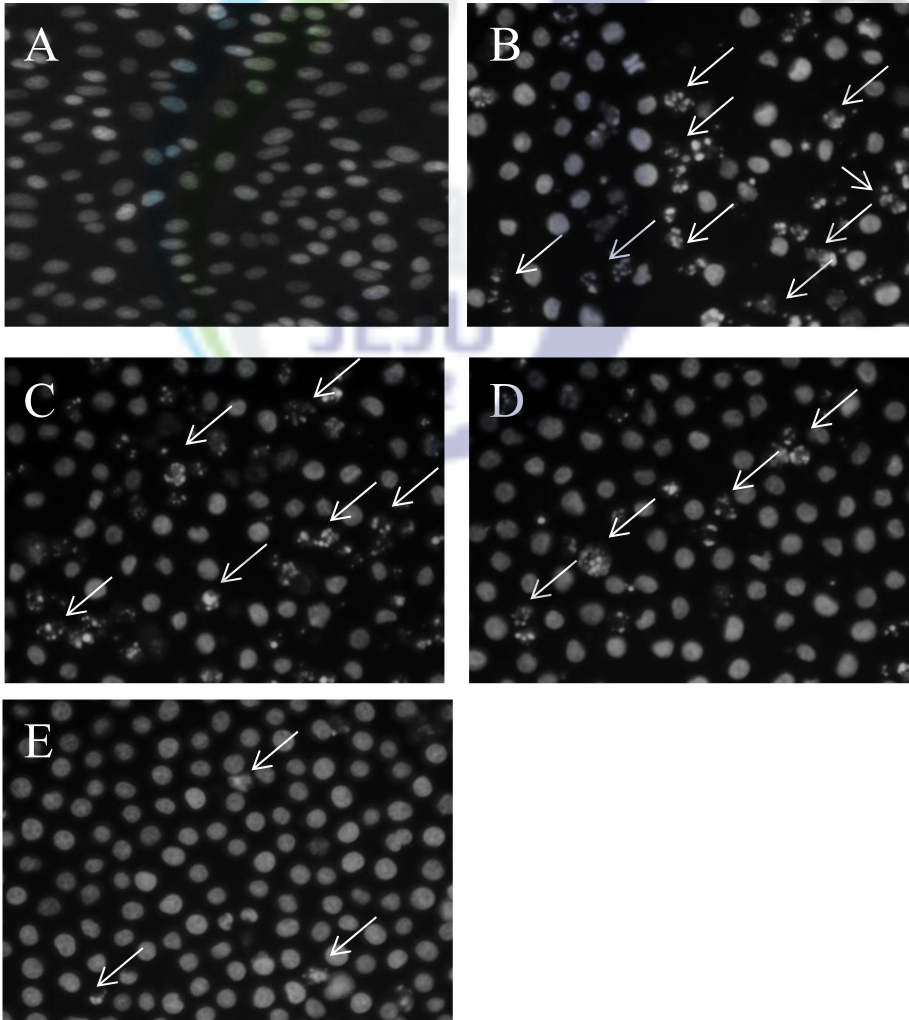


Fig. 4-6. Continued.

pretreatment of RINm5F pancreatic β cells with OPA results in a reduce in expression of cleaved caspase-3, -9 and PARP in the STZ treated cells.

3.8. Glucose-stimulated insulin secretion

As shown in **Fig. 4-8**, glucose-stimulated insulin secretion in RINm5F pancreatic β cells was reduced significantly as the result of STZ treatment. Also, after culturing with STZ, stimulation with 25 mM glucose resulted in a 2.5-fold increase in insulin secretion as compared with 5 mM glucose treatment. OPA pretreatment dose-dependently increased insulin secretion in the cells stimulated with 5 mM and 25 mM glucose under treated STZ conditions.

3.9. Levels of blood glucose and plasma insulin and body weight *in vivo*

To assess the potential of OPA to protect against STZ-mediated diabetes, ICR mice were administered with OPA, and then injected with a single high dose of STZ (150 mg/kg). Levels of fasting blood glucose at day 7 were significantly higher in the STZ-treated group than in the normal group (**Table 4-2**). Conversely, STZ-treated group exhibited decreased body weight. Reduction in body weight along with an increase in blood glucose level is a marker for the development of diabetes. This pathophysiology has been observed in STZ

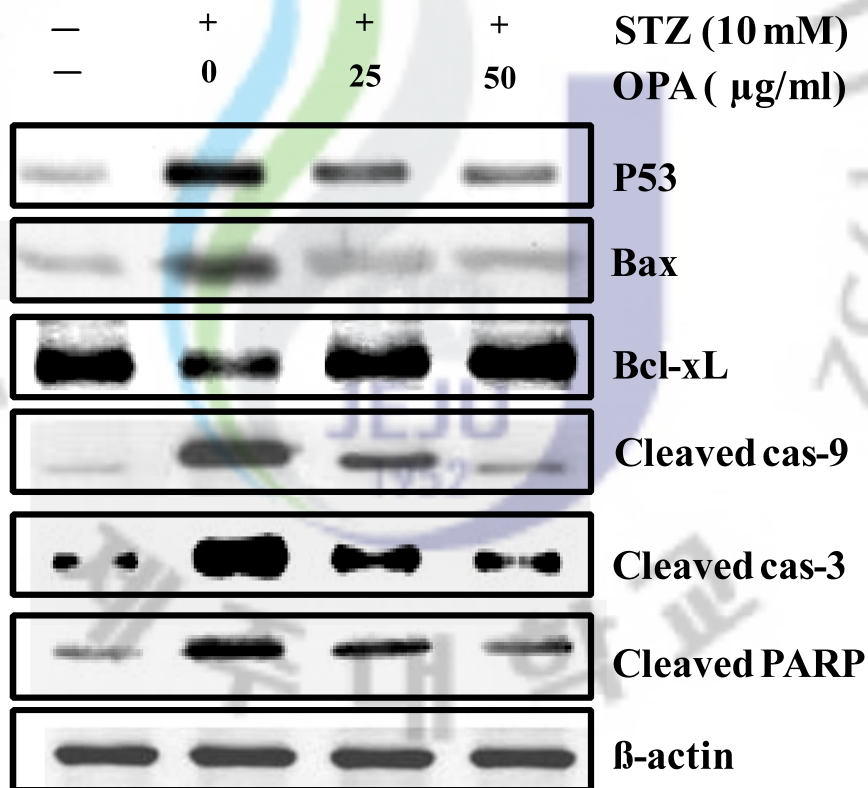


Fig. 4-7. OPA modulated the expression levels of apoptosis-related protein in RINm5F pancreatic β cells. Cells were pretreated with or without the indicated concentrations of OPA for 3 h, and then treated with the STZ for 24 h. The cell lysates were analyzed via Western blotting using anti-P53, anti-Bax, anti-Bcl-xL, anti-caspase-3, -9 and anti-PARP. Figures are representative of three independent experiments.

treated animals suggesting their diabetic nature. OPA pretreated group, however, significantly lowered the fasting blood glucose level and prevented the loss in body weight compared to the STZ-treated group. Plasma insulin levels were significantly lower in the STZ group than in the normal group. However, the plasma insulin levels were significantly higher in the OPA pretreated group than in the STZ group (**Table 4-2**).

3.10. Lipid peroxidation and antioxidant enzyme activities *in vivo*

Table 4-3 shows the level of malondialdehyde (MDA), a secondary product of lipid peroxidation in the pancreatic tissue homogenate. When mice were treated with STZ group (STZ treated group), MDA level was significantly increased compared to the normal group (non-treated control group). However, OPA pretreated group (OPA+STZ group) significantly decreased the MDA level compared to the STZ group. **Table 4-3** demonstrate the activities of SOD, CAT and GSH-px in pancreas of normal group, STZ group and OPA+STZ group. STZ group significantly decreased the activities of SOD, CAT and GSH-px in pancreatic tissue compared to the normal group. The activities of SOD, CAT and GSH-px of pancreas were significantly increased in OPA pretreated group when compared with STZ group.

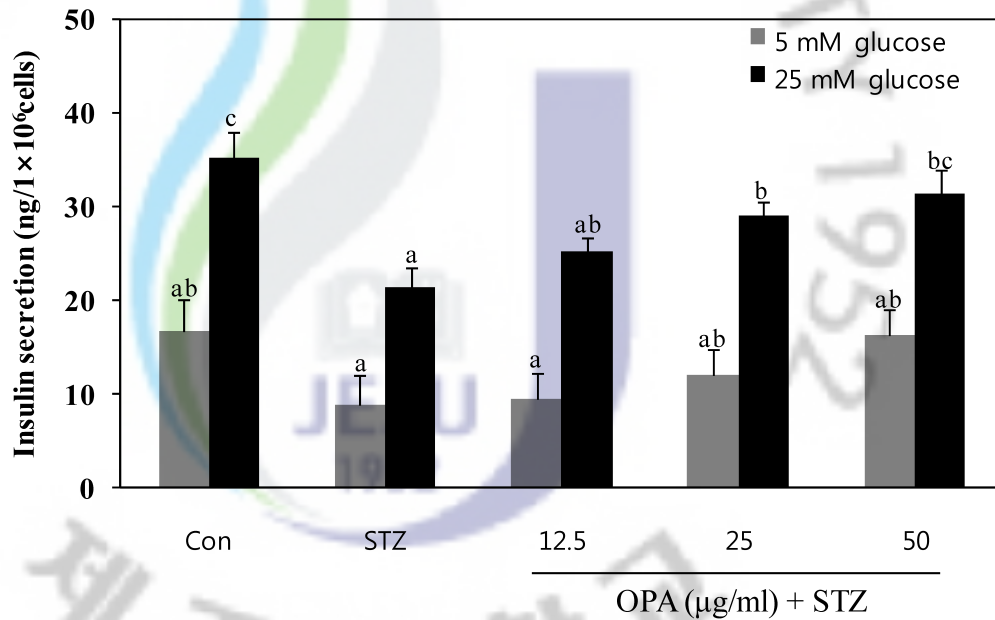


Fig. 4-8. Effects of OPA on insulin secretion in STZ-treated RINm5F pancreatic β cells.

Cells (1×10^6) in 10 mm dishes were pretreated with the indicated concentrations of OPA for 3 h, and then incubated with STZ for 24 h. Insulin secretion from RIN-m5F cells in response to glucose (5 and 25 mM) concentration. Each value is expressed as mean \pm S.E. ^{a-c}Values with different alphabets differ significantly at $p < 0.05$ as analyzed by Duncan's multiple range test.

Table 4-2. Effects of OPA on the levels of blood glucose, plasma insulin and body weight in STZ-treated mice¹.

	Normal ²	STZ ³	OPA-5 ⁴	OPA-10 ⁵
Blood glucose (mg/dl)				
Initial	129.0±20.8 ^a	138.3±20.0 ^a	133.0±33.8 ^a	129.3±9.1 ^a
Final	122.7±31.1 ^a	356.3±41.0 ^c	175.7±38.7 ^b	142.0±28.8 ^{ab}
Plasma insulin (ng/ml)				
	2.1±0.23 ^c	0.3±0.07 ^a	1.1±0.32 ^b	1.8±0.16 ^c
Body weight (g)				
Initial	25.9±0.87 ^a	27.8±1.28 ^{ab}	23.8±0.57 ^a	23.8±3.38 ^a
Final	27.3±4.34 ^c	24.3±4.28 ^{ab}	21.6±5.33 ^a	23.3±3.38 ^b

The OPA dissolved saline was administered orally into mice, receiving at a dose of 5 mg/kg or 10 mg/kg body weight first at 12 h and then again at 2 h before the administration of STZ .

¹ Means ± SE (n = 6).

² Non-treated normal group.

³ STZ -treated group.

⁴ OPA (5 mg/kg B.W) + STZ group.

⁵ OPA (10 mg/kg B.W) + STZ group.

^{a-c} Means not sharing a common letter are significantly different between groups (P < 0.05).

Table 4-3. Effects of OPA on the lipid peroxidation and antioxidant enzyme activities in STZ-treated mice¹.

	Normal ²	STZ ³	OPA -5 ⁴	OPA -10 ⁵
TBARS (nmol/ mg tissue)	1.30±0.33 ^a	4.84±0.79 ^c	3.19±0.19 ^b	2.41±0.12 ^{ab}
SOD activity (%)	87.98±2.79 ^c	71.09±3.12 ^a	78.95±3.45 ^b	85.63±2.59 ^c
CAT(μmole/mg protein/min)	6.41±0.14 ^c	4.86±0.42 ^a	5.25±0.95 ^b	5.67±0.48 ^{bc}
GSH-px (μmole/mg protein)	1.58±0.09 ^c	0.99±0.03 ^a	1.30±0.08 ^b	1.44±0.02 ^c

The OPA dissolved saline was administered orally into mice, receiving at a dose of 5 mg/kg or 10 mg/kg body weight first at 12 h and then again at 2 h before the administration of STZ .

¹ Means ± SE (n = 6).

² Non-treated normal group.

³ STZ -treated group.

⁴ OPA (5 mg/kg B.W) + STZ group.

⁵ OPA (10 mg/kg B.W) + STZ group.

^{a-c} Means not sharing a common letter are significantly different between groups (P < 0.05).

3.11. Effects of OPA on expression levels of apoptosis-related protein *in vivo*

To determine whether OPA induces expression of proteins related to STZ-induced apoptosis *in vivo*, ICR mice were administered with OPA, and then injected with a single high dose of STZ (150 mg/kg). As shown in **Fig. 4-9**, the level of the P53 and Bax pro-apoptotic protein expression was clearly higher in STZ-treated group than in normal group. However, the expression level by the OPA pretreated group were reduced markedly. In addition, expression of anti-apoptosis related protein such as Bcl-XL tends to decrease in STZ-treated group. On the other hand, the OPA pretreated group showed higher Bcl-XL expression than the STZ-treated group. Furthermore, expression levels of the active form of cleaved caspase-3 was increased significantly in the STZ-treated group. However, the OPA pretreated group results in an reduce in expression of cleaved caspase-3 in the STZ treated group.

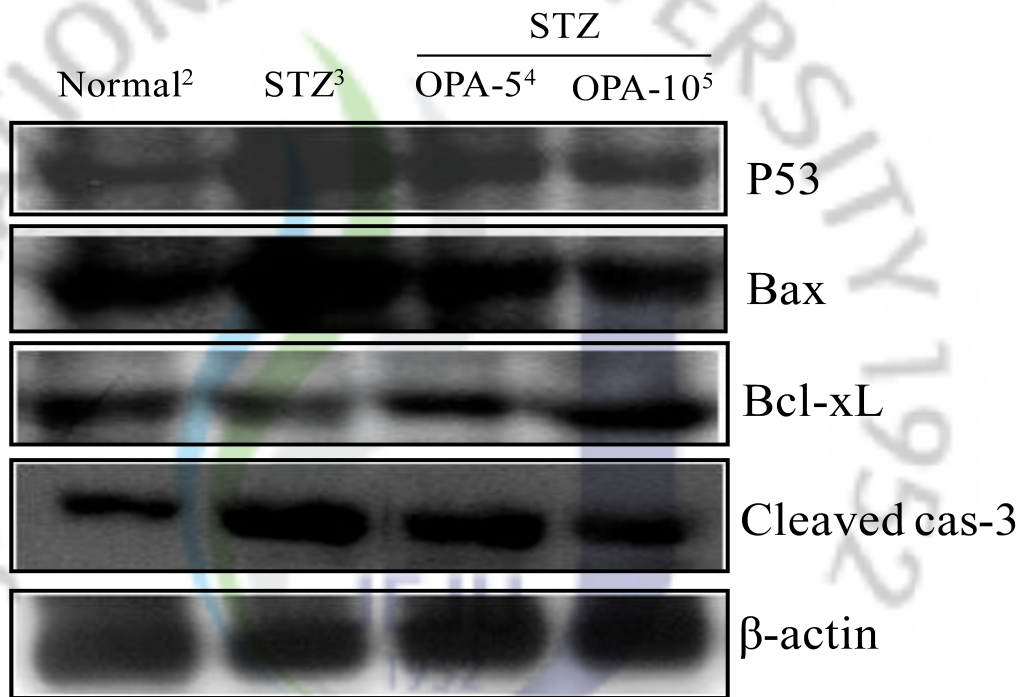


Fig. 4-9. Effects of OPA expression levels of apoptosis-related protein in STZ-treated mice¹. The OPA dissolved saline was administered orally into mice, receiving at a dose of 5 mg/kg or 10 mg/kg body weight first at 12 h and then again at 2 h before the administration of STZ. The pancreatic tissue lysates were analyzed via Western blotting using anti-P53, anti-Bax, anti-Bcl-xL and anti-caspase-3. Figures are representative of experiments.

¹ Means \pm SE (n = 6).

² Non-treated normal group.

³ STZ -treated group.

⁴ OPA (5 mg/kg B.W) + STZ group.

⁵ OPA (10 mg/kg B.W) + STZ group.

4. DISCUSSION

Oxidative stress induced by the increase of hyperglycemia causes diabetes-associated pathological damage (Fraga et al., 1988; Uemura et al., 2001). Acute streptozotocin (STZ) injection has been used to study cellular or tissue oxidative damage because it produces reactive oxygen species and reduces antioxidant enzyme activity, especially in pancreatic tissues (Coskun et al., 2005). In fact, streptozotocin can stimulate H₂O₂ generation in islet cells (Friesen et al., 2004) where the activity of antioxidant enzymes such as superoxide dismutase, catalase and glutathione peroxidase is relatively low when compared to other tissues (Tiedge et al., 1997). By STZ, most islet cells are impacted to death and remaining islet cells almost exhibit a significant decrease in the activity of these enzymes compared to normal rats (Srivivasan et al., 2003). Several studies have demonstrated that exposure of β cells to STZ results in β cell dysfunction and apoptosis (Srivivasan et al., 2003; Coskun et al., 2005). Pancreatic β cell dysfunction plays a key role in the pathogenesis of type 2 diabetes. Thus, in order to reduce the risk of pathological damage such as diabetes, it is important to find ways to protect the β cell damage induced by oxidative stress. There is a great deal of interest in identifying antioxidant compounds that do not cause side effects or exhibit toxicity.

The phlorotannins, which constitute one of the most diverse and widespread groups of natural compounds, are probably the most abundant natural phenolics found in marine algae.

These compounds exhibit a broad spectrum of chemical and biological activities, including antioxidant properties (Kang et al., 2003; Ahn et al., 2007; Heo et al., 2009). Present study demonstrates the prophylactic role of OPA, a kind of phlorotannin, was a marine algal polyphenolic compound isolated from *I. sinicola* against STZ-induced pancreatic β cell damage developed under hyperglycemia *in vitro* and *in vivo*.

To measure cell viability, MTT assays were conducted. The exposure of RINm5F pancreatic β cells to STZ resulted in significant reductions in cell viability. However, OPA pretreatment was shown to inhibit cell death, thereby suggesting that OPA protects RINm5F pancreatic β cells against STZ-induced cytotoxicity.

Lipid peroxidation may be a form of cell damage mediated by free radicals (Sevanian and Hochstein, 1985). Presently, STZ treatment has been shown to induce lipid peroxidation in RINm5F pancreatic β cells and OPA was shown to effectively inhibit TBARS formation. One of the more serious consequences of lipid peroxidation is damage to biomembranes such as mitochondrial and plasma membranes. During lipid peroxidation, low molecular-weight end products, most notably malondialdehyde (MDA), are formed via the oxidation of polyunsaturated fatty acids. These end products can react with two molecules of thiobarbituric acid to generate a pinkish-red chromogen. The presently-demonstrated protective action of OPA on TBARS formation can be attributed to its antiperoxidative

effects.

High ROS levels induce oxidative stress, which can result in a variety of biochemical and physiological lesions. Such cellular damage frequently impairs metabolic function, and result in cell death (finkel and Holbrook, 2000). Our results demonstrated that the treatment of RINm5F pancreatic β cells with STZ significantly increased intracellular ROS levels. However, OPA inhibited STZ-induced ROS generation. These results indicate that OPA alleviates oxidative stress via the inhibition of ROS generation induced by STZ treatment.

ROS may play a major role as endogenous initiators and promoters of DNA damage and mutations that contribute to cancer, diabetes and other age-related diseases. Oxidative DNA damage is shown to be extensive and has been proposed as a major cause of the physiological changes associated with aging and the degenerative diseases related to aging, such as cancer and diabetes (Ames, 1989). Our results demonstrated that the treatment of RINm5F pancreatic β cells with STZ significantly increased cellular DNA damage. However, OPA protected STZ-induced cellular DNA damage. Therefore, we expected that OPA would protect against oxidative DNA damage, and may reduce the risk of STZ-induced diabetic complications.

Cells are protected from activated oxygen species by endogenous antioxidant enzymes such as catalase (CAT), superoxide dismutase (SOD), and glutathione peroxidase (GSH-px). We

observed in this study that the application of STZ treatment to RINm5F pancreatic β cells with OPA resulted in increases in CAT activity, SOD activity, and GSH-px activity. SOD, the endogenous scavenger, catalyzes the dismutation of the highly reactive superoxide anion to H_2O_2 (Husain and Somani, 1998). GSH-px catalyzes the reduction of H_2O_2 at the expense of reduced GSH. H_2O_2 is also scavenged by CAT (Runnegar et al., 1987). The reduced activities of both CAT and GSH-px in the RINm5F pancreatic β cells treated with STZ demonstrate a highly reduced capacity to scavenge H_2O_2 produced in the cells, with increases in ROS and oxidative stress occurring in response to STZ treatment (Alptekin et al., 1996). High superoxide anion radical production inhibits CAT activity (Kono and Fridovich, 1982). The excess of the superoxide anion radical, as a consequence of a reduction in SOD activity, might prove responsible for the reduction in the activities of CAT in STZ-treated RINm5F pancreatic β cells.

ROS are by products of normal cellular oxidative stress processes, and are generated in the mitochondria and from other sources. They inflict serious damages on nucleic acids, protein and membrane lipids, and they have been suggested to regulate the processes involved in the initiation of apoptotic signaling. Several recent studies have demonstrated that ROS generation performs a crucial function in the pro-apoptotic activities. Members of the Bcl-2 family (such as Bcl-xL) of proteins are critical regulators of the apoptotic pathway (Zanke et

al., 1996). Bcl-2 and Bcl-xL are an upstream molecule in the apoptotic pathway and is identified as a potent suppressor of apoptosis (Szatrowski and Nathan, 1991). Previous reports have demonstrated that Bcl-2 family-mediated caspase-3 activation is responsible for ROS-induced apoptosis (Chen and Chang, 2009). Caspase-3, -9 is one of the key executioners of apoptosis, as it is cleavage of many key proteins such as the nuclear enzyme poly (ADP-ribose) polymerase (PARP) (Fernandes-Alnemri et al., 1994). In this study, we demonstrate that OPA protects damage in RINm5F pancreatic β cells under STZ treatment. These effects were mediated by suppressing apoptosis and were associated with increasing in anti-apoptotic Bcl-XL expression, and reduces in pro-apoptotic cleaved caspase 3, 9, PARP and P53 expression. In addition, Cell cycle analysis was performed to determine the proportion of apoptotic sub-G₁ hypodiploid cells. The exposure of RINm5F pancreatic β cells to STZ resulted in increases in apoptosis cells rate. However, OPA pretreatment was shown to reduce the number of apoptosis cells. The results of two assays provide substantial evidence that OPA plays a protective role during STZ-induced apoptosis.

Pancreatic β cells perform an important function in maintaining glucose homeostasis via the secretion of insulin in response to changes in the extracellular glucose (Hou et al., 2008). Previous data suggested that the oxidative stress induced by STZ exerts a variety of harmful effects, including the inhibition of glucose-stimulated insulin secretion (GSIS), impairment

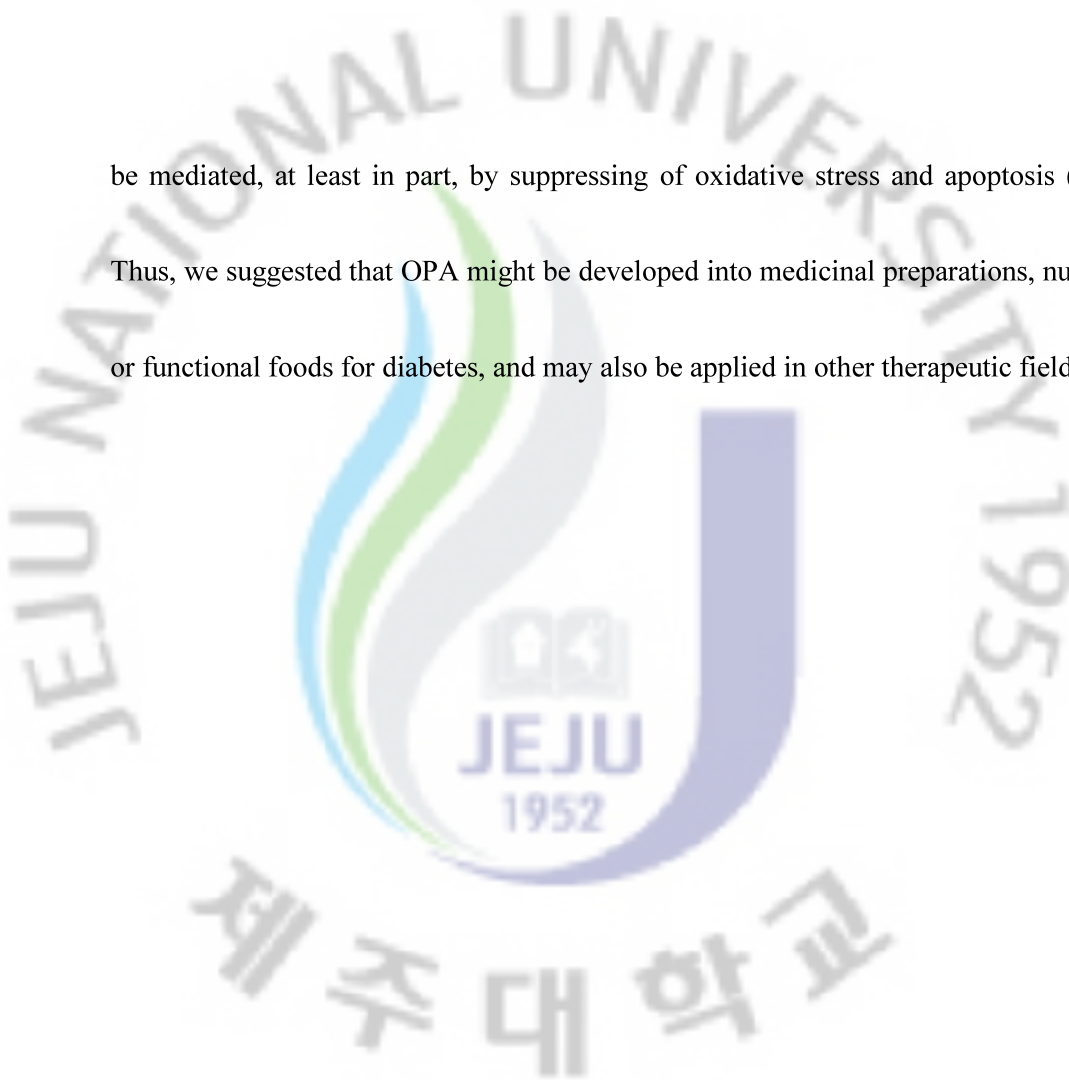
of insulin gene expression, and the induction of cell death in β cells (Kaneto et al., 2005). In this study, we demonstrate that OPA increases insulin secretion in pancreatic β -cells under STZ treatment. These effects were mediated by reducing oxidative stress and were associated with reductions in ROS generation, and increases in cell survival.

Present study demonstrated the prophylactic role of OPA against STZ-induced β cells damage *in vitro*. Therefore, additionally, we investigated the protective effects of OPA against pancreatic β cells damage in STZ-induced diabetic mice. Thereby, we demonstrate that OPA not only protected RINm5F pancreatic β cells against STZ toxicity, but also protected against STZ-induced diabetes. OPA treatment prior to STZ administration reduces blood glucose level and increases plasma insulin level. The weight loss detected in the STZ treated animals is most likely due to the induction of insulinitis and/or the lack of insulin. No weight loss was registered in the animals treated with OPA prior to STZ, probably those animals were not as hyperglycemic as that of STZ treated group. Moreover, OPA treatment prior to STZ administration was found to inhibit lipid peroxidation and apoptosis, and increase of antioxidant enzyme activities.

In summary, this study is the first to demonstrate that OPA has a β -cell protective effect. Specifically, OPA protected β -cells from STZ-induced injury *in vitro* and counteracted the diabetes development in response to streptozotocin *in vivo*. This β -cell protective effect may

be mediated, at least in part, by suppressing of oxidative stress and apoptosis (**Fig. 4-10**).

Thus, we suggested that OPA might be developed into medicinal preparations, nutraceuticals, or functional foods for diabetes, and may also be applied in other therapeutic fields.



REFERENCES

- Ahn, G.N., Kim, K.N., Cha, S.H., Song, C.B., Lee, J.H., Heo, M.S., Yeo, I.K., Lee, N.H., Jee, Y.H., Kim, J.S., Heu, M.S., Jeon, Y.J., 2007. Antioxidant activities of phlorotannins purified from *Ecklonia cava* on free radical scavenging using ESR and H₂O₂ –mediated DNA damage. *Eur Food Res Technol.* 226, 71-79.
- Ames, B.N., 1989. Endogeneous oxidative DNA damage, aging, and cancer. *Free Radic. Res.* 7, 121–128.
- Athukorala, Y., Jeon, Y.J., 2005. Screening for angiotensin 1-converting enzyme inhibitory activity of *Ecklonia cava*. *J. Food Sci. Nutr.* 10, 134-139.
- Barrow, C., Shahidi, F., 2008. *Marine nutraceuticals and functional foods*, CRC Press, New York, USA.
- Baron, A.D., 1998. Postprandial hyperglycemia and α -glucosidase inhibitors. *Diabetes Res Clin Pract.* 40, S51-S55.
- Bhandari, M.R., Jong-Anurakkun, N., Hong, G., Kawabata, J., 2008. α -Glucosidase and α -amylase inhibitory activities of Nepalese medicinal herb Pakhanbhed (*Bergenia ciliata*, Haw.). *Food Chem.* 106, 247–252.
- Campbell, R.K., 2009. Type 2 diabetes: where we are today: an overview of disease burden, current treatments, and treatment strategies. *J. Am. Pharm. Assoc.* 49, S3–S9.

Chang, M.S., Oh, M.S., Kim, D.R., Jung, K.J., Park, S., Choi, S.B., Ko, B.S., Park, S.K.,
2006. Effects of Okchun-San, a herbal formulation, on blood glucose levels and body
weight in a model of type 2 diabetes. *J Ethnopharmacol* 103, 491-95.

Charpentier, G., Riveline, J.P., Varroud-Vial, M., 2000. Management of drugs affecting
blood glucose in diabetic patients with renal failure. *Diabetes Metab.* 26, 73-85.

Cheng, J.Y., Shih, M.F., 2006. Improving glycogenesis in Streptozotocin (STZ) diabetic
mice after administration of green algae *Chlorella*. *Life Sci.* 78, 1181-1186.

Clark, A., Wells, C.A., Buley, I.D., Cruickshank, J.K., Vanhegan, R.I., Matthews, D.R.,
Cooper, G.J., Holman, R.R., Turner, R.C., 1988. Islet amyloid, increased A-cells, reduced
B-cells and exocrine fibrosis: quantitative changes in the pancreas in type 2 diabetes.
Diabetes Res. 9, 151-159.

Cormont, M.J., Tanti, F., Zahraoui, A., Van Obberghen, E., Tavitian, A., Le, Y., 1993.
Marchand-Brustel, Insulin and okadaic acid induce Rab4 redistribution in adipocytes. *J.*
Biol. Chem. 268, 19491-19497.

Coskun, O., Kanter, M., Korkmaz, A., Oter, S., 2005. Quercetin, a flavonoid antioxidant,
prevents and protects streptozotocin-induced oxidative stress and beta-cell damage in rat
pancreas. *Pharmacol. Res.* 51, 117-123.

DeFronzo RA, Jacot E, Jequier E, Maeder E, Wahren J, Felber JP. The effect of insulin on

the disposal of intravenous glucose. Results from indirect calorimetry and hepatic and femoral venous catheterization. *Diabetes* 1981; 30: 1000-1007.

DeFronzo, R.A., 1999. Pharmacologic therapy for type 2 diabetes mellitus. *Ann Intern Med.* 131, 281-303.

Dennis, J.W., Laferte, S., Waghorne, C., Breitman, M.L., Kerbel, R.S., 1987. Beta 1-6 branching of Asn-linked oligosaccharides is directly associated with metastasis. *Science.* 236, 582-585.

Diaz-Gutierrez, F.L., Ladero, J.M., Diaz-Rubio, M., 1998. Acarbose-induced acute hepatitis. *Am. J. Gastroenterol.* 93, 481-481.

Dugani, C.B., Randhawa, V.K., Cheng, A.W., Patel, N., Klip, A., 2008. Selective regulation of the perinuclear distribution of glucose transporter 4 (GLUT4) by insulin signals in muscle cells. *Eur. J. Cell Biol.* 87, 337-351.

Eizirik, D.L., Mandrup-Poulsen, T., 2001. A choice of death: the signal-transduction of immune-mediated β -cell apoptosis. *Diabetologia* 44, 2115-2133.

Fautz, R., Husen, B., Hechenberger, C., 1991. Application of the neutral red assay (NR assay) to monolayer cultures of primary hepatocytes: rapid colorimetric viability determination for the unscheduled DNA synthesis test (UDS). *Mutat. Res.* 253, 173-179.

Fraga, C.G., Leibovita, R.M., Roeder, R.G., 1988. Lipid peroxidation measured as

thiobarbituric-reactive substances in tissue slices: Characterization and comparison with homogenates and microsomes. *Free Radic. Biol. Med.* 4, 155-161.

Friesen, N.T., Buchau, A.S., Schott-Ohly, P., Lgssiar, A., Gleichmann, H., 2004. Generation of hydrogen peroxide and failure of antioxidative responses in pancreatic islets of male C57BL/6 mice are associated with diabetes induced by multiple low doses of streptozotocin. *Diabetologia* 47, 676–685.

Fryer, L.G., Parbu-Patel, A., Carling, D., 2002. The anti-diabetic drugs rosiglitazone and metformin stimulate AMP-activated protein kinase through distinct signaling pathways. *J. Biol. Chem.* 277, 25226–25232.

Gray, D.M., 1995. Carbohydrate digestion and absorption role of small intestine. *N. Engl. J. Med.* 29, 1225-1230.

Green, C.D., Jump, D.B., Olsen, L.K., 2009. Elevated insulin secretion from liver X receptor-activated pancreatic β cells involves increased de novo lipid synthesis and triacylglyceride turnover. *Endocrinology* 150, 2637-2645.

Gruters, R.A., Neeffjes, J.J., Tersmette, M., De Goede, R.E.Y., Tulp, A., Huisman, H.G., Miedema, F., Ploegh, H.L., 1987. Interference with HIV-induced syncytium formation and viral infectivity by inhibitors of trimming glucosidase. *Nature.* 330, 74–77.

Gschwind, M., Huber, G., 1995. Apoptotic cell death induced by β -amyloid 1-42 peptide is

cell type dependent. J. Neurochem. 65, 292-300.

Guiot, Y., Sempoux, C., Moulin, P., Rahier, J., 2001. No decrease of the β -cell mass in type 2 diabetic patients. Diabetes 50 (Suppl. 1). S188

Halliwell, B., Gutteridge, J.M.C., 1999. Antioxidant defenses. In: Free radicals in biology and medicine, 3rd ed. pp. 105-159. Oxford Science Publications, Oxford, UK.

Hanefeld, M., 1998. The role of acarbose in the treatment of non-insulin-dependent diabetes mellitus. J. Diabetes Complicat. 12, 228-237.

Hara, Y., Honda, M., 1990. The inhibition of α -amylase by tea polyphenols. Agric. Biol. Chem. 54, 1939-1945.

Harder, J., Bartels, J., Christophers, E., Schroder, J.M., 2001. Isolation and characterization of human β -defensin-3, a novel human inducible peptide antibiotic. J. Biol. Chem. 276, 5707-5713.

Heo, S.J., Pak, E.J., Lee, K.W., Jeon, Y.J., 2005a. Antioxidant activities of enzymatic extracts from brown seaweeds. Bioresource Technol. 96, 1613-1623.

Heo, S.J., Park, P.J., Park, E.J., Kim, S.K., Jeon, Y.J., 2005b. Antioxidant activity of enzymatic extracts from a brown seaweed *Ecklonia cava* by electron spin resonance spectrometry and comet assay. Eur. Food Res. Technol. 221, 41-47.

Heo, S.J., Kim, J.P., Jung, W.K., Lee, N.H., Kang, H.S., Jun, E.M., Park, S.H., Kang, S.M.,

Lee, Y.J., Park, P.J., Jeon, Y.J., 2008. Identification of chemical structure and free radical scavenging activity of diphlorethohydroxycarmalol isolated from a brown alga, *Ishige okamurae*. J. Microbiol. Biotechnol. 18, 676–681.

Heo, S.J., Hwang, J.Y., Choi, J.I., Han, J.S., Kim, H.J., Jeon, Y.J., 2009a.

Diphlorethohydroxycarmalol isolated from *Ishige okamurae*, a brown algae, a potent α -glucosidase and α -amylase inhibitor, alleviates postprandial hyperglycemia in diabetic mice. Eur J Pharmacol 615, 252-256.

Heo, S.J., Jeon, Y.J., 2009b. Evaluation of diphlorethohydroxycarmalol isolated from *Ishige*

okamurae for radical scavenging activity and its protective effect against H₂O₂-induced cell damage. Process Biochem. 44, 412–418.

Hotamisligil, G.S., 2006. Inflammation and metabolic disorders. Nature 444, 860–867.

Inoue, I., Takahashi, K., Noji, S., Awata, T., Negishi, K., Katayama, S., 1997. Acarbose

controls postprandial hyper-proinsulinemia in non-insulin-dependent diabetes mellitus. Diabetes Res. Clin. Pract. 36, 143–151.

Jorgensen, L.V., Madsen, H.L., Thomsen, M.K., Dragsted, L.O., Skibsted, L.H., 1999.

Regulation of phenolic antioxidants from phenoxyl radicals: an ESR and electrochemical study of antioxidant hierarchy. Free Radic. Res. 30, 207–220.

Jung, U.J., Baek, N.I., Chung, H.G., Bang, M.H., Yoo, J.S., Jeong, T.S., Lee, K.T., Kang, Y.J., Lee, M.K., Yeo, J.Y., Choi, M.S., 2007. The anti-diabetic effects of ethanol extract from two variants of *Artemisia princeps* Pampanini in C57BL/KsJ-*db/db* mice. *Food Chem Toxicol* 45, 2022-2029.

Kaneto, H., Nakatani, Y., Kawamori, D., Miyatsuka, T., Matsuoka, T., Matsuhisa, M., Yamasaki, Y., 2005. Role of oxidative stress, endoplasmic reticulum stress, and c-Jun N-terminal kinase in pancreatic β cells dysfunction and insulin resistance. *Int. J. Biochem. Cell. Biol.* 37, 1595-1608.

Kang, K., Park, Y., Hwang, H.J., Kim, S.H., Lee, J.G., Shin, H.C., 2003. Antioxidative properties of brown algae polyphenolics and their perspectives as chemopreventive agents against vascular risk factors. *Arch. Pharm. Res.* 26, 286–293.

Kang, S.I., Jin, Y.J., Ko, H.C., Choi, S.Y., Hwang, J. H., Whang, I., Kim, M.H., Shin, H.S., Jeong, H.B., Kim, S.J., 2008. *Petalonia* improves glucose homeostasis in streptozotocin-induced diabetic mice. *Biochem. Biophys. Res. Commun.* 373, 264-269.

Keen, H., Clark, C., Laakso, M., 1999. Reducing the burden of diabetes: managing cardiovascular disease. *Diabetes Metab. Res. Rev.* 15, 186–196.

Kim, J.S., 2004. Effect of *rhemanniae radix* on the hyperglycemic mice induced with streptozotocin. *J. Korea Soc. Food Sci. Nut.* 33, 1133–1138.

Kim, K.Y., Nam, K.A., Kurihara, H., Kim, S.M., 2008. Potent α -glucosidase inhibitors purified from the red alga *Grateloupia elliptica*. *Phytochemistry*. 69, 2820–2825.

Klein, R., Klein, B.E., Moss, S.E., Cruickshanks, K.J., 1996. The medical management of hyperglycemia over a 10-year period in people with diabetes. *Diabetes Care* 19, 744–750.

Kloppel, G., Lohr, M., Habich K, Oberholzer, M., Heitz, P.U., 1985. Islet pathology and the pathogenesis of type 1 and type 2 diabetes mellitus revisited. *Surv Synth Pathol Res*. 4, 110–125.

Kong, C.S., Kim, J.A., Yoon, N.Y., Kim, S.K., 2009. Induction of apoptosis by phloroglucinol derivative from *Ecklonia cava* in MCF-7 human breast cancer cells. *Food Chem. Toxicol.* 47, 1653–1658.

Kotake-Nara, E., Asai, A., Nagao, A., 2005. Neoxanthin and fucoxanthin induce apoptosis in PC-3 human prostate cancer cells. *Cancer lett.* 220, 75-84.

Krentz, A.J., Bailey, C.J., 2005. Oral antidiabetic agents. Current role in type 2 diabetes mellitus. *Drugs*. 65, 385-411.

Lee, S.H., Han, J.S., Heo, S.J., Hwang, J.Y., Jeon, Y.J., 2010a. Protective effects of dieckol isolated from *Ecklonia cava* against high glucose-induced oxidative stress in human umbilical vein endothelial cells. *Toxicol. In vitro* 24, 375-381.

Lee, S.H., Park, M.H., Heo, S.J., Kang, S.M., KO, S.C., Han, J.S., Jeon, Y.J., 2010b. Dieckol isolated from *Ecklonia cava* inhibits α -glucosidase and α -amylase in vitro, and alleviates postprandial hyperglycemia in streptozotocin-induced diabetic mice. *Food Chem Toxicol* 48, 2633-2637.

Li, Y., Wen, S., Kota, B.P., Peng, G., Li, G.Q., Yamahara, J., 2005. *Punica granatum* flower extract, a potent α -glucosidase inhibitor, improves postprandial hyperglycemia in Zucker diabetic fatty rats. *J. Ethnopharmacol.* 99, 239–244.

Lizard, G., Fournel, S., Genestier, L., Dhedin, N., Chaput, C., Flacher, M., Mutin, M., Panaye, G., Revillard, J.P., 1995. Kinetics of plasma membrane and mitochondrial alterations in the cells undergoing apoptosis. *Cytometry* 21, 275-283.

Matsui, T., Tanaka, T., Tamura, S., Toshima, A., Miyata, Y., Tanaka, K., Matsumoto, K., 2007. Alpha-glucosidase inhibitory profile of catechins and theaflavins. *J. Agric. Food Chem.* 55, 99–105.

Mayer, A.M.S., Hamann, M.T., 2002. Marine Pharmacology in 1999: compounds with antibacterial, anticoagulant, antifungal, anthelmintic, anti-inflammatory, antiplatelet, antiprotozoal and antiviral activities affecting the cardiovascular, endocrine, immune and nervous systems, and other miscellaneous mechanisms of action. *Comparative Biochemistry and Physiology Part C.* 132, 315-339.

Mayer, A.M.S., Hamann, M.T., 2005. Marine pharmacology in 2001–2002: marine compounds with anthelmintic, antibacterial, anticoagulant, antidiabetic, antifungal, anti-inflammatory, antimalarial, antiplatelet, antiprotozoal, anti-tuberculosis, and antiviral activities; affecting the cardiovascular, immune and nervous systems and other miscellaneous mechanisms of action. *Comp. Biochem. Physiol. C* 140, 265–286.

Moller, D.E., Flier, J.S., 1992. Insulin resistance: mechanisms, syndromes, and implications. *N. Engl. J. Med.* 325, 938–942.

Moller, D.E., 2001. New drug targets for type 2 diabetes and the metabolic syndrome. *Nature* 414, 821–827.

Musi, N., Goodyear, L.J., 2003. AMP-activated protein kinase and muscle glucose uptake. *Acta Physiol. Scand.* 178, 337–345.

Nagayama, K., Iwamura, Y., Shibata, T., Hirayama, I., Nakamura, T., 2002. Bactericidal activity of phlorotannins from the brown alga *Ecklonia kurome*. *J. Antimicrob. Chemother.* 50, 889–893.

Nakatani, Y., Kaneto, H., Kawamori, D., Yoshiuchi, K., Hatazaki, M., Matsuoka, T., Ozawa, K., Ogawa, S., Hori, M., Yamasaki, Y., Matsuhisa, M., 2005. Involvement of endoplasmic reticulum stress in insulin resistance and diabetes. *J. Biol. Chem.* 280, 847–851.

Nicoletti, I., Migliorati, G., Pagliacci, M.C., Grignani, F., Riccardi, C., 1991. A rapid and

simple method for measuring thymocyte apoptosis by propidium iodide staining and flow cytometry. *J. Immunol. Methods* 139, 271-279.

Nisizawa, K., Noda, H., Kikuchi, R., Watamaba, T., 1987. The main seaweed foods in Japan. *Hydrobiol.* 151/152, 5-29.

Okada, T., Kawano, Y., Sakakibara, T., Hazeki, O., Ui, M., 1994. Essential role of phosphatidylinositol 3-kinase in insulin-induced glucose transport and antilipolysis in rat adipocytes. Studies with a selective inhibitor wortmannin. *J Biol Chem.* 269, 3568-3573.

Ozawa, K., Miyazaki, M., Matsuhisa, M., Takano, K., Nakatani, Y., Hatazaki, M., Tamatani, T., Yamagata, K., Miyagawa, J., Kitao, Y., Hori, O., Yamasaki, Y., Ogawa, S., 2005. The endoplasmic reticulum chaperone improves insulin resistance in type 2 diabetes. *Diabetes.* 54, 657-663.

Ozcan, U.Q., Cao, E., Yilmaz, A.H., Lee, N.N., Iwakoshi, E., Ozdelen, G., Tuncman, C., Gorgun, L.H., Glimcher, G.S., Hotamisligil, 2004. Endoplasmic reticulum stress links obesity, insulin action, and type 2 diabetes. *Science.* 306, 457-461.

Ozcan, U., Yilmaz, E., Ozcan, L., Furuhashi, M., Vailancourt, E., Smith, R.O., Gorgun, C.Z., Hotamisligil, G.S., 2006. Chemical chaperones reduce ER stress and restore glucose homeostasis in a mouse model of type 2 diabetes. *Science.* 313, 1137-1140.

Raj, P.A., Dentino, A.R., 2002. Current status of defensins and their role in innate and adaptive immunity. *FEMS Microbiol. Lett.* 206, 9–18.

Rashid, M.A., Lee, S., Tak, E., Lee, J., Choi, T.G., Lee, J.W., Kim, J.B., Youn, J.H., Kang, I., Ha, J., Kim, S.S., 2010. Carbonyl reductase 1 protects pancreatic β cells against oxidative stress-induced apoptosis in glucotoxicity and glucolipotoxicity. *Free Radical Biol. Med.* 49, 1522-1533.

Ricketts, E., Calvin, J., 1962. *Between pacific tides*. 3rd ed. Revised by Hedgpeth, J. Stanford, California: Stanford University Press. Smith, G. M. 1944. *Marine algae of the monterey peninsula*. Stanford, California: Stanford University Press.

Rice-Evans, C.A., Miller, N.J., Bolwell, P.G., Bramley, P.M., Pridham, J.B., 1995. The relative antioxidant activities of plant-derived polyphenolic flavonoids. *Free Radic. Res.* 22, 375–383.

Ruperez, P., 2001. Antioxidant activity of sulphated polysaccharides from the Spanish marine seaweed Nori. In *Proceedings of the COST 916 European conference on bioactive compounds in plants foods* (p. 114). Tenerife, Canary Islands, Spain: Health Effects and Perspectives for the Food Industry.

Saito, N., Sakai, H., Sekihara, H., Yajima, Y., 1998. Effect of an α -glucosidase inhibitor (volibose), in combination with sulphonylureas, on glycaemic control in type 2 diabetes

patients. *J. Int. Med. Res.* 26, 219–232.

Sels, J.P., Huijberts, M.S., Wolffenbuttel, B.H., 1999. Miglitol, a new alpha-glucosidase inhibitor. *Expert Opin. Pharmacother.* 1, 149–156.

Shahidi, F., Zhong, Y., 2008. Bioactive peptides. *Journal of AOAC International.* 91, 914–931.

Sheetz, M.J., King, G.L., 2002. Molecular understanding of hyperglycemia's adverse effects for diabetic complications. *JAMA.* 288, 2579–2588.

Shibata, T., Fujimoto, K., Nagayama, K., Yamaguchi, K., Nakamura, T., 2002. Inhibitory activity of brown algal phlorotannins against hyaluronidase. *Int. J. Food Sci. Technol.* 37, 703–709.

Singh, I.P., Bharate, S.B., 2006. Phloroglucinol compounds of natural origin. *Nat. Prod. Rep.* 23, 558–591.

Srikanta, S., Ganda, O.P., Jackson, R.A., Gleason, R.E., Kaldany, A., Garovoy, M.R., Milford, E.L., Carpenter, C.B., Soeldner, J.S., Eisenbarth, G.S., 1983. Type I diabetes mellitus in monozygotic twins: chronic progressive β cell dysfunction. *Ann Intern Med.* 99, 320–326.

Srivivasan, A., Menon, V.P., Periaswamy, V., Rajasekaran, K.N., 2003. Protection of pancreatic beta-cell by the potential antioxidant bis-hydroxycinnamoyl methane, analogue

of natural curcuminoid in experimental diabetes. *J. Pharm. Pharm. Sci.* 6, 327–333.

Stand, E., Baumgartl, H.J., Fuchtenbusch, M., Stemplinger, J., 1999. Effect of acarbose on additional insulin therapy in type 2 diabetic patients with late failure of sulphonylurea therapy. *Diabetes. Obes. Metab.* 1, 215–220.

Stephens, J.M., Pilch, P.F., 1995. The metabolic regulation and vesicular transport of GLUT4, the major insulin-responsive glucose transporter. *Endocr. Rev.* 16, 529–546.

Stern, J.L., Hagerman, A.E., Steinberg, P.D., Mason, P.K., 1996. Phlorotannins–protein interactions. *J. Chem. Ecol.* 22, 1877–1899.

Taniguchi, C.M., Emanuelli, B., Kahn, C.R., 2006. Critical nodes in signalling pathways: insights into insulin action. *Nat. Rev. Mol. Cell Biol.* 7, 85–96.

Tan, M.J., Ye, J.M., Turner, N., Hohnen-Behrens, C., Ke, C.Q., Tang, C.P., Chen, T., Weiss, H.C., Gesing, E.R., Rowland, A., James, D.E., Ye, Y., 2008. Antidiabetic activities of triterpenoids isolated from bitter melon associated with activation of the AMPK pathway. *Chem. Biol.* 15, 263–273.

Tiedge, M., Lortz, S., Drinkgern, J., Lenzen, S., 1997. Relation between antioxidant enzyme gene expression and antioxidative defense status of insulin-producing cells. *Diabetes* 46, 1733–1742.

Towler, M.C., Hardie, D.G., 2007. AMP-activated protein kinase in metabolic control and insulin signaling. *Circ. Res.* 100, 328–341.

U.K. Prospective Diabetes Study Group, 1995. U.K. Prospective Diabetes Study 16. Overview of 6 years' therapy of type II diabetes: a progressive disease. *Diabetes* 44, 1249 – 1258.

UK Prospective Diabetes Study Group, 1998. Effect of intensive blood-glucose control with metformin on complications in overweight patients with type 2 diabetes (UKPDS 34). *Lancet* 352, 854–865.

Wang, Q., Somwar, R., Bilan, P.J., Liu, Z., Jin, J., Woodgett, J.R., Klip, A., 1999. Protein kinase B/Akt participates in GLUT4 translocation by insulin in L6 myoblasts. *Mol Cell Biol.* 19, 4008-4018.

Wang, X. W., Zhan, Q., Coursen, J.D., Khan, M.A., Kontny, H.U., Yu, L., Hollander, M.C., O'Connor, P.M., Fornace, A.J., Harris, C.C., 1993. GADD45 induction of a G2/M cell cycle checkpoint. *Proc. Natl. Acad. Sci. U.S.A.* 96, 3706-3711.

Watanabe, J., Kawabata, J., Kurihara, H., Niki, R., 1997. Isolation and identification of alpha-glucosidase inhibitors from Tochucha (*Eucommia ulmoides*). *Bioscience, Biotechnology, and Biochemistry.* 61, 177–178.

Winchester, B., Fleet, G.W., 1992. Amino-sugar glycosidase inhibitors: versatile tools for glyco biologists. *Glycobiology*. 2, 199–210.

Yokozawa, T., Kim, Y.A., Kim, H.Y., Lee, Y.A., Nonaka, G., 2007. Protective effect of persimmon peel polyphenol against high glucose-induced oxidative stress in LLC-PK₁ cells. *Food Chem. Toxicol.* 45, 1979-1987.

Zaid, H., Antonescu, C.N., Randhawa, V.K., Klip, A., 2008. Insulin action on glucose transporters through molecular switches, tracks and tethers. *Biochem. J.* 413, 201–215.

Zhou, G., Myers, R., Li, Y., Chen, Y., Shen, X., Fenyk-Melody, J., Wu, M., Ventre, J., Doebber, T., Fujii, N., Musi, N., Hirshman, M.F., Goodyear, L.J., Moller, D.E., 2001. Role of AMP-activated protein kinase in mechanism of metformin action. *J. Clin. Invest.* 108, 1167–1174.

Zimmet, P., Alberti, K., Shaw, J., 2001. Global and societal implications of the diabetes epidemic. *Nature*. 414, 782-87.

Acknowledgement

학부 2 학년으로 연구실에 입문하여 박사학위논문이라는 내 노력의 결실을 얻기까지 많은 분들의 관심과 도움이 있었기에 이 자리를 빌어 감사의 말씀을 드리고자 합니다. 먼저 수 많은 시간 동안 험난한 시련과 포기라는 것이 내 앞을 가로막을 때마다 용기를 잃지않게 자신감을 심어주시고 사랑과 세심한 가르침으로 부족한 저를 잘 이끌어주신 전유진 교수님께 머리 숙여 진심으로 감사 드립니다. 또한 바쁘신 가운데서도 논문이 좀 더 나은 방향으로 나아 갈 수 있게 심사해 주시고 관심을 보여주신 김기영 교수님, 이대호 교수님, 이승헌 교수님, 김대경 박사님과 학부시절부터 대학원 기간 동안 늘 많은 관심과 조언을 해주셨던 이기완 교수님, 송춘복 교수님, 최광식 교수님, 이제희 교수님, 허문수 교수님, 여인규 교수님, 이경준 교수님, 정준범 교수님, 김수현 교수님께도 깊은 감사를 드립니다.

다사다난한 연구실에서 동고동락하며 부족한 선배인 저를 잘 따라주며 많은 협조를 통해 힘을 실어준 강성명, 고석천 후배님과 연구실의 많은 일을 잘 이끌고 나가는 이원우 후배님, 잔소리에도 변함없이 잘 따라주고 바쁜 중에도 혼자 해낼 수 없는 실험에 많은 도움을 준 고주영, 강민철, 이지혁, 고창익, 양혜미, 강나래, 김은아, 오재영 후배님 및 한국 생활을 잘 적응해 나가는 양수동, 자나카, 칼파 이 모든 해양생물자원이용공학연구실 가족에게 감사의 마음을

전합니다. 또한 자랑스런 저희 연구실 출신으로 사회에 나가 참된 연구자의 길을
걸고 계시는 허수진 선배님, 김길남 선배님, 차선희 후배님, 안긴내 후배님,
김원석 선배님, 양현필 선배님의 많은 조언과 관심에 깊은 감사를 드립니다.

학부시절과 대학원생활 동안 항상 옆에 있어주며 같은 길을 걸어가고 있는
친구이자 동기인 김주상, 한송헌에게 고마운 마음을 전하며 돈독한 선후배로
뭉친 학과 선·후배님들께도 감사의 마음을 전합니다. 또한 관련 실험에 큰
도움을 주었던 의과대학 관건 학생과 멀리서 저에게 많은 관심과 조언을 해주신
조선대학교 정원교 교수님께도 고마운 마음을 전합니다.

철없던 학창시절부터 많은 시간이 흐른 지금까지 언제나 함께하고 힘들 때
부담없이 술잔을 기울일 수 있는 소중한 친구들에게 항상 고맙고 앞으로 더욱
발전된 모습으로 함께하자는 말을 전합니다. 공부한다는 이유로 자주 찾아뵙지도
못하는 부족한 막내 사위를 위해 잘되라고 기도해주시는 장인어른과 장모님께
깊은 감사의 마음을 드리며 두 분의 건강을 기원합니다. 또한 저를 친동생처럼
잘 챙겨주시는 큰 처형과 형님, 작은 처형께도 고마운 마음을 전합니다. 아들
하나만을 잘되기만을 간절히 바라시며 눈물과 땀과 헌신적인 사랑으로 오늘의
저를 있게 해주신 아버지와 어머니께 깊은 감사를 드리며 평생 갚아도 부족할
그 은혜 꼭 보답하겠습니다. 철없는 남동생을 항상 격려해주는 누나 내외분들,
하나뿐인 동생 내외에게도 고마운 마음을 전합니다.

마지막으로 꽃다운 나이에 저를 만나 두 아이의 엄마가 되기까지 힘든 시간 잘 참고 사랑과 헌신으로 연구와 학업에 몰두할 수 있도록 용기를 준 나의 사랑하는 아내 최숙진에게 미안하고 고마운 마음을 전하며 이 작은 결실이 당신의 것이기도 하며 앞으로도 믿음과 사랑 변치 않겠다는 저의 마음과 이 논문을 바칩니다. 그리고 제가 살아가는 힘의 원천이자 세상 무엇과도 바꿀 수 없는 나의 아들 재훈이와 나의 딸 시현이 정말 사랑하고 사람 냄새나는 사람으로 자라길 바란다는 마음을 전합니다.

이 논문이 인생에서 아주 작은 결실이라면, 앞으로 가꾸고 수확할 열매가 더욱 풍성할 것입니다. 항상 낮은 자세로 앞으로도 학문과 연구에 더욱 정진하며 언제 어디에 서더라도 부끄러움 없는 제 자신을 다짐하며 이 글을 마칩니다.